Electronic Supplementary Material (ESI) for New Journal of Chemistry.

Cu(II), Ir(I) and CuO nano catalysed mild synthesis of luminescent bis(triazolylmethyl)quinoxalines: biocompatibility, cytotoxicity, live cell imaging and biomolecular interaction

Santanu Maiti, Nilmadhab Roy, Lavanya Thilak Babu, Prithvi Moharana, Athira C C, Darsana Sreedhar E, Sourav De, Ashok Kumar S K and Priyankar Paira*

General procedure for the synthesis of 2,3-bis (bromomethylquinioxaline) series (3a, 3b)

O-Phenylenediamine derivatives (**1a**, **1b**) (100mg) and 1,4-dibromobutane-2,3-dione (**2**) (1.1 equivalent) were dissolved in ethanol and adequate amount of silica gel was added to it to make the slurry. The slurry was further dried under vacuum. The mixture was taken in microwave vessel and kept for stirring under microwave at 60 watt (100˚ C) for 10 min. The progress of reaction was monitored by TLC using hexane/ethyl acetate (3:1) solvent system. After completion of the reaction the silica gel slurry was washed three times using hexane followed by filtration. The collected filtrate was evaporated to dryness and further recrystallized from hexane.White needle like crystals of 2,3-bis bromomethylquinoxalines (**3a**,**3b**) were formed with 90-95% yield.

Characterization of 2,3-bis (bromomethylquinioxaline)series (3a, 3b)

2,3-bis(bromomethyl)quinoxaline (3a): Yield: 95%;mp: 150˚-155˚ C;R_f: 0.75 (1:3 ethylacetate :hexane); ^{1}H NMR ($CDCl_3$, 400 MHz): δ 8.07 (dd, 2H, J_1 = 6.4 Hz, J_2 = 3.6 Hz, ArH, H-1,H-4), 7.79 (dd, 2H, J_1 = 6.4 Hz, J_2 = 3.6 Hz, ArH,H-2, H-3), 4.93 (s, 4H, CH_2, H-9, H-10); ^{13}C NMR (400 MHz, $CDCl_3$): δ 30.5 (2 x CH_2, C-9, C-10), 129.7 (2 x CH,C-7, C-8), 130.9 (2 x CH, C-5, C-6), 143.6 (2 x CH, C-1, C-4), 150.9 (2 x CH,C-2, C-3); IR (KBr, cm^{-1}): 3018 (sp3 C-H stretching), 2962 (C–H Ar stretching), 1485 (C-H bending), 1425 (CH_2 bending), 1209(C-N stretching), 765 (C-H stretching of o-di-substituted group),628(C-Br stretching); LC-MS (CH_3OH): m/z 317 $[M+H]^+$.

6-bromo-2,3-bis(bromomethyl)quinoxaline (3b):^{1}H NMR (400 MHz, $CDCl_3$): Yield: 98%, mp: 165˚ C-168° C, R_f: 0.79 (1:3 ethylacetate : hexane); ^{1}H NMR ($CDCl_3$, 400 MHz): δ 8.25 (s, 1H, H-4), 7.92 (d, J = 8.8 Hz, 1H, H-2), 7.85 (d, J = 8.8 Hz, 1H, H-1), 4.89 (s, 4H, CH_2,H-9, H-10); ^{13}C NMR (400 MHz, $CDCl_3$): δ 151.8 (CH, C-7), 151.2 (CH, C-8) ,142.1 (CH, C-5), 140.3 (CH, C-6), 134.5 (CH, C-4), 131.40 (CH, C-1), 130.3 (CH, C-2), 125.1 (CH, C-3), 30.21 (CH_2,C-9), 30.11 (CH2, C-10); IR (KBr, cm^{-1}): 3028 (sp^3 C-H stretching), 2972 (C–H Ar stretching), 1595 (C=C), 1473, 1415 (CH_2 bending), 1209.37 (C-N stretching) 721.38 (C-H stretching of *o*-di-substituted group). 634, 567 (C-Br stretching); LC-MS (CH_3OH): m/z 395 $[M+H]^+$.

General procedure for the synthesis of 2,3-bis (azidomethylquinioxaline)series (4a, 4b)

2,3 bromomethylquinoxalines (**3a, 3b**) (50 mg) and sodium azide (2.5 equivalent) were dissolved in ethanol followed by the addition of adequate amount of silica gel (100-200 mesh) to make the slurry. After complete air drying the solid supported form of this reaction mixture was kept for stirring in microwave for 10 min at 70° C (270 watt). The progress of the reaction was monitored by TLC (3:1 Hexane/Ethayl Acetate). After completion of the reaction, the mixture was transferred into a 250 ml of beaker followed by addition of ethanol to extract the desired product from the silica gel. Finally, the ethanol was evaporated to isolate the blackish crystals of azidomethylquinoxalines (**4a, 4b**).

Characterization of 2,3-bis(azidomethylquinioxaline) series (4a, 4b)

2,3-bis(azidomethyl)quinoxaline (4a): Yield: 95%; mp: 145˚-148˚C, R_f0.68 (1:3 ethylacetate : hexane); ^{1}H NMR ($CDCl_3$, 400 MHz): δ 8.10 (dd, 2H, J_1 = 6.4 Hz, J_2 = 3.6 Hz, ArH, H-1,H-4), 7.78 (dd, 2H, J_1 = 6.4 Hz, J_2 = 3.6 Hz, ArH, H-2, H-3), 4.70 (s, 4H, CH_2, H-9,H-10); ^{13}C NMR (400 MHz, $CDCl_3$): δ 148.3 (2 x CH, C-7, C-8), 140.9 (2 x CH, C-5,C-6), 130.3 (2 x CH, C-2, C-3), 128.7 (2 x CH, C-1, C-4), 52.9(2 x CH_2, C-9, C-10); IR(KBr, cm^{-1}): 3053 (sp^3 C-H stretching), 2129, 2083 (N=N=N Stretching), 1566 (C-H bending), 1452 (CH_2 bending), 1240 (C-N stretching), 761 (C-H stretching of *o*-di-substituted group); LC-MS (CH_3OH): m/z 241 $[M+H]^+$.

2,3-bis(azidomethyl)-6-bromoquinoxaline (4b): Yield: 95%, mp: 145˚-148° C, R_f 0.68 (1:3 ethylacetate :hexane); ^{1}H NMR ($CDCl_3$, 400 MHz): δ 8.32 (s, 1H,ArH, H-4), 8.0 (d,1H, *J* = 9.2 Hz, ArH, H-2), 7.90 (d,1H,*J*= 10.8 Hz,ArH, H-1), 4.71 (s, 4H, CH_2); ^{13}C NMR (400 MHz, $CDCl_3$): δ 150.4 (CH, C-7), 149.7 (CH, C-8), 141.9 (CH, C-5), 140.1 (CH, C-6), 134.3 (CH, C-1), 131.5 (CH,C-4), 130.4 (CH, C-2), 124.5 (CH, C-3), 53.3 (CH_2, C-9), 53.2 (CH_2, C-10),IR(KBr, cm^1): 3045 (sp3 C-H stretching), 2943 (C–H Ar stretching), 2094, 2069 (N=N=N Stretching), 1597 (C-H bending), 1477 (CH_2 bending), 1427 (CH_2 bending), 1143 (C-N stretching), 740 (C-H stretching of *o*-disubstituted group); LC-MS (CH3OH): m/z 319 $[M+H]^+$.

Synthesis of CuO Nanoparticle

- 25ml of ethanolic solution of 0.2 M $Cu(CH_3COO)_2$ mixed with 25 ml of ethanolic solution of 0.01mol NaOH in R. B. flask. Then, 0.5 g of PEG was added to the reaction mixture. It was kept in microwave for 10 min. After 10 min brown black precipitate was obtained and then it was cooled at room temperature. Then the precipitates were washed with distilled water, ethanol followed by acetone. Finally, CuO nano particles were dried at room temperature and characterized.

^{1}H NMR of compound 3a

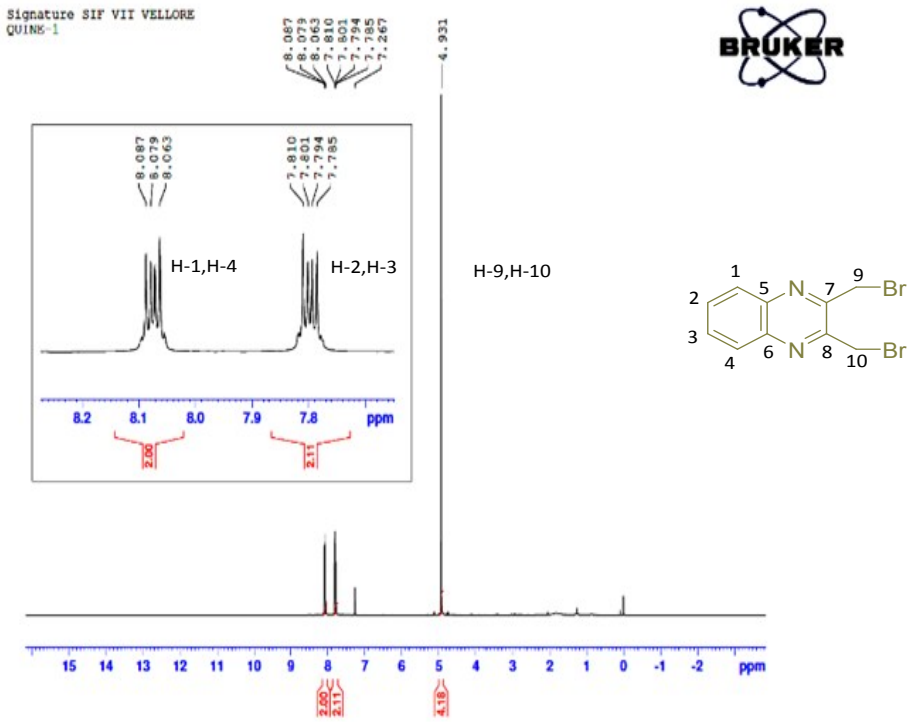

^{13}C NMR of compound 3a

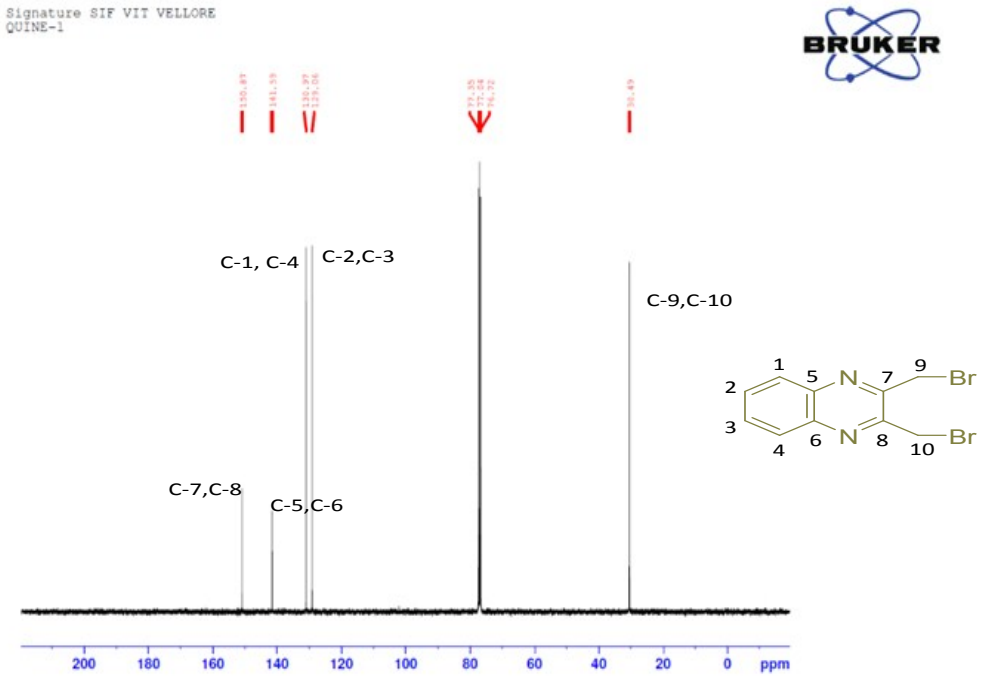

IR spectra of compound 3a

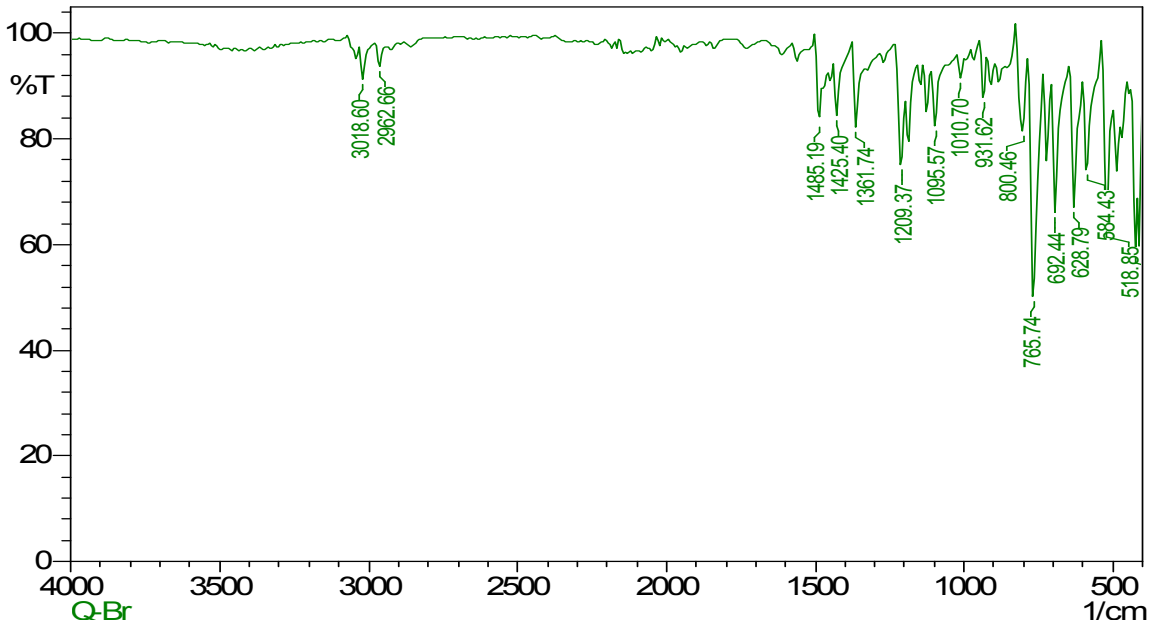

LCMS of compound 3a

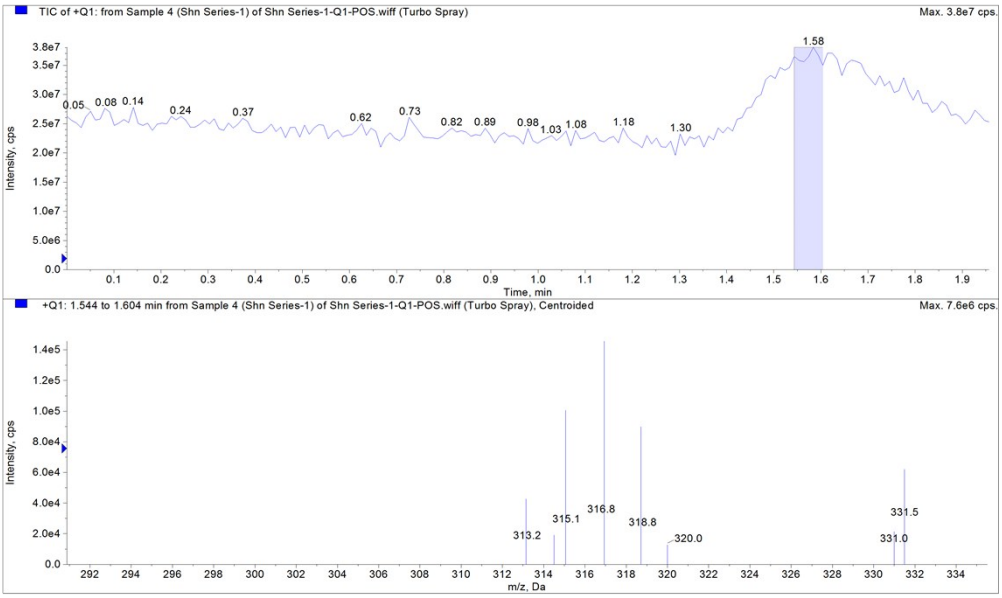

^{1}H NMR of compound 3b

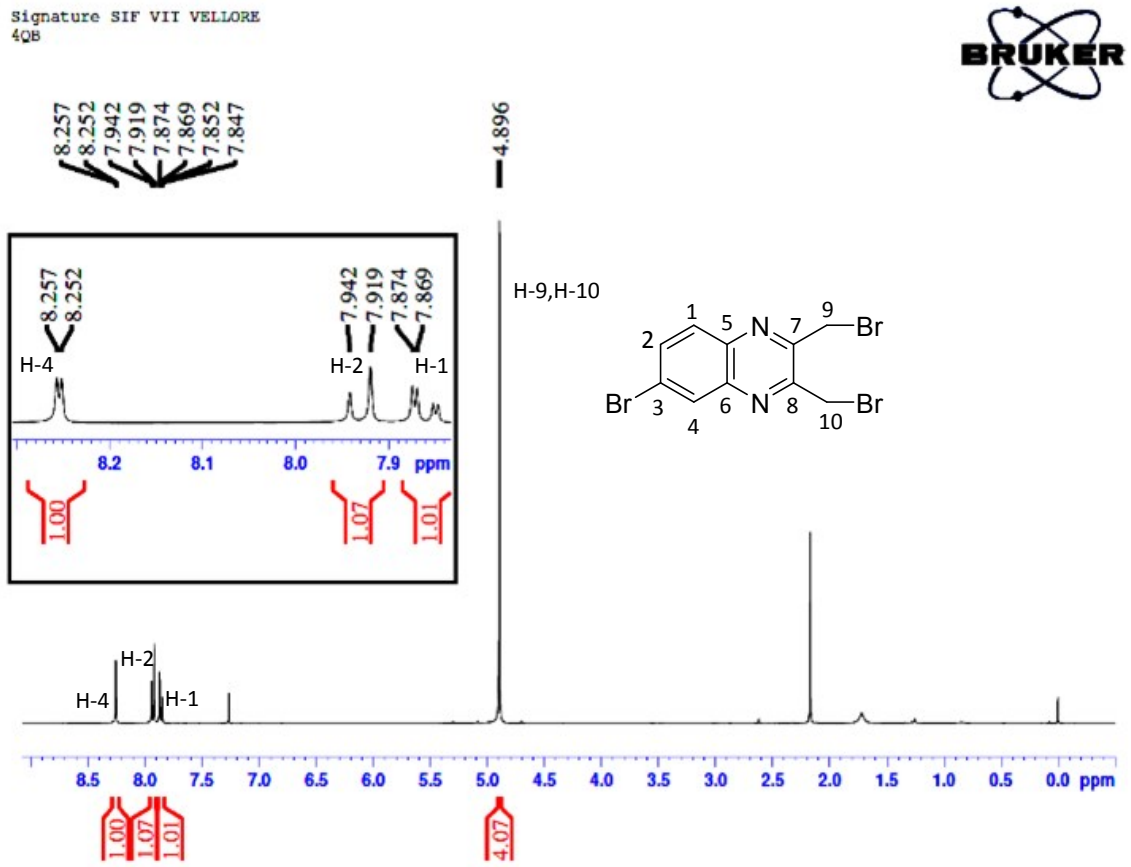

^{13}C NMR of compound 3b

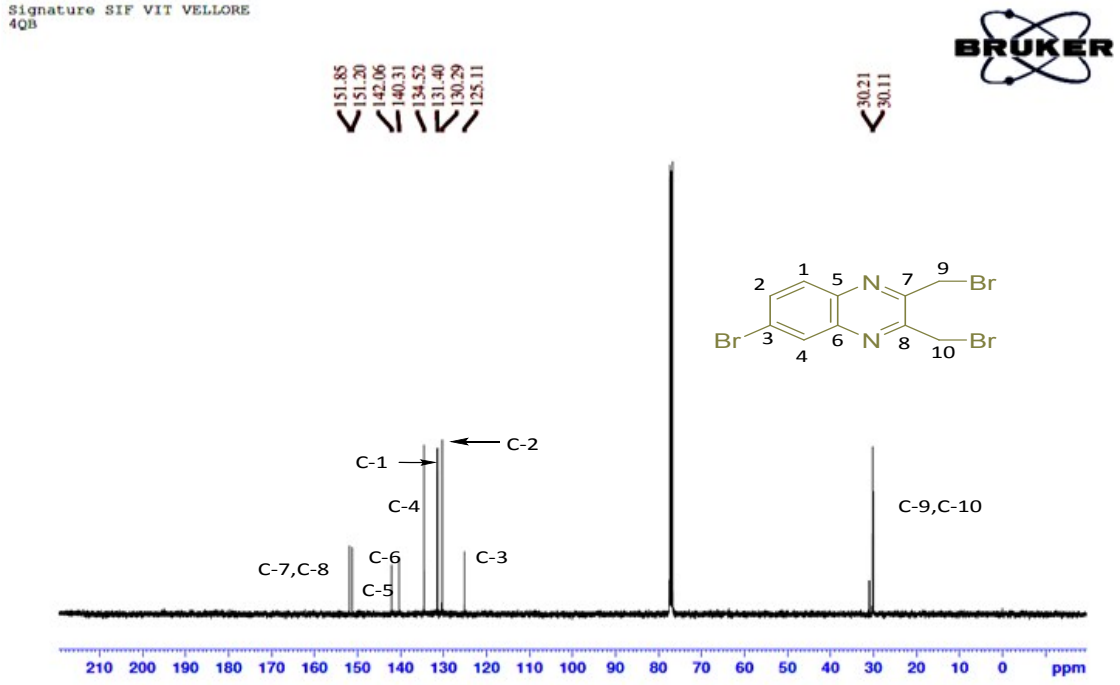

IR spectra of compound 3b

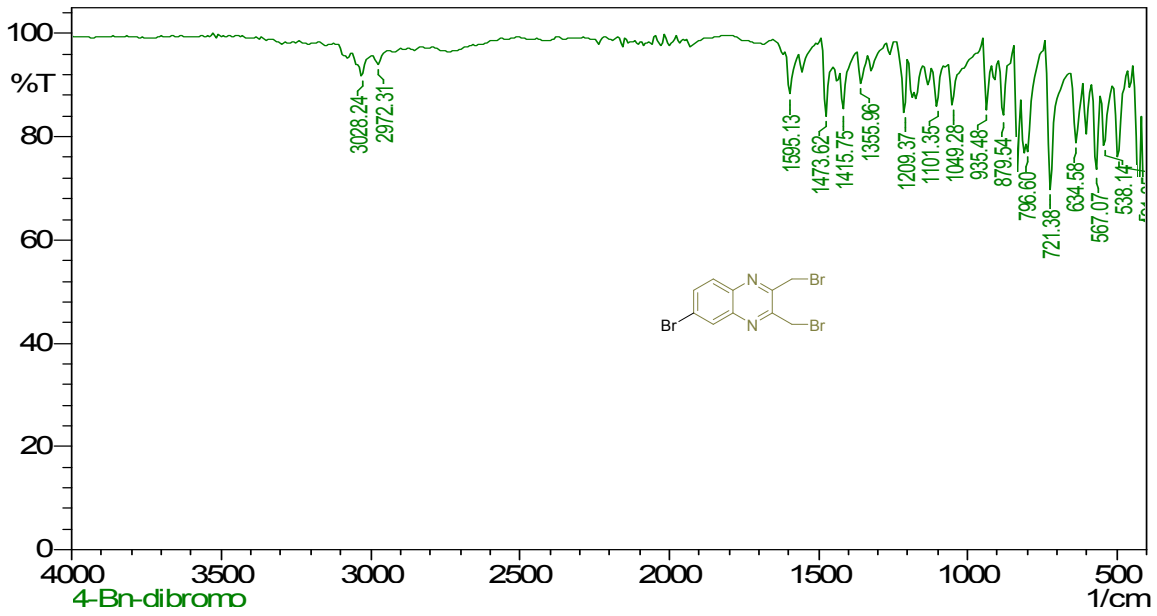

LCMS of compound 3b

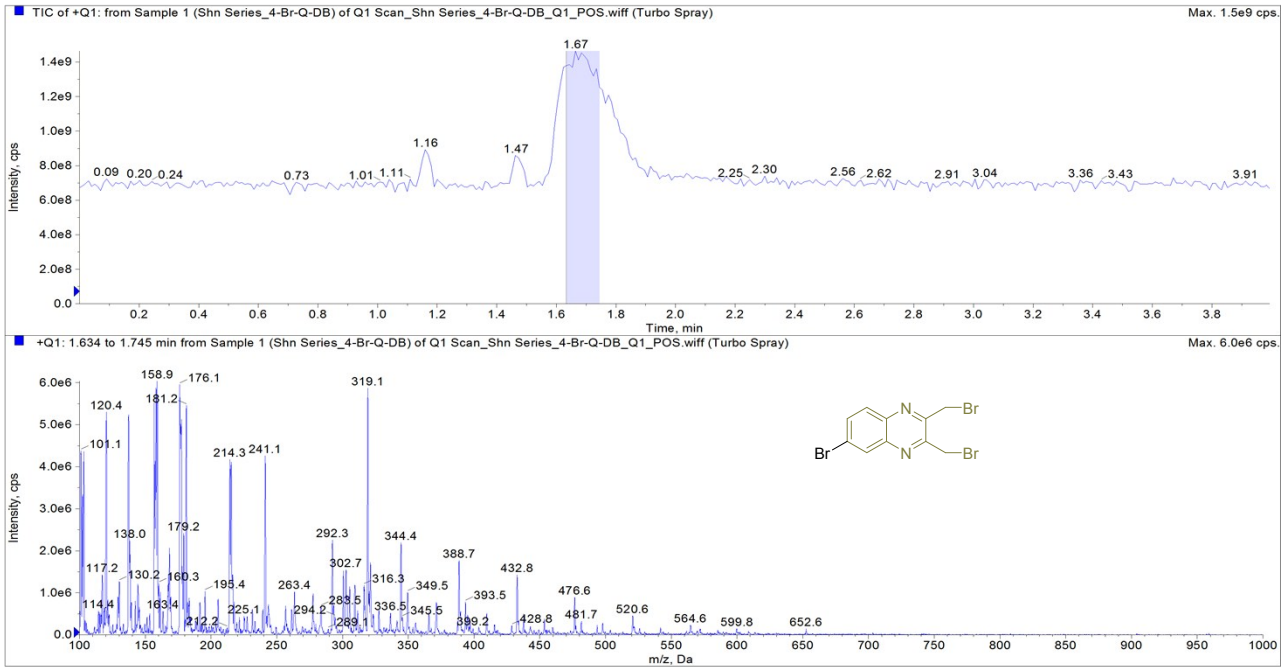

^{1}H NMR of compound 4a

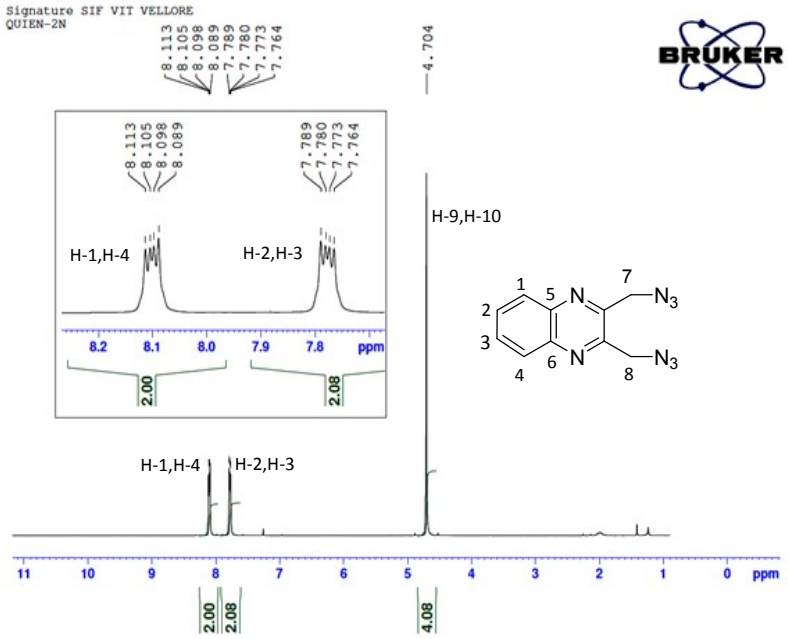

^{13}C NMR of compound 4a

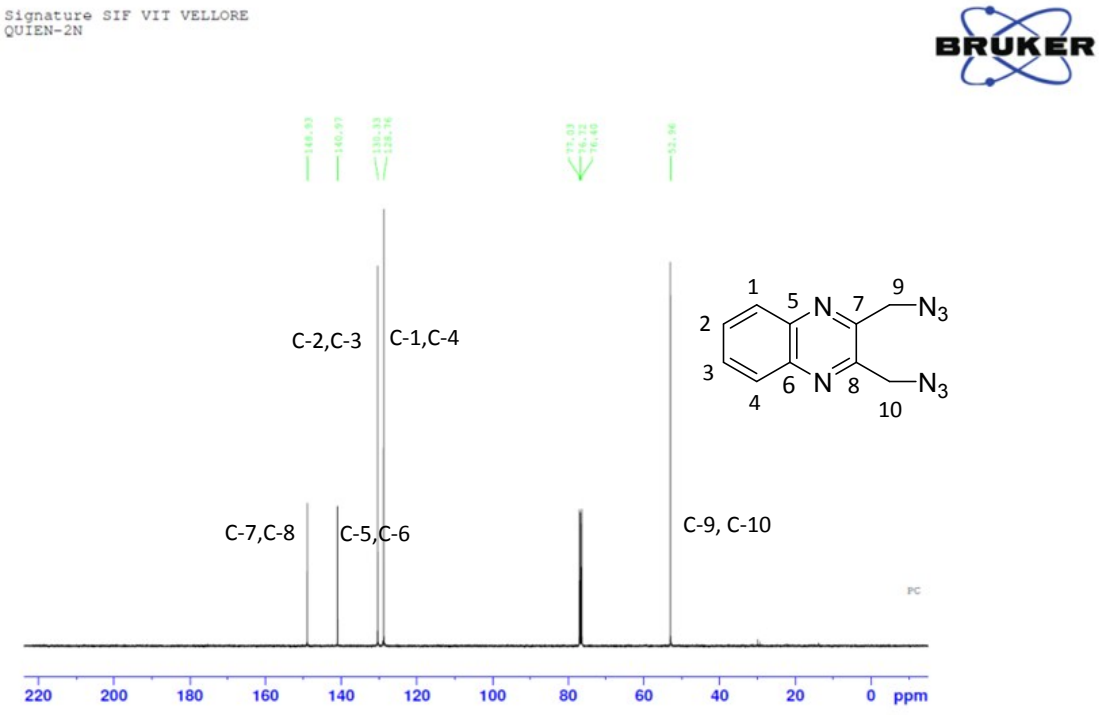

IR spectra of compound 4a

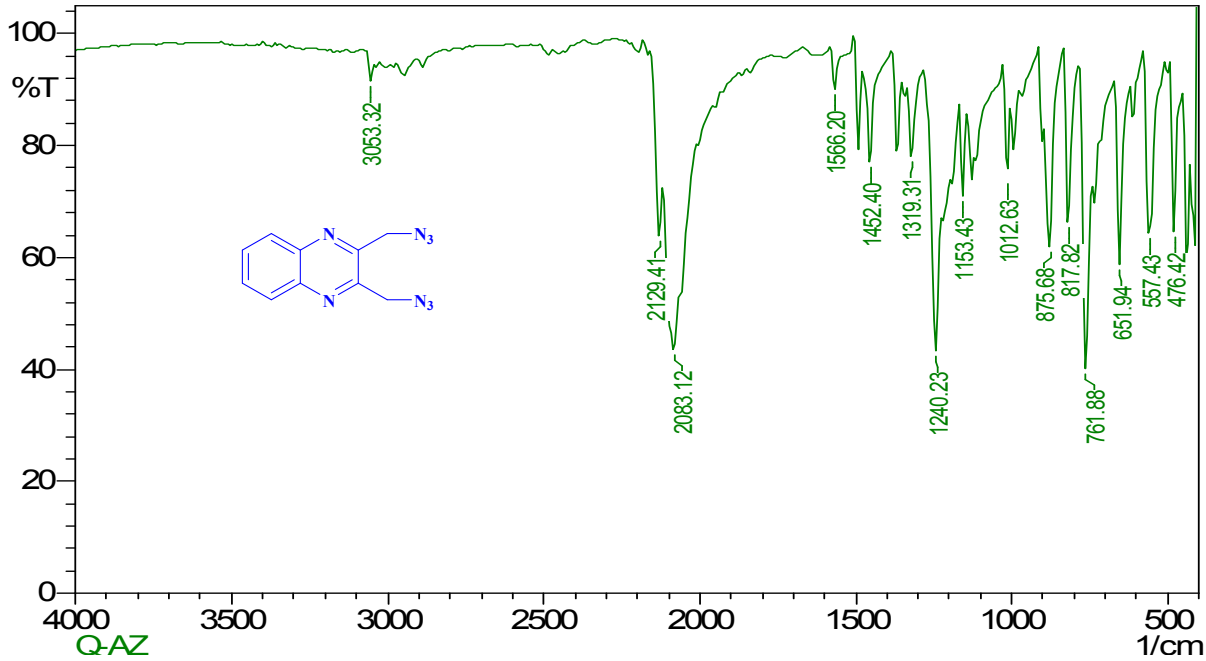

LCMS of compound 4a

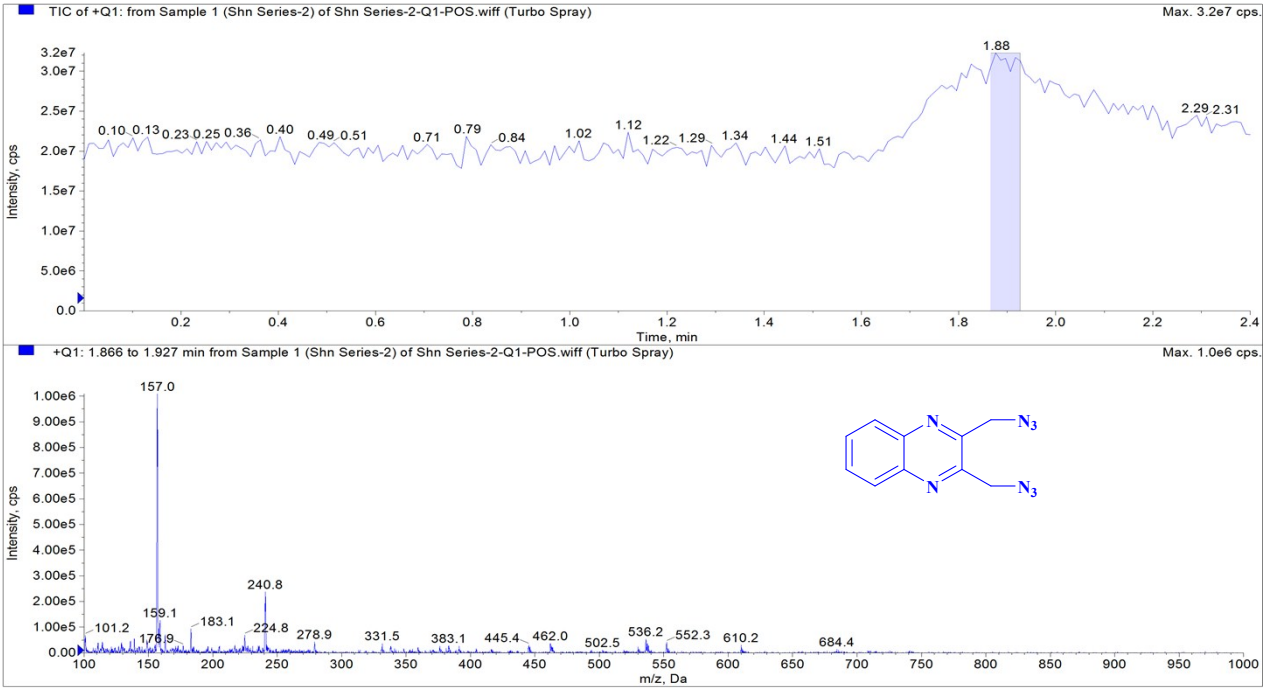

^{1}H NMR of compound 4b

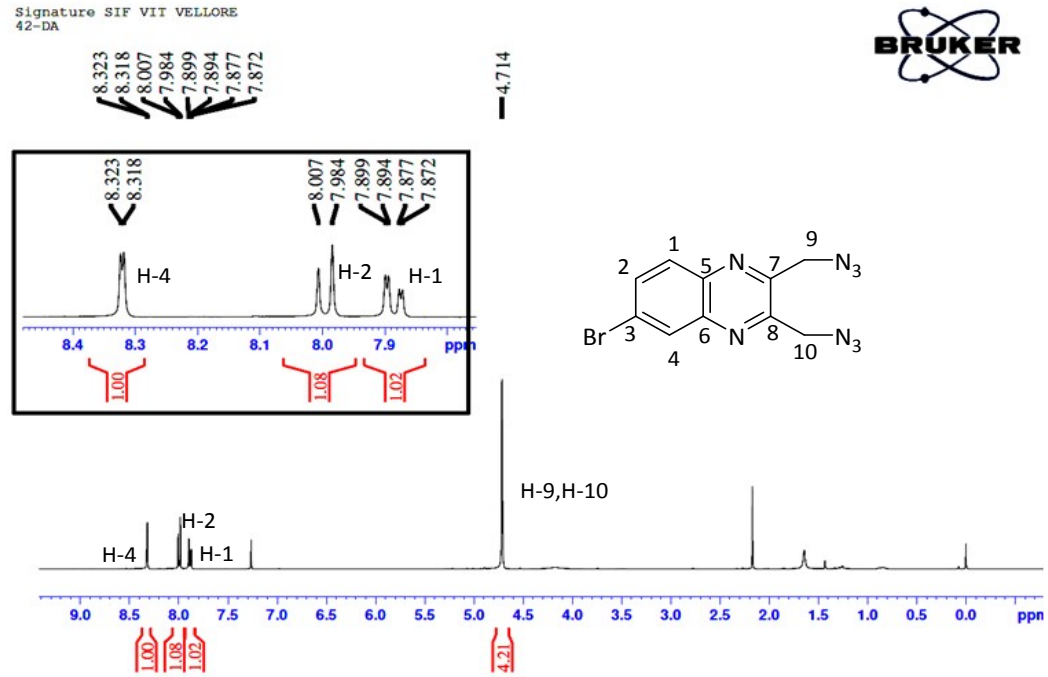

^{13}C NMR of compound 4b

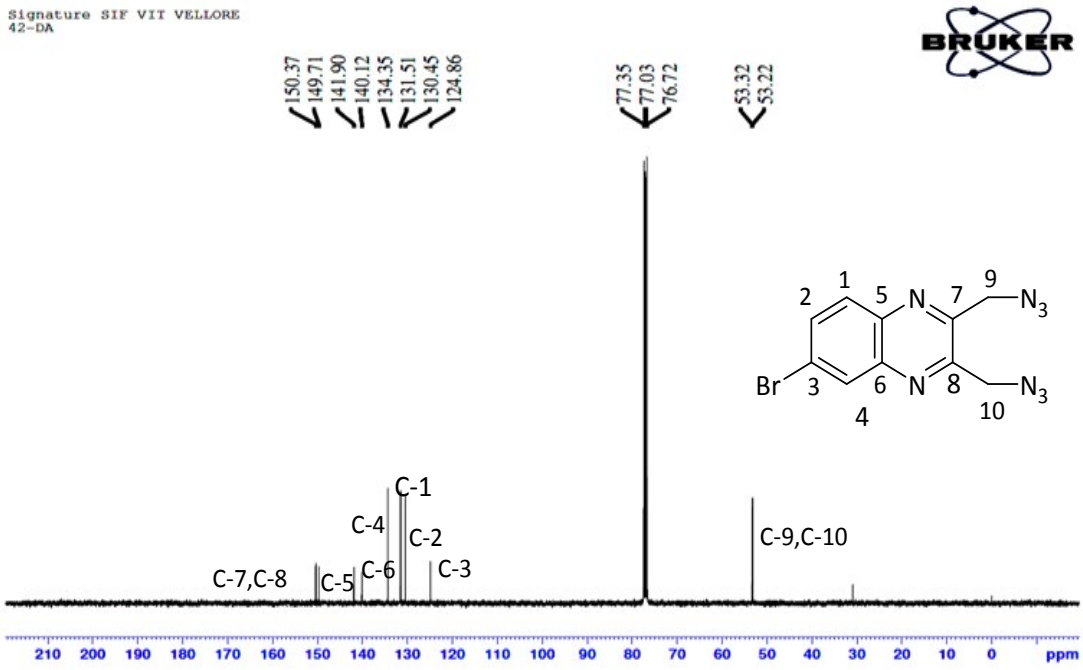

IR spectra of compound 4b

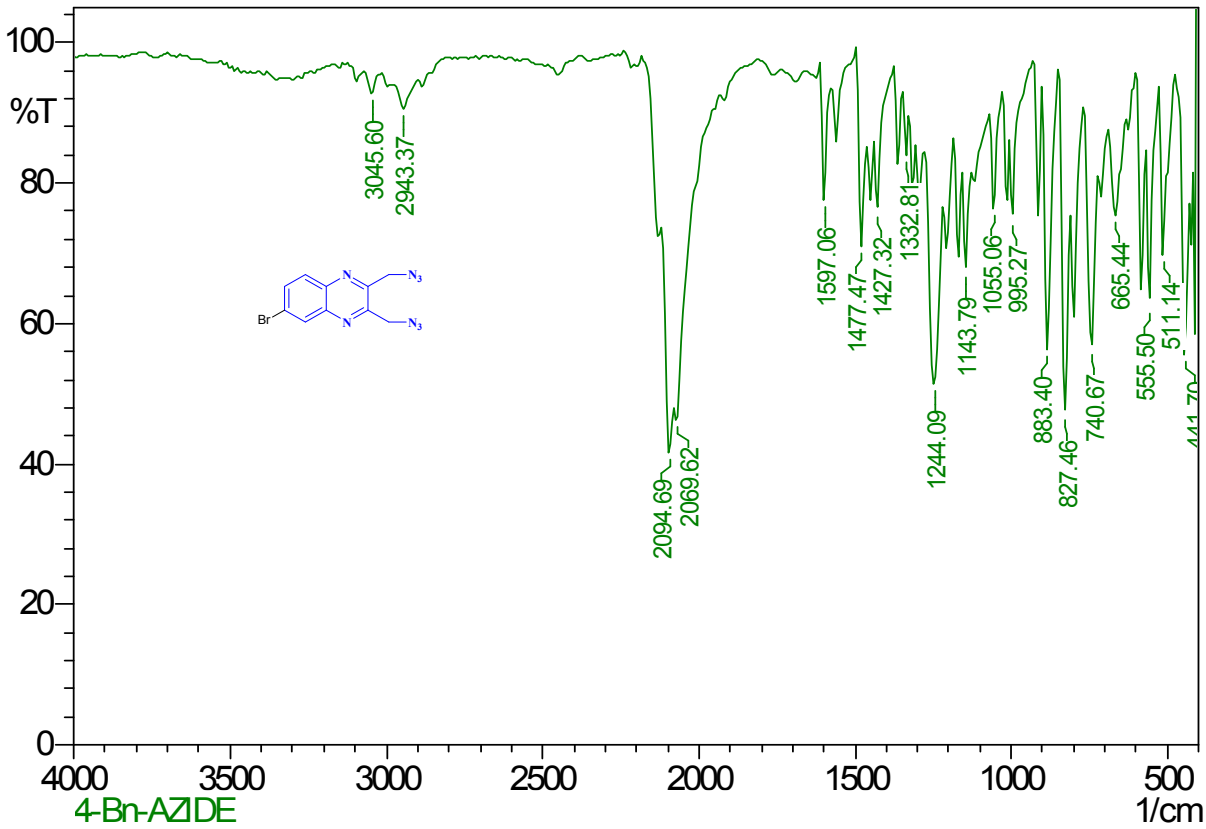

LCMS of compound 4b

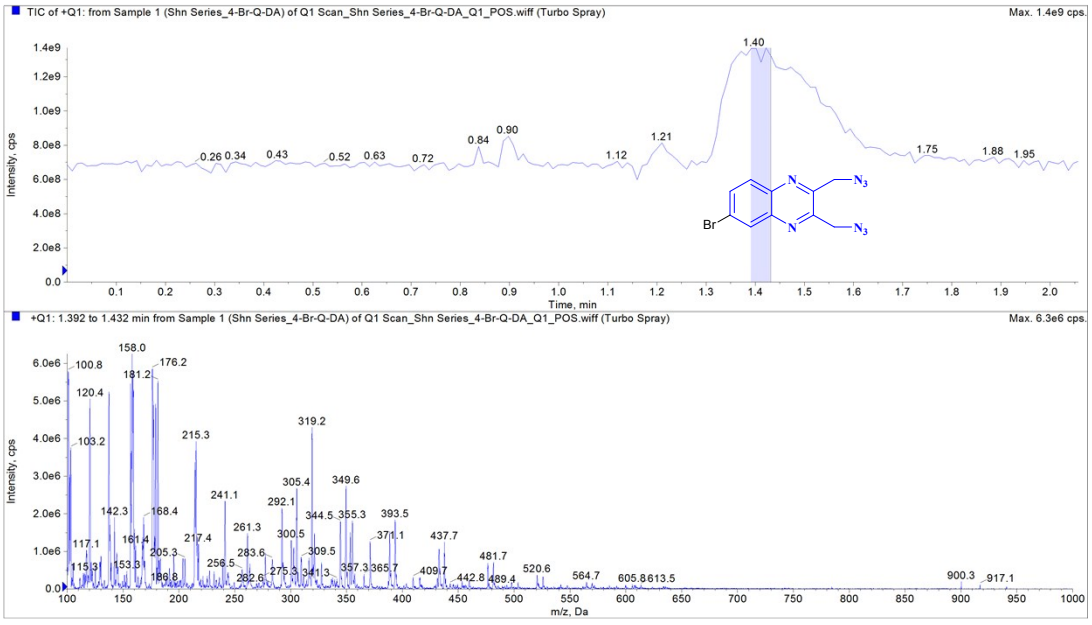

^{1}H NMR of compound 6a

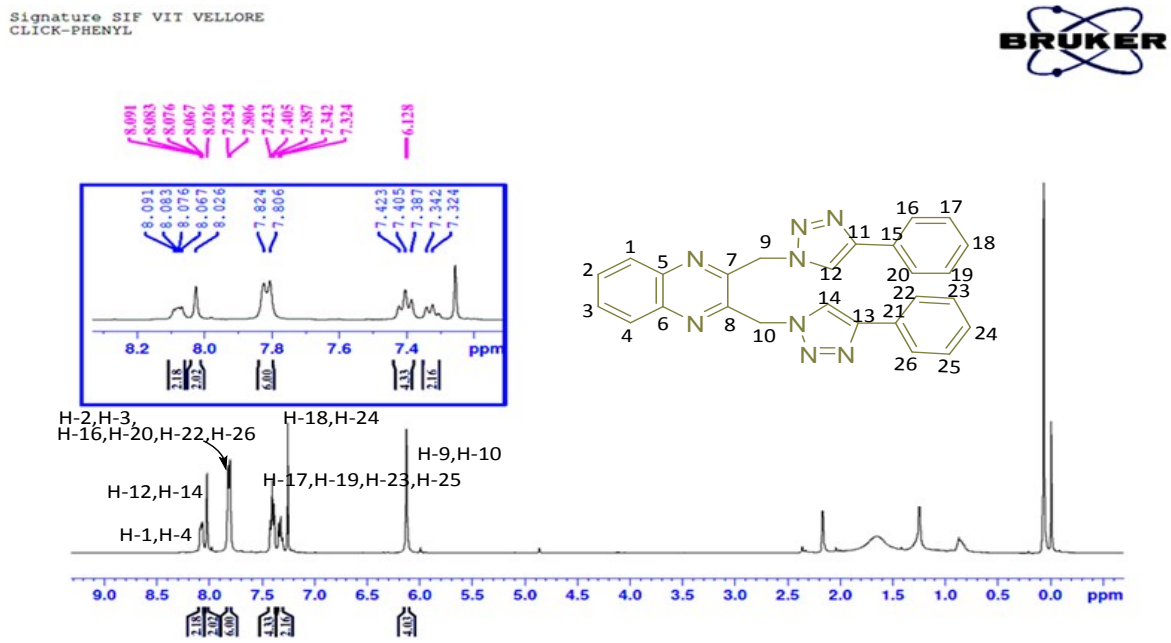

^{13}C NMR of compound 6a

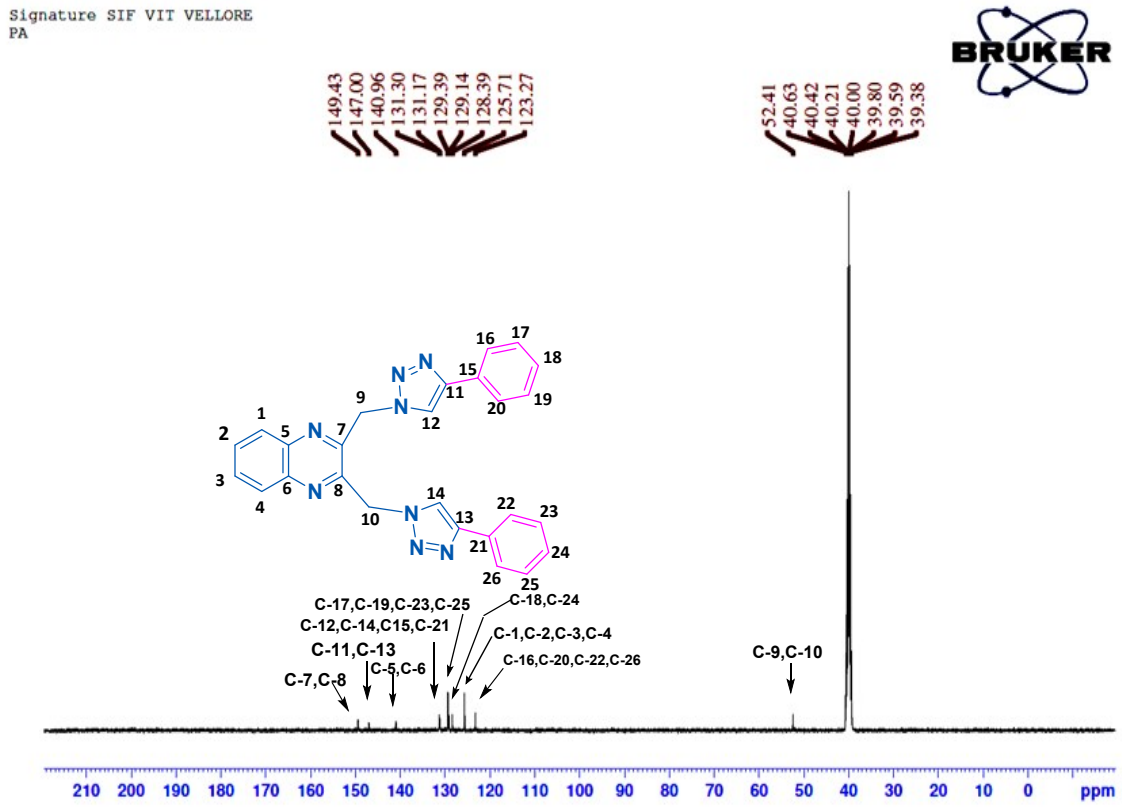

IR spectra of compound 6a

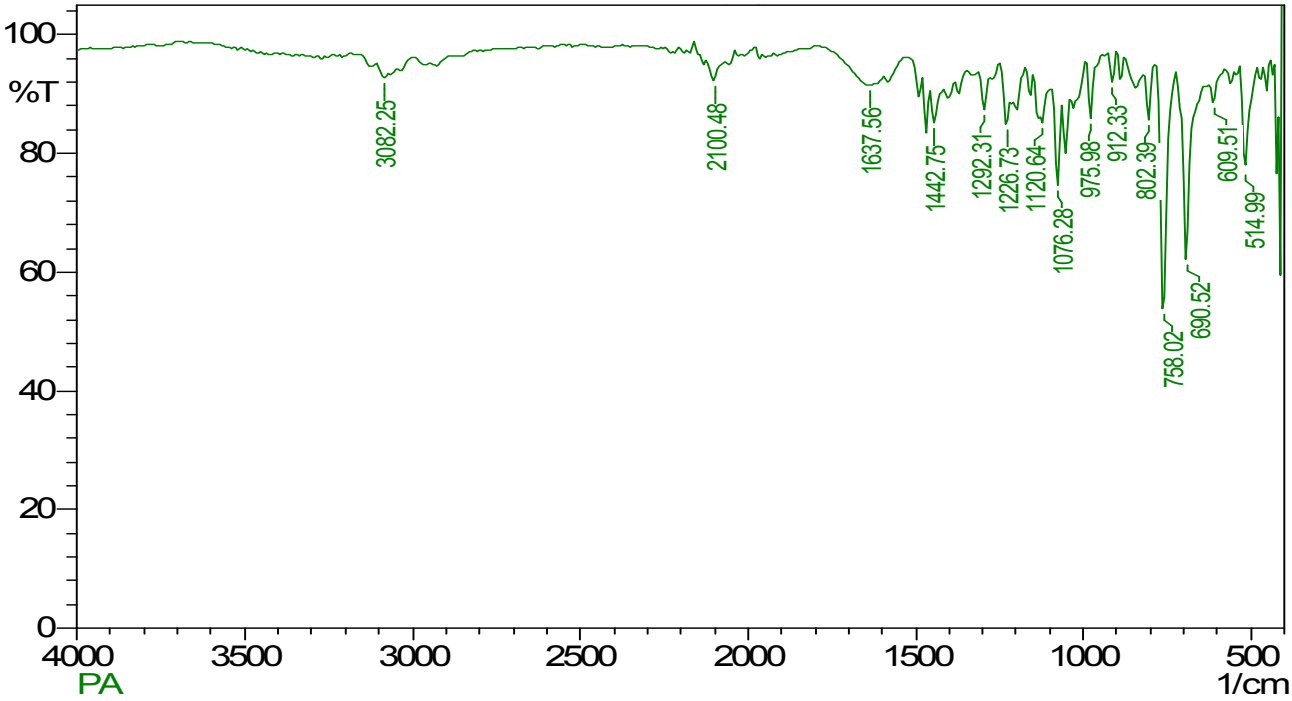

LCMS of compound 6a

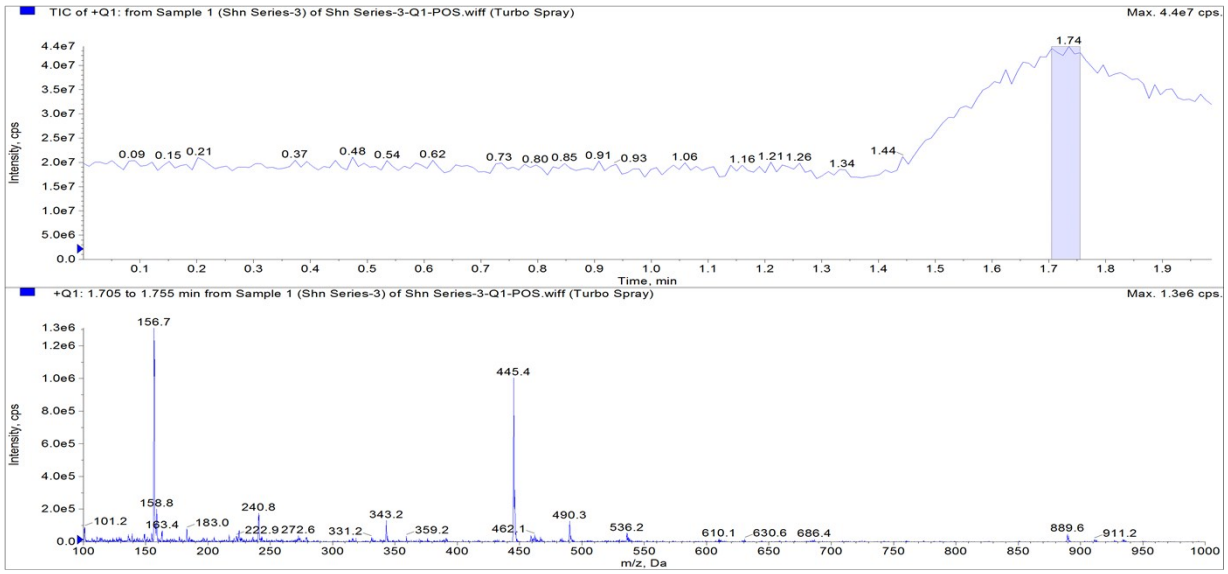

[1]H NMR of compound 6b

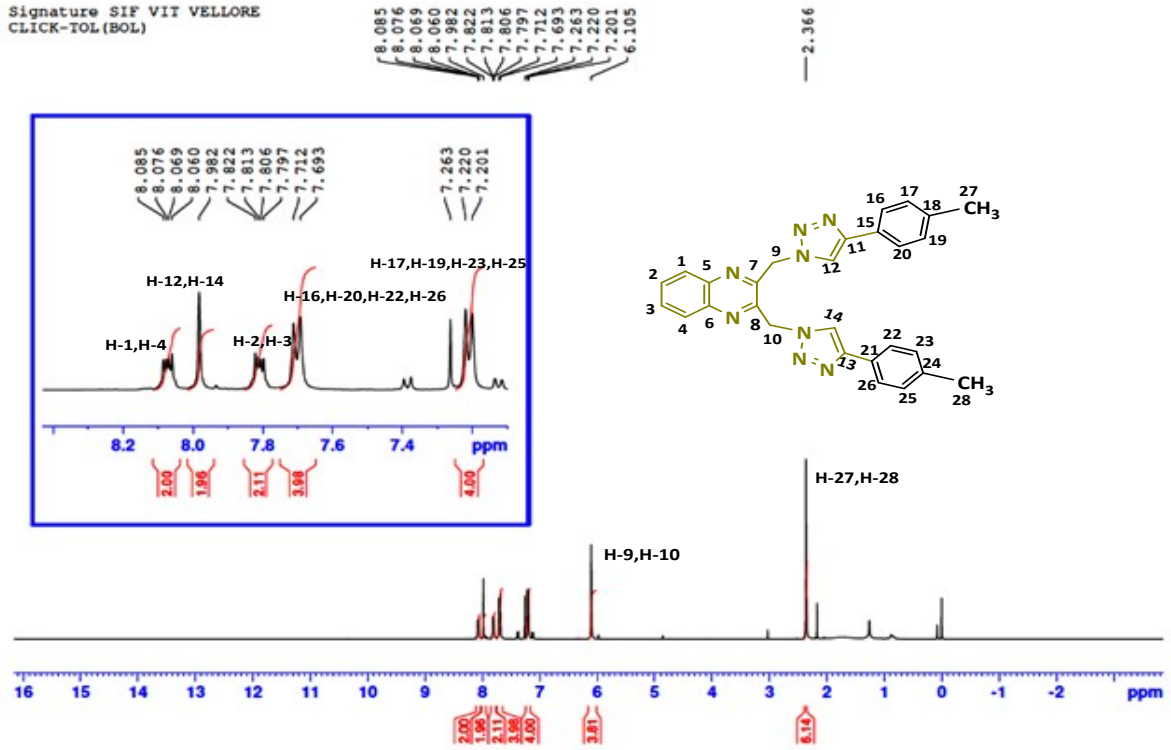

^{13}C NMR of compound 6b

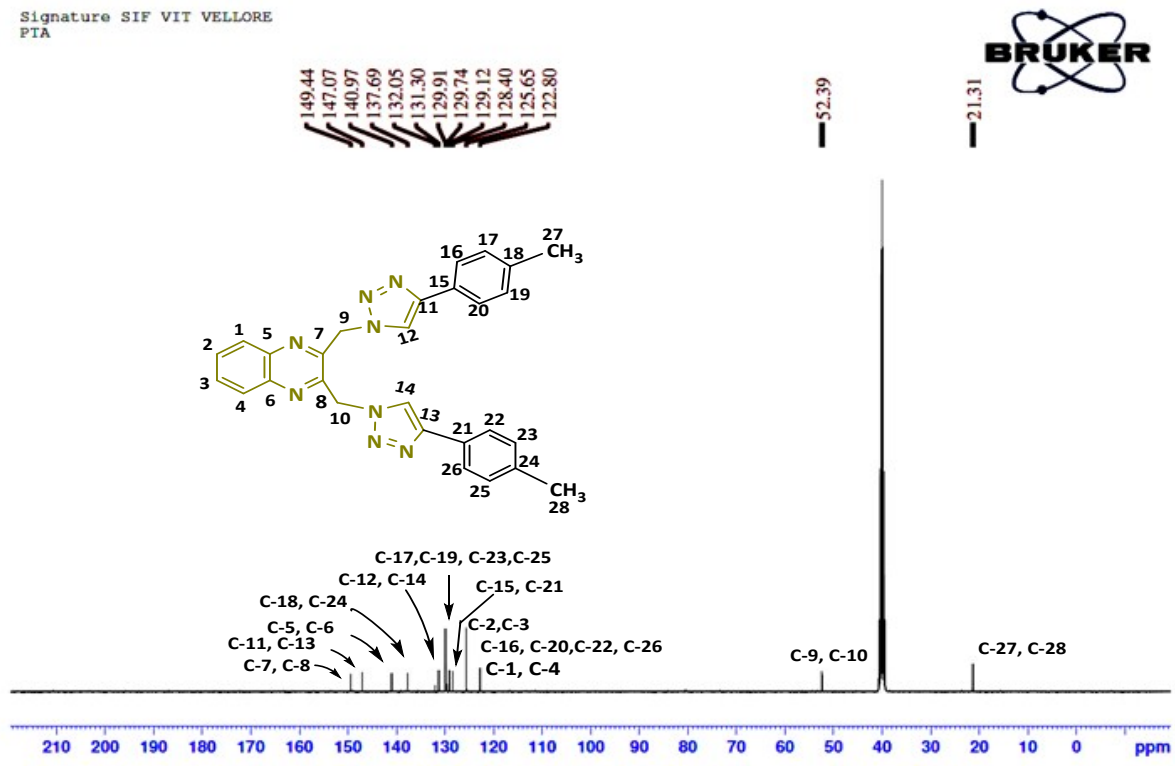

IR spectra of compound 6b

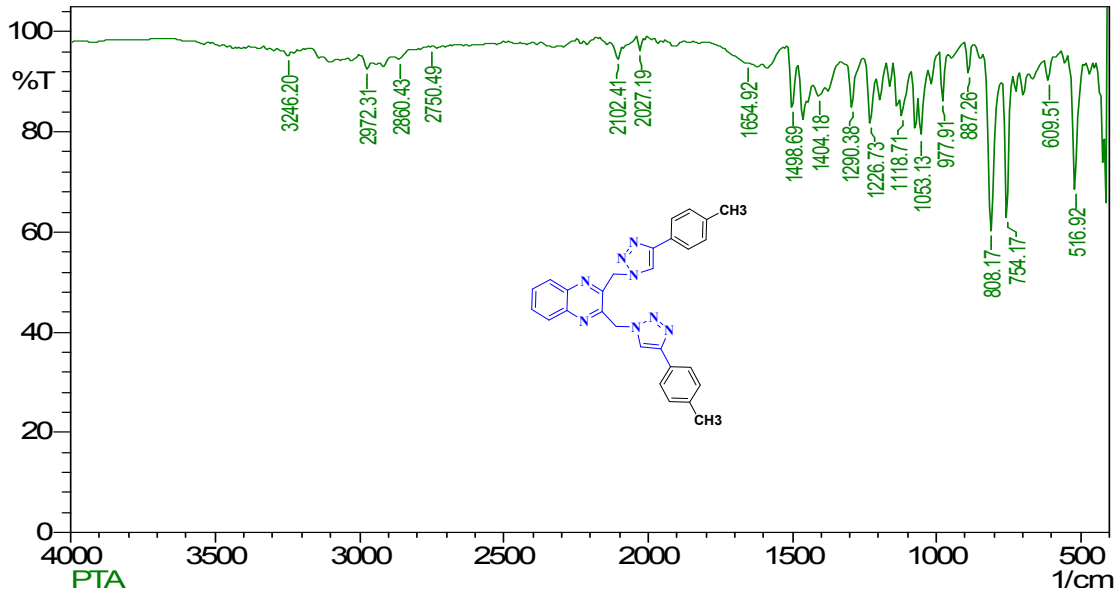

LCMS of compound 6b

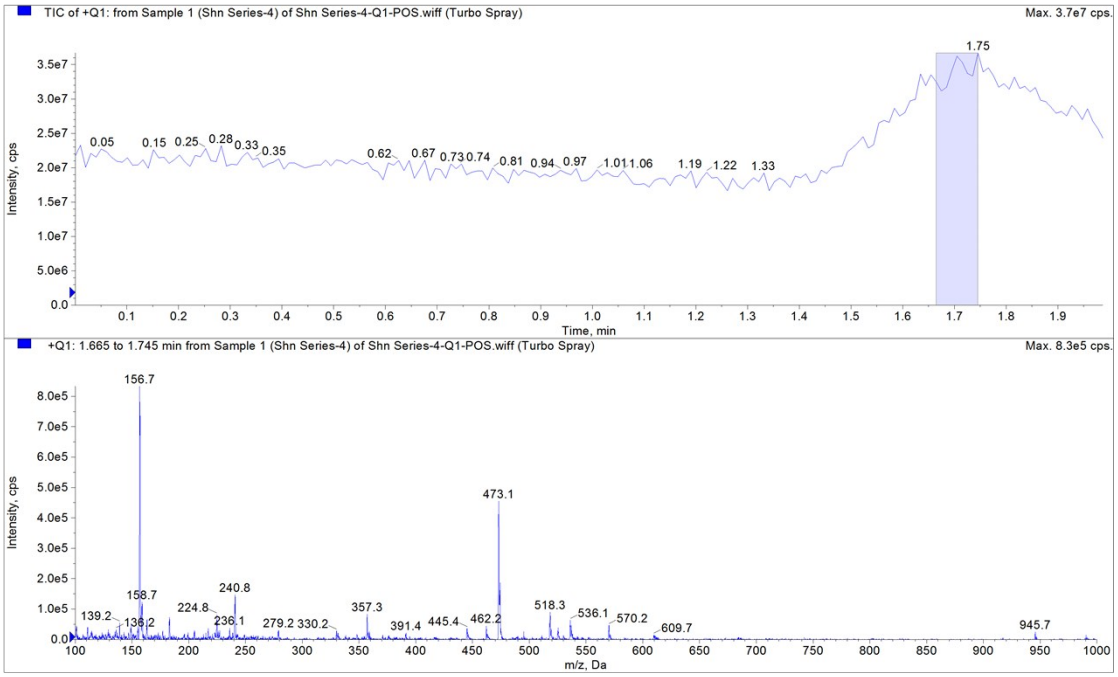

^{1}H NMR of compound 6c

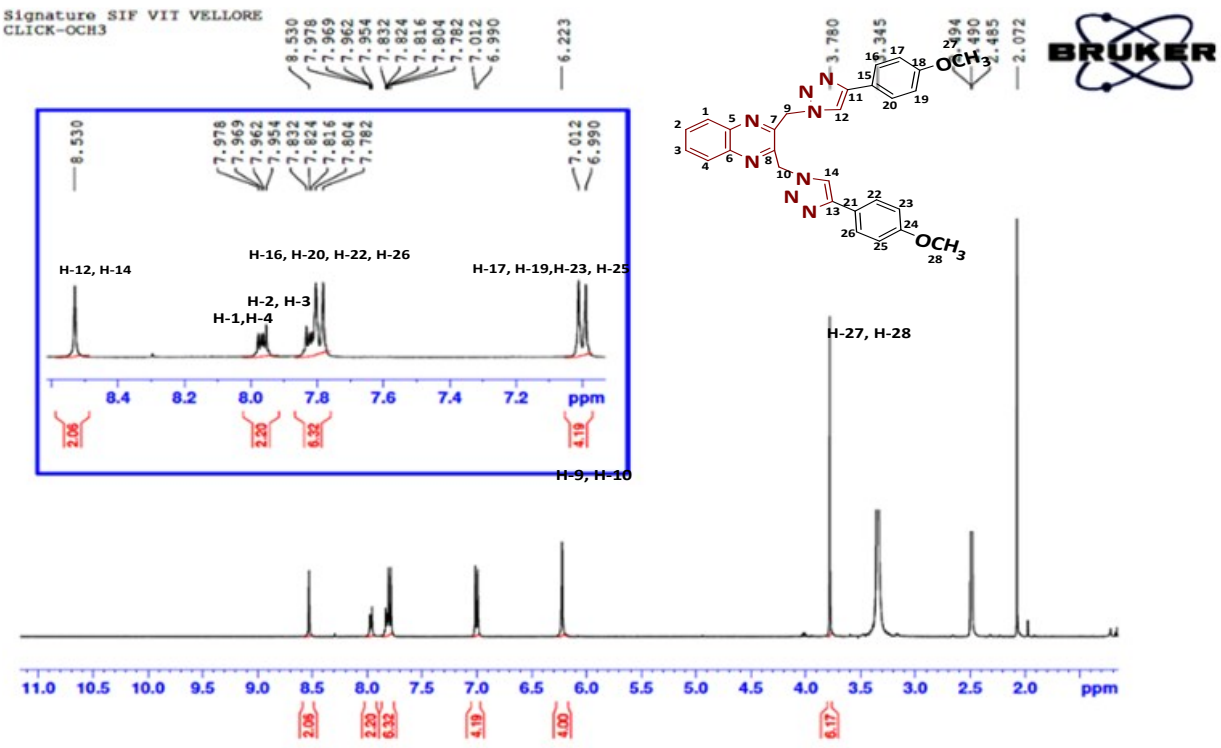

^{13}C NMR of compound 6c

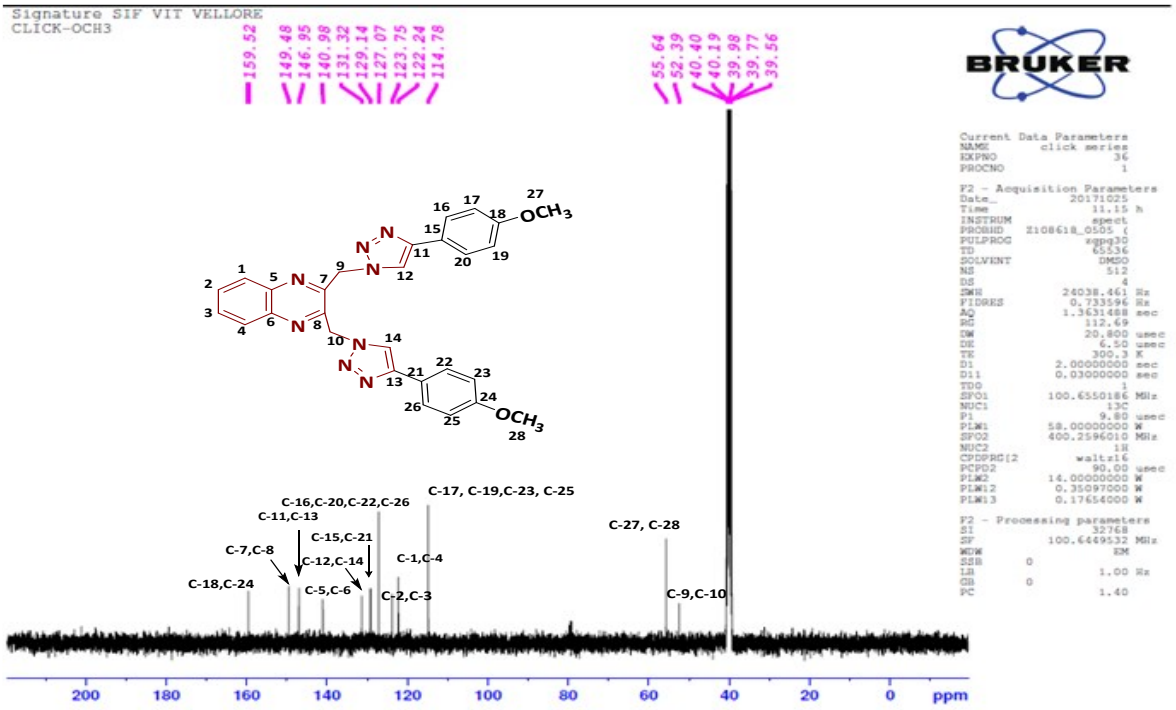

IR spectra of compound 6c

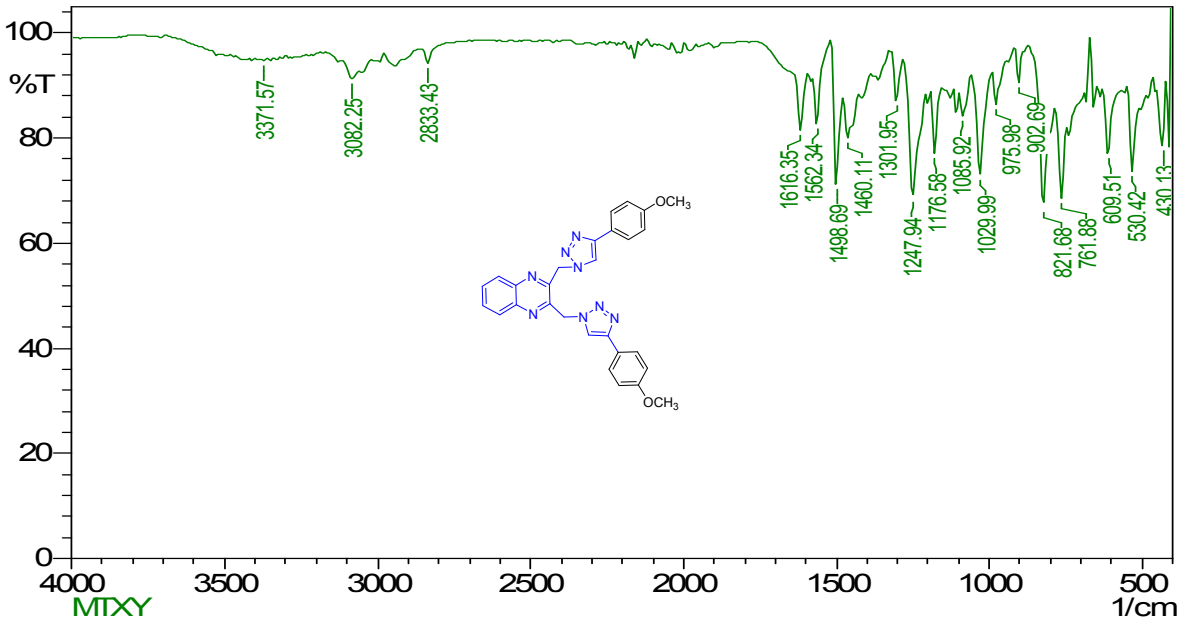

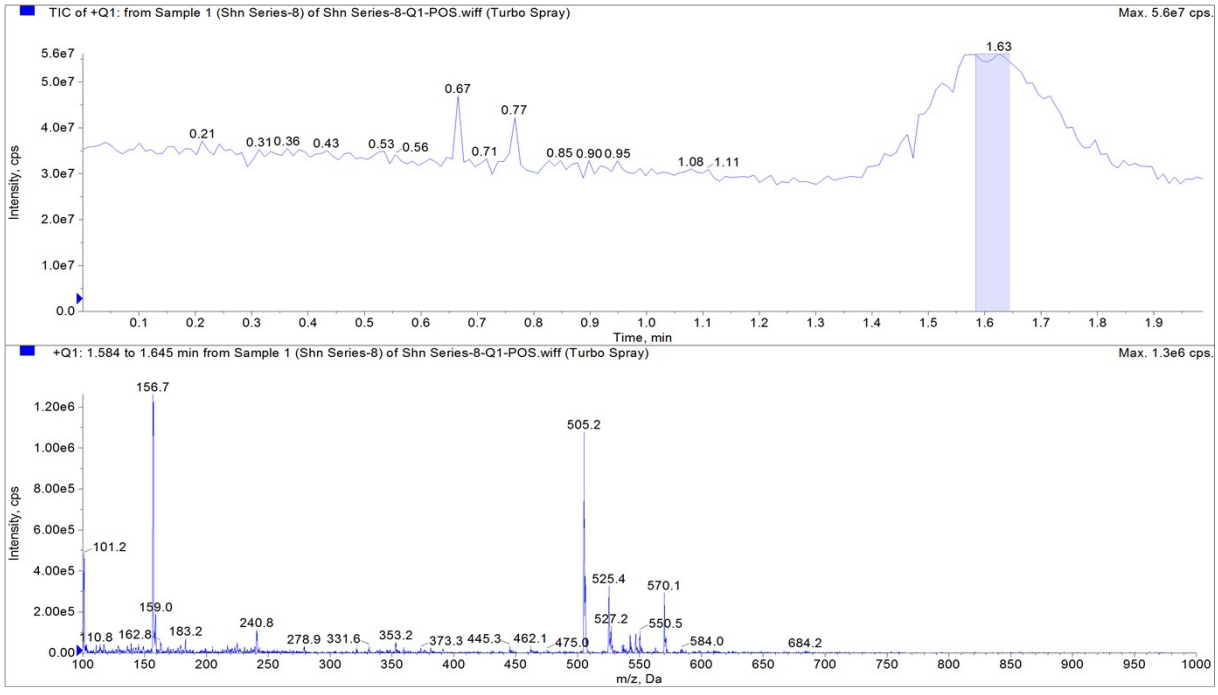

LCMS of compound 6c

^{1}H NMR of compound 6d

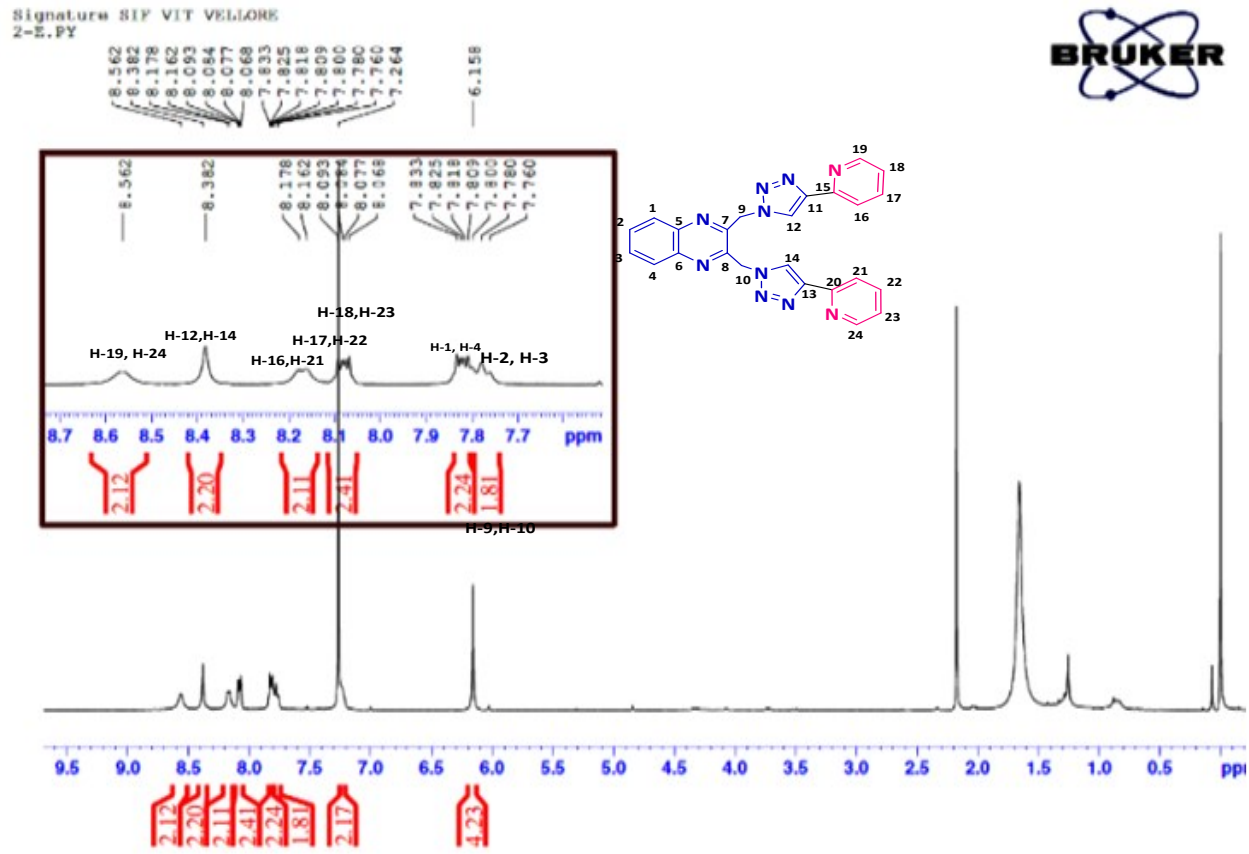

IR spectra of compound 6d

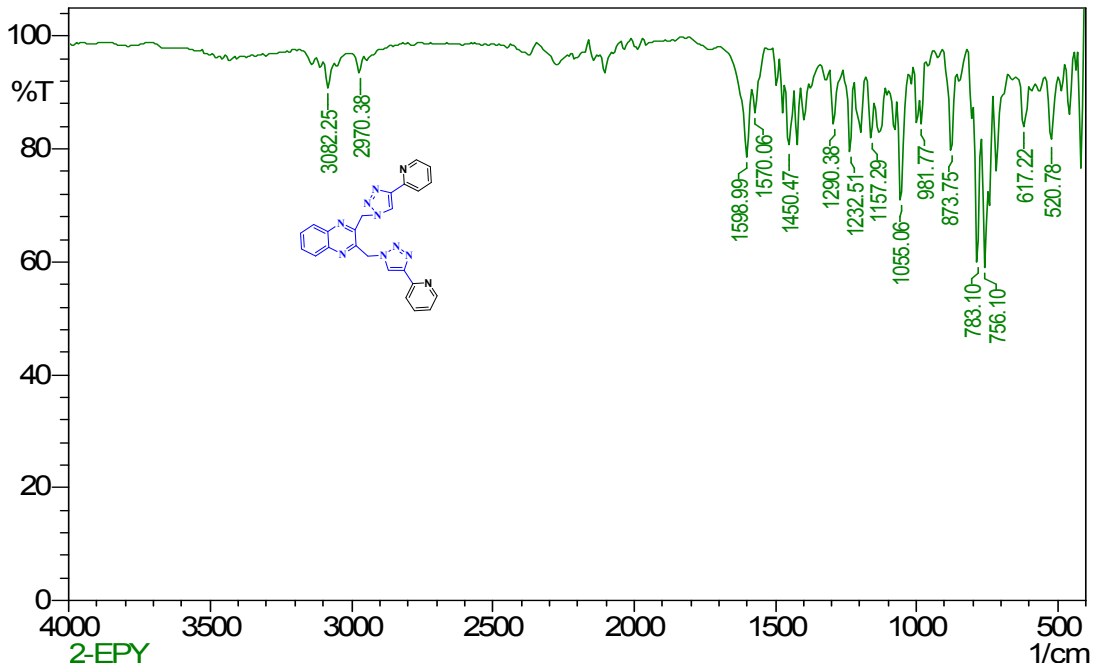

LCMS of compound 6d

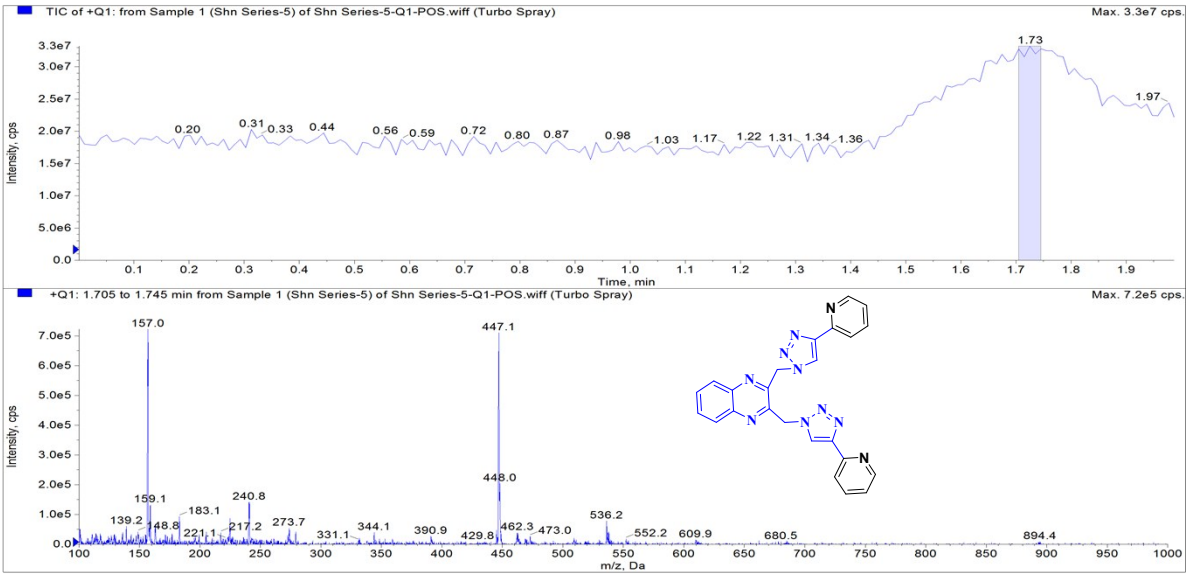

^{1}H NMR of compound 6e

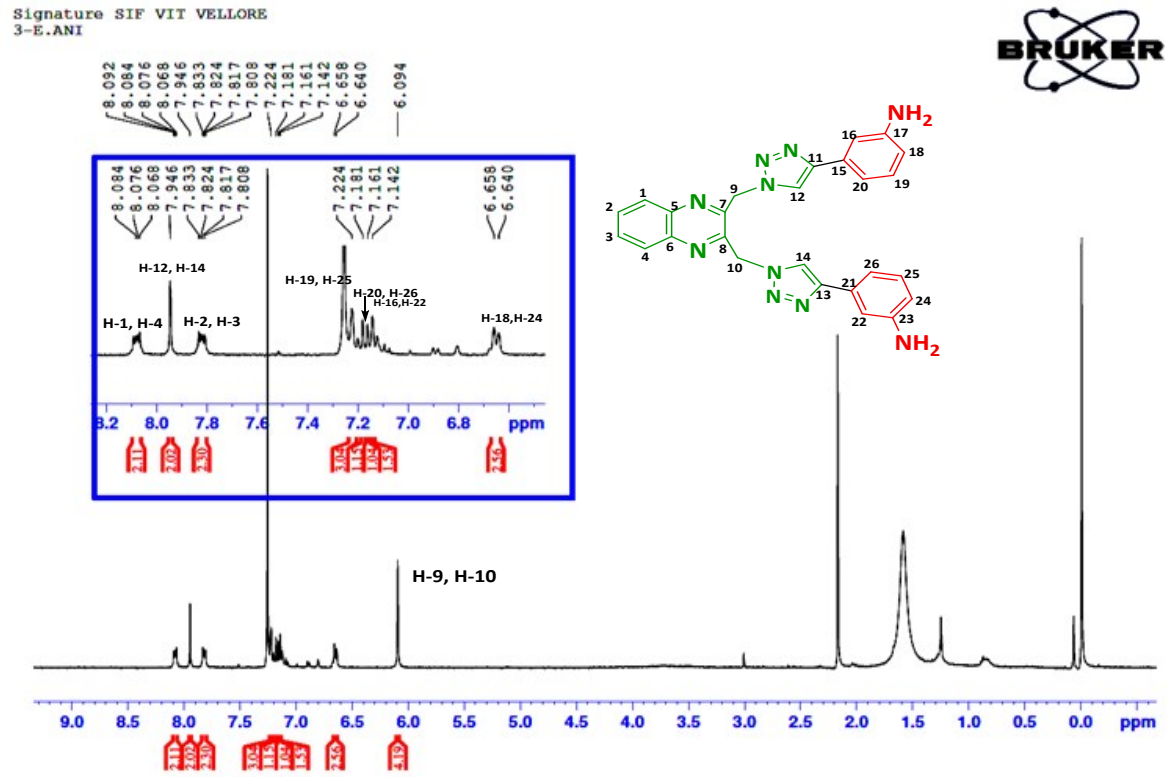

^{13}C NMR of compound 6e

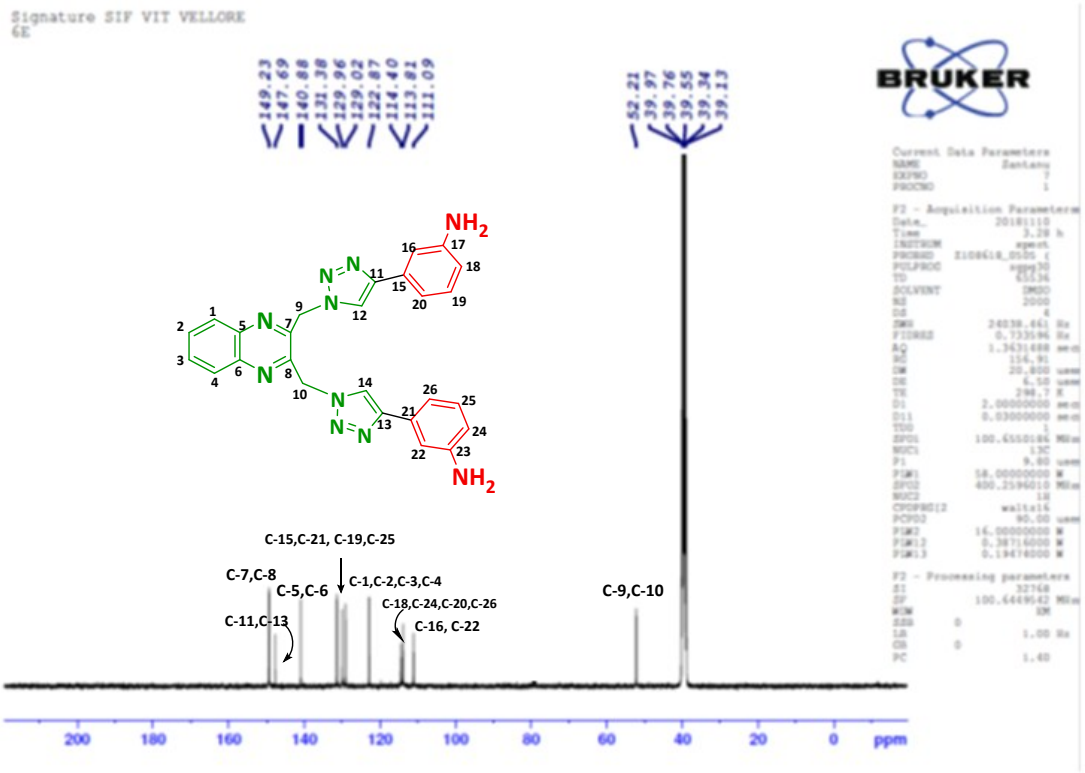

IR spectra of compound 6e

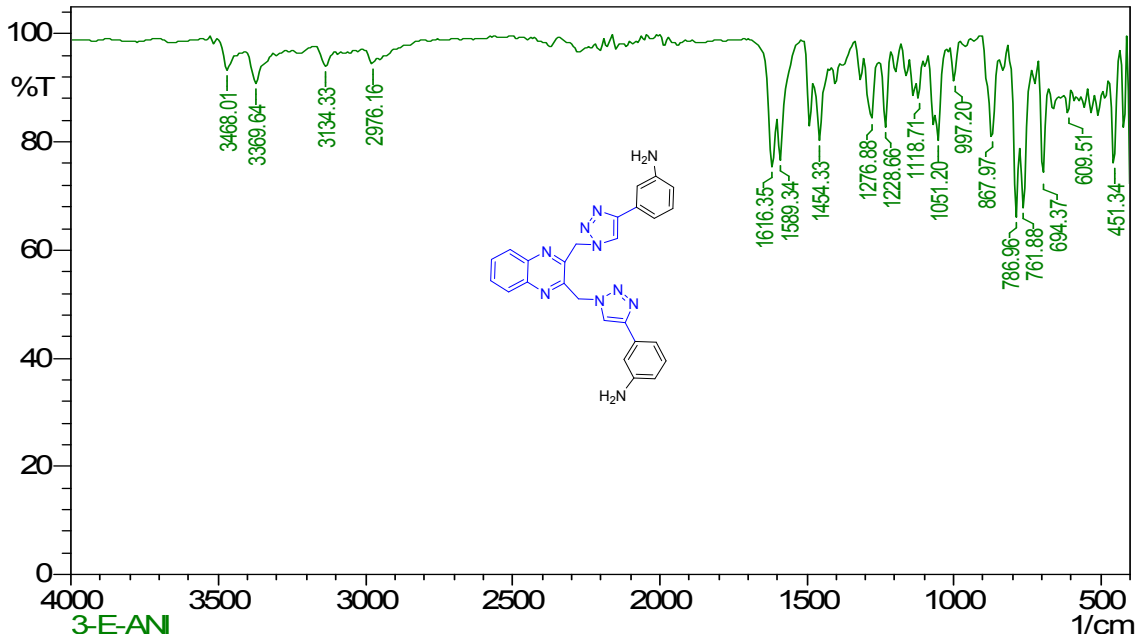

LCMS of compound 6e

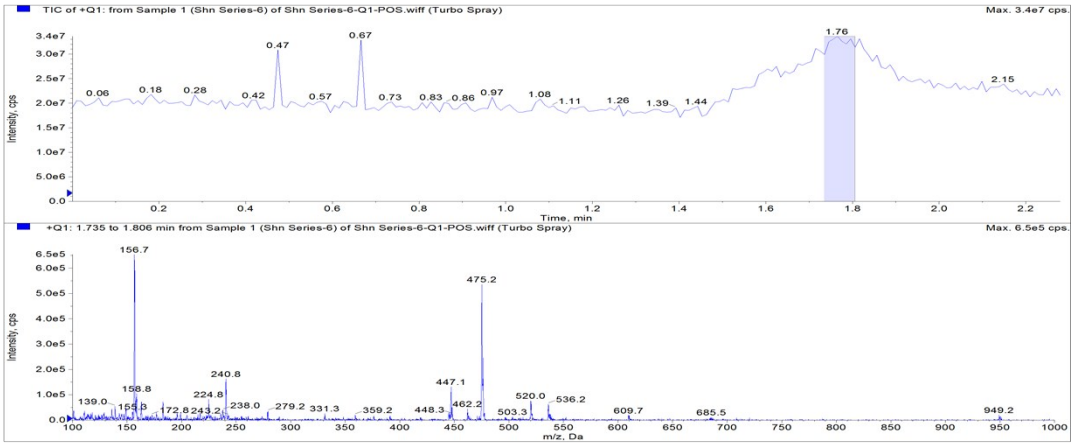

^{1}H NMR of compound 6f

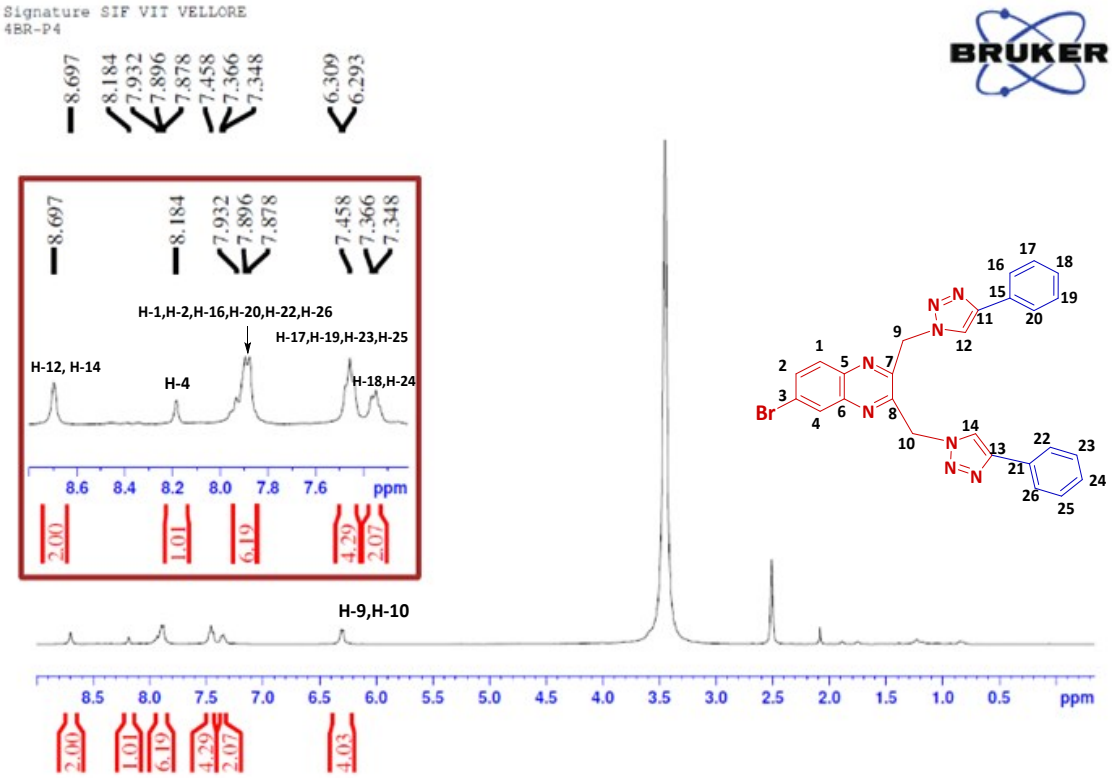

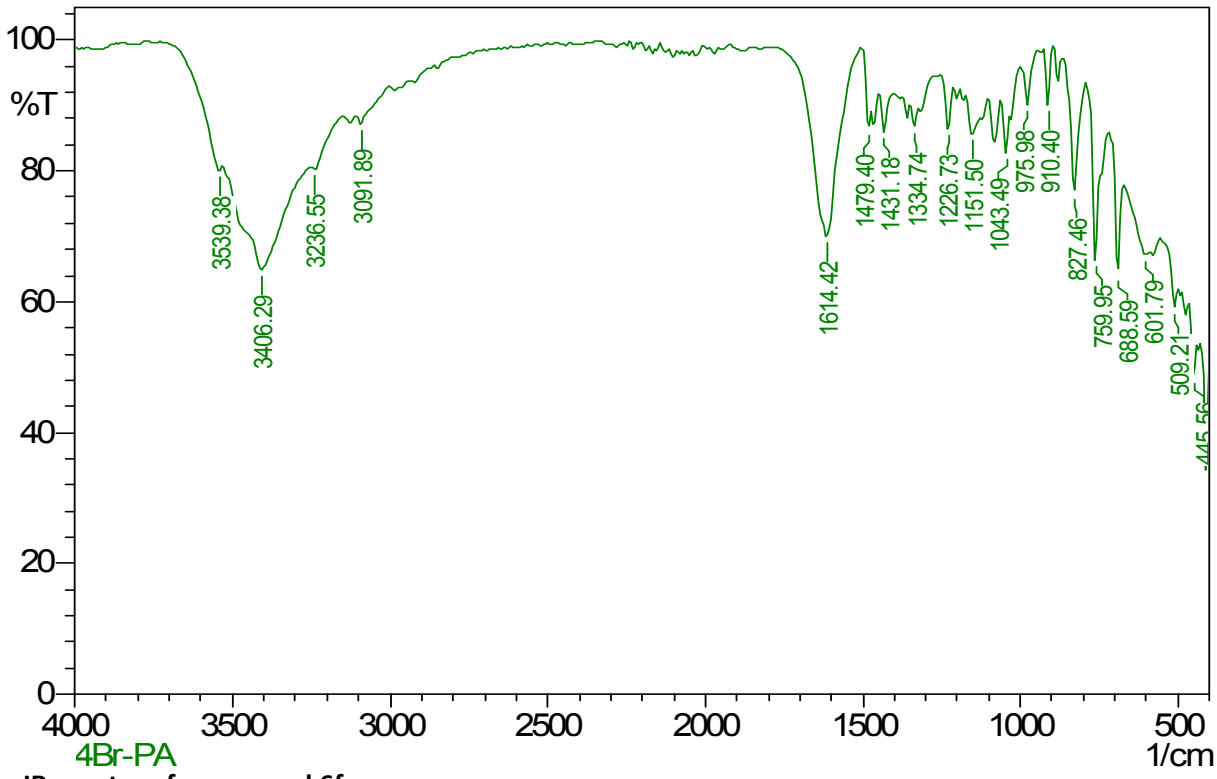

IR spectra of compound 6f

LCMS of compound 6f

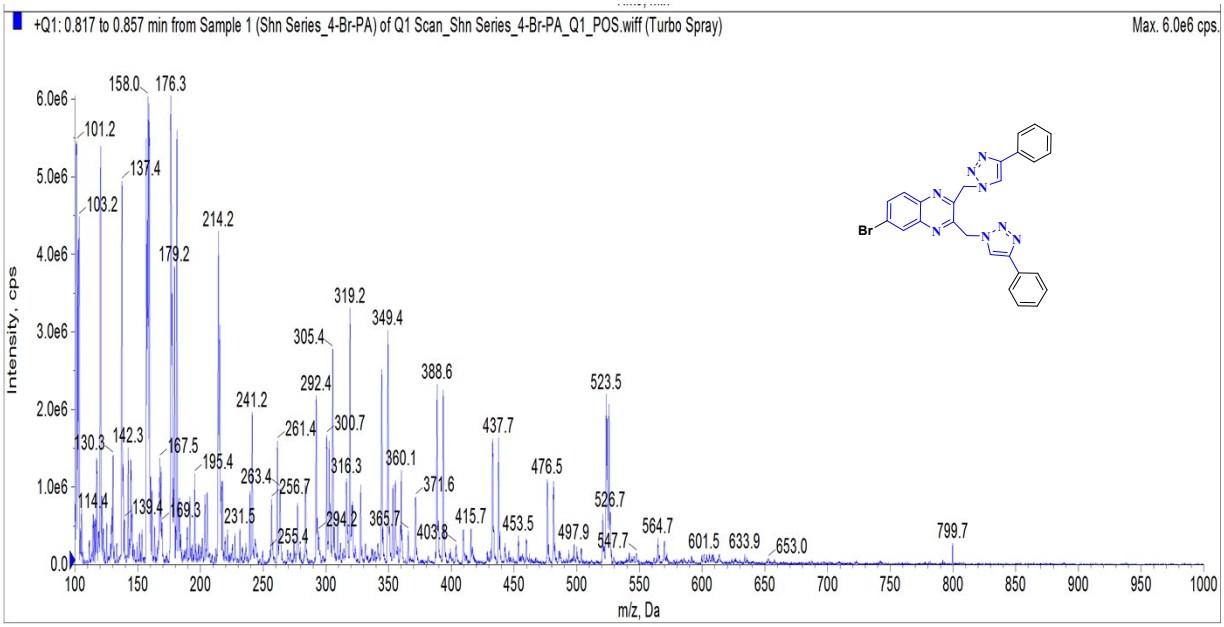

^{1}H NMR of compound 6g

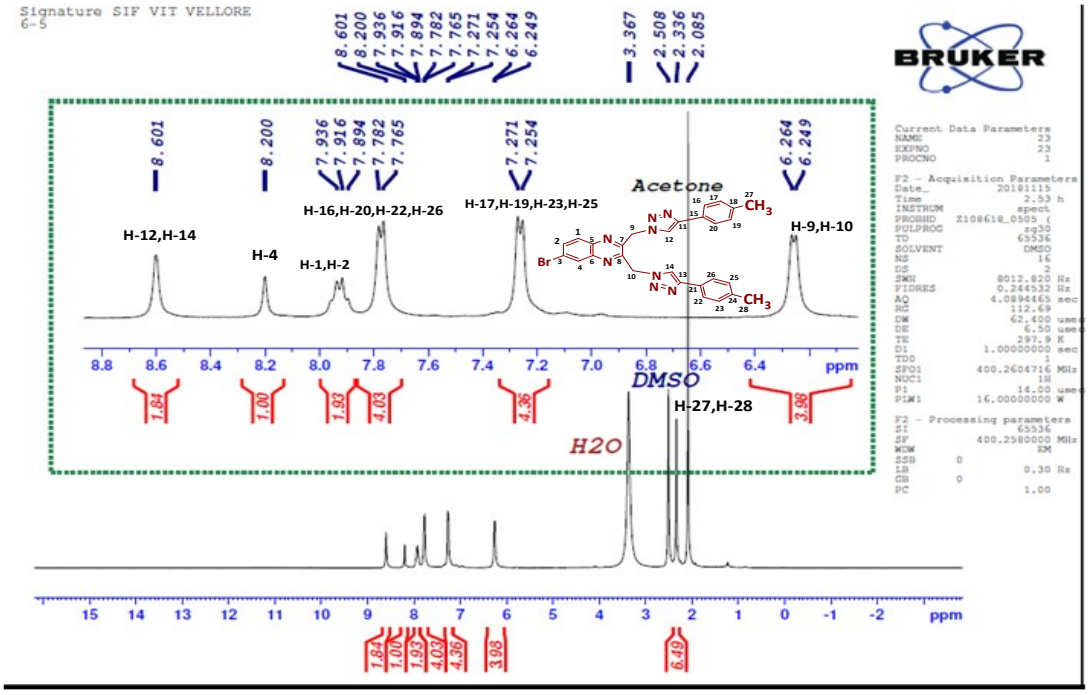

^{13}C NMR of compound 6g

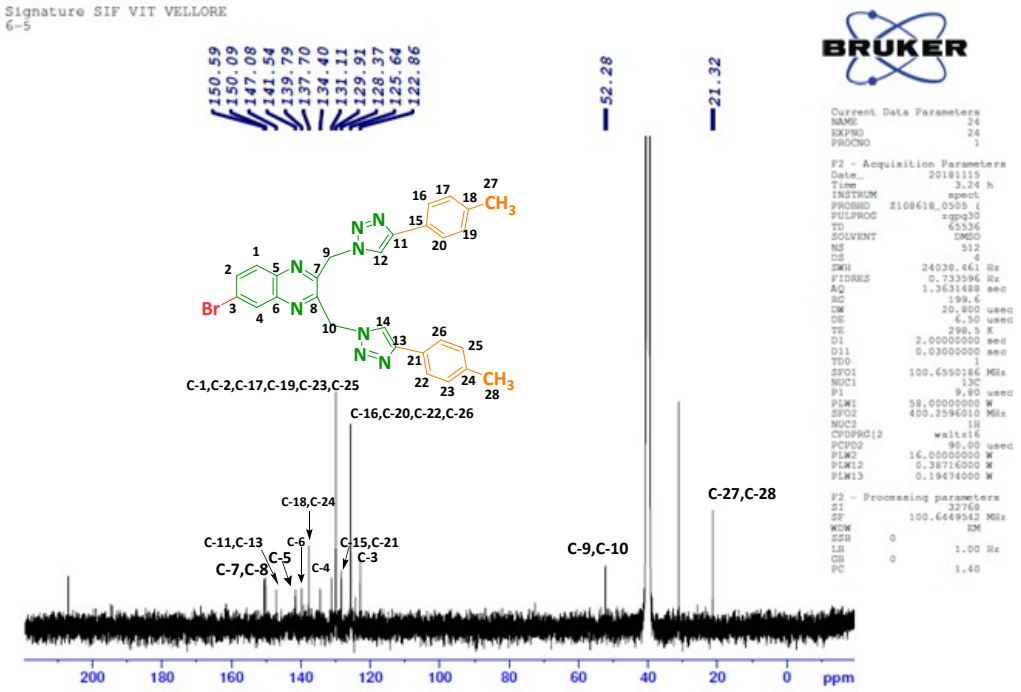

IR spectra of compound 6g

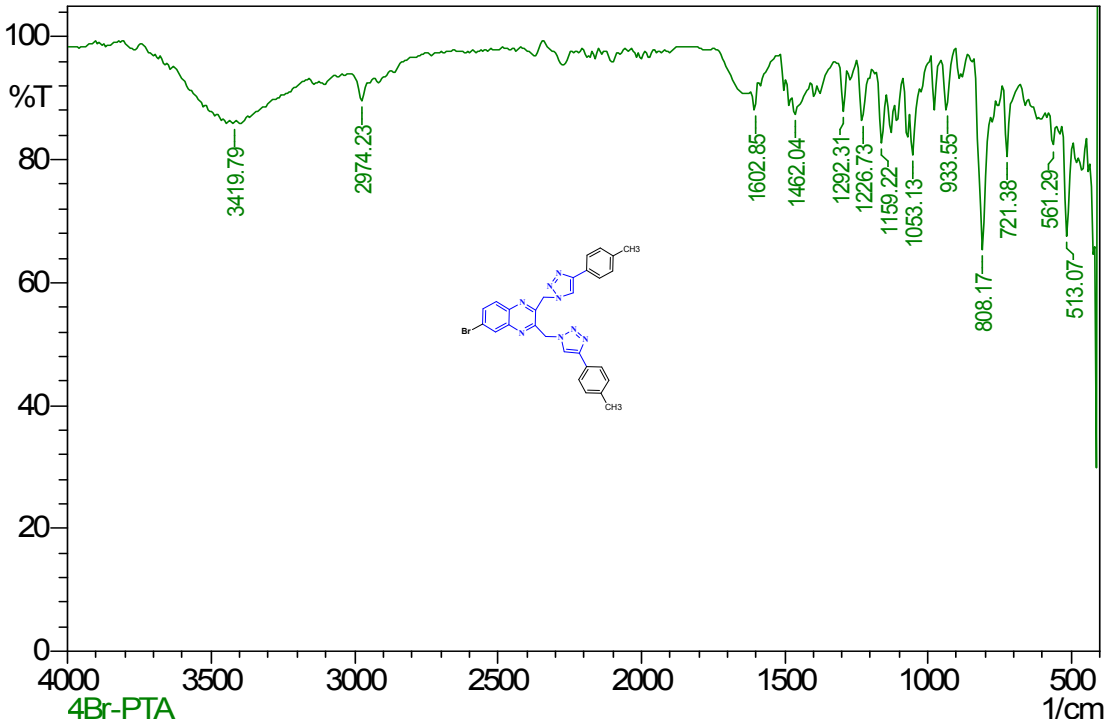

LCMS of compond 6g

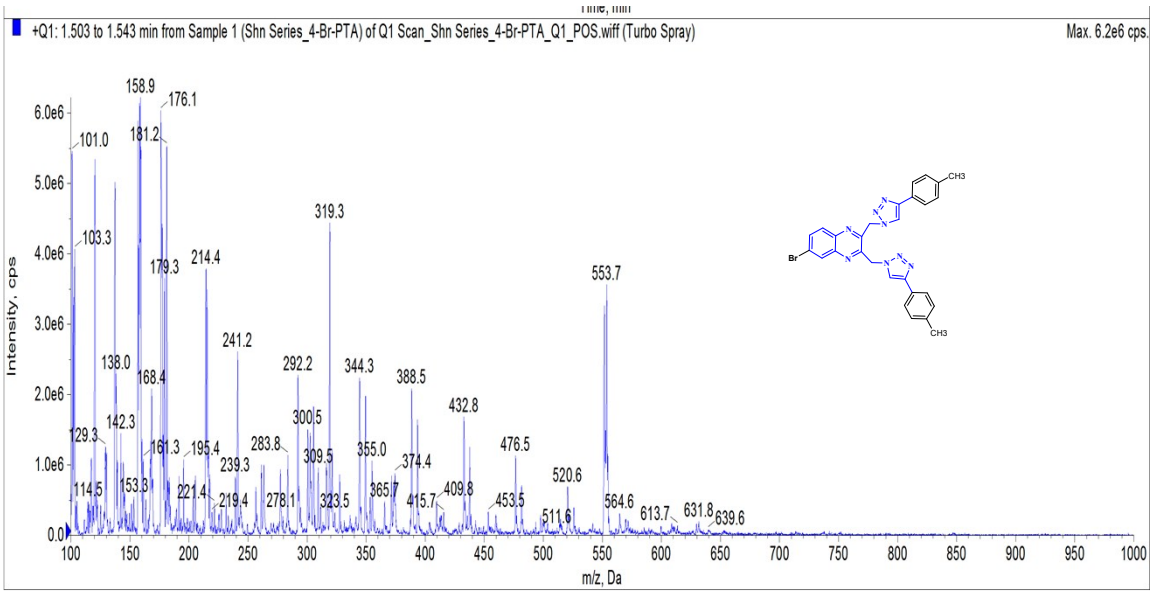

^{1}H NMR of compound 6h

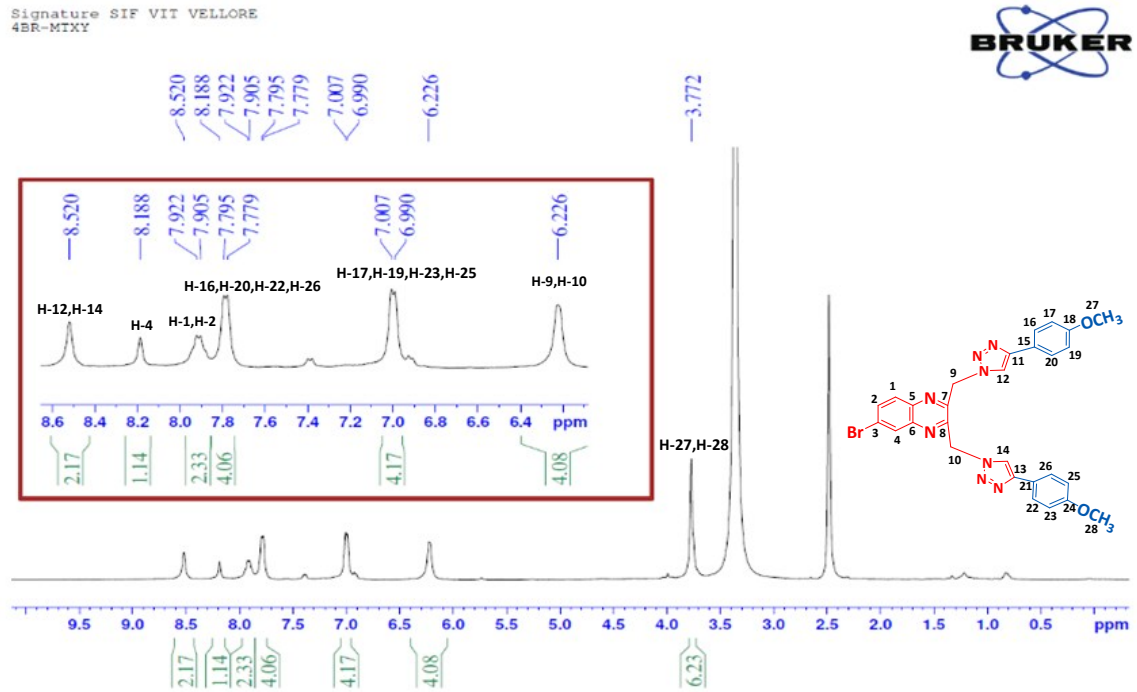

IR spectra of compound 6h

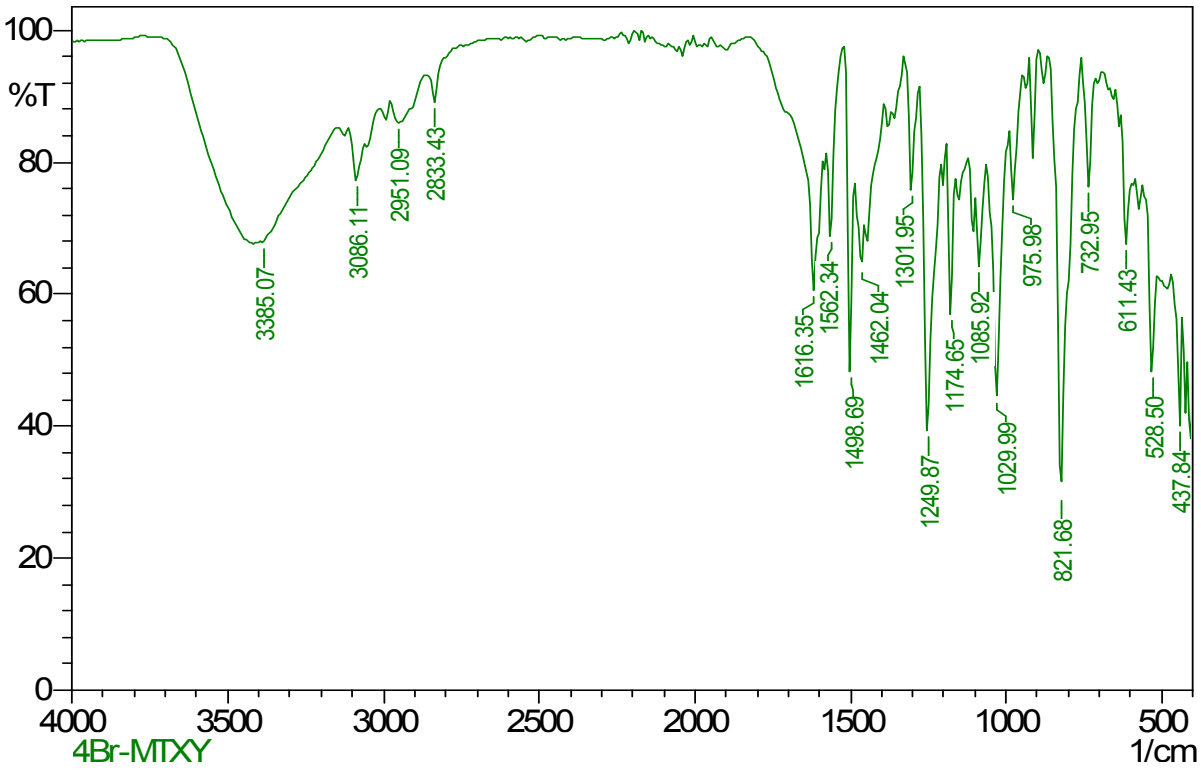

^{1}H NMR of compound 6i

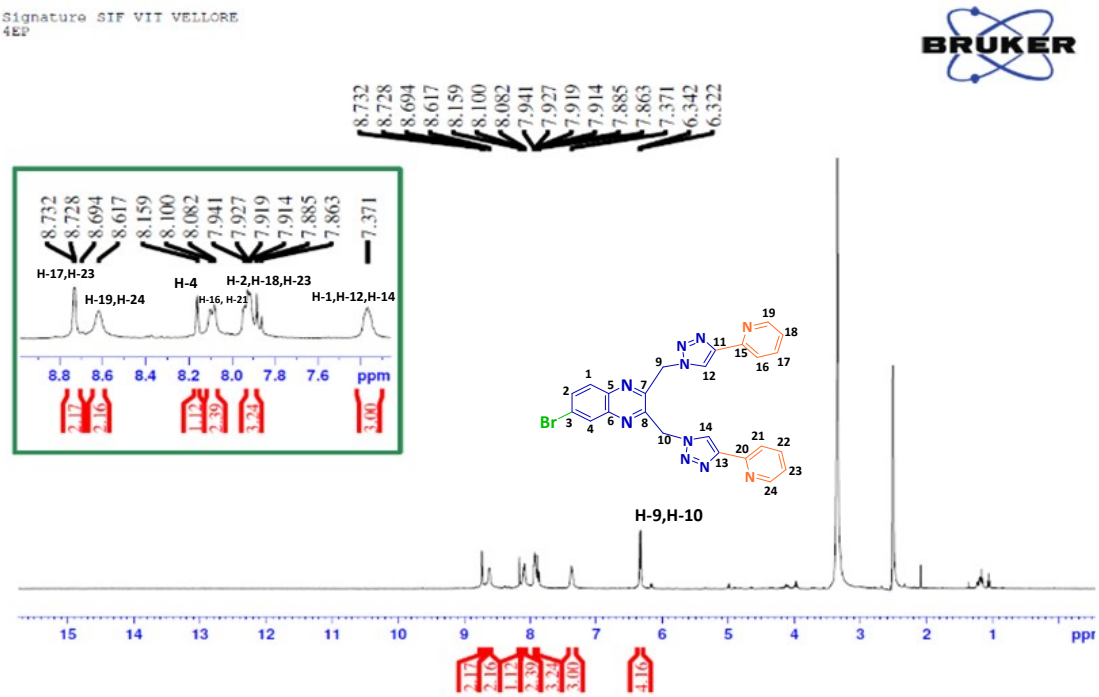

IR spectra of compound 6i

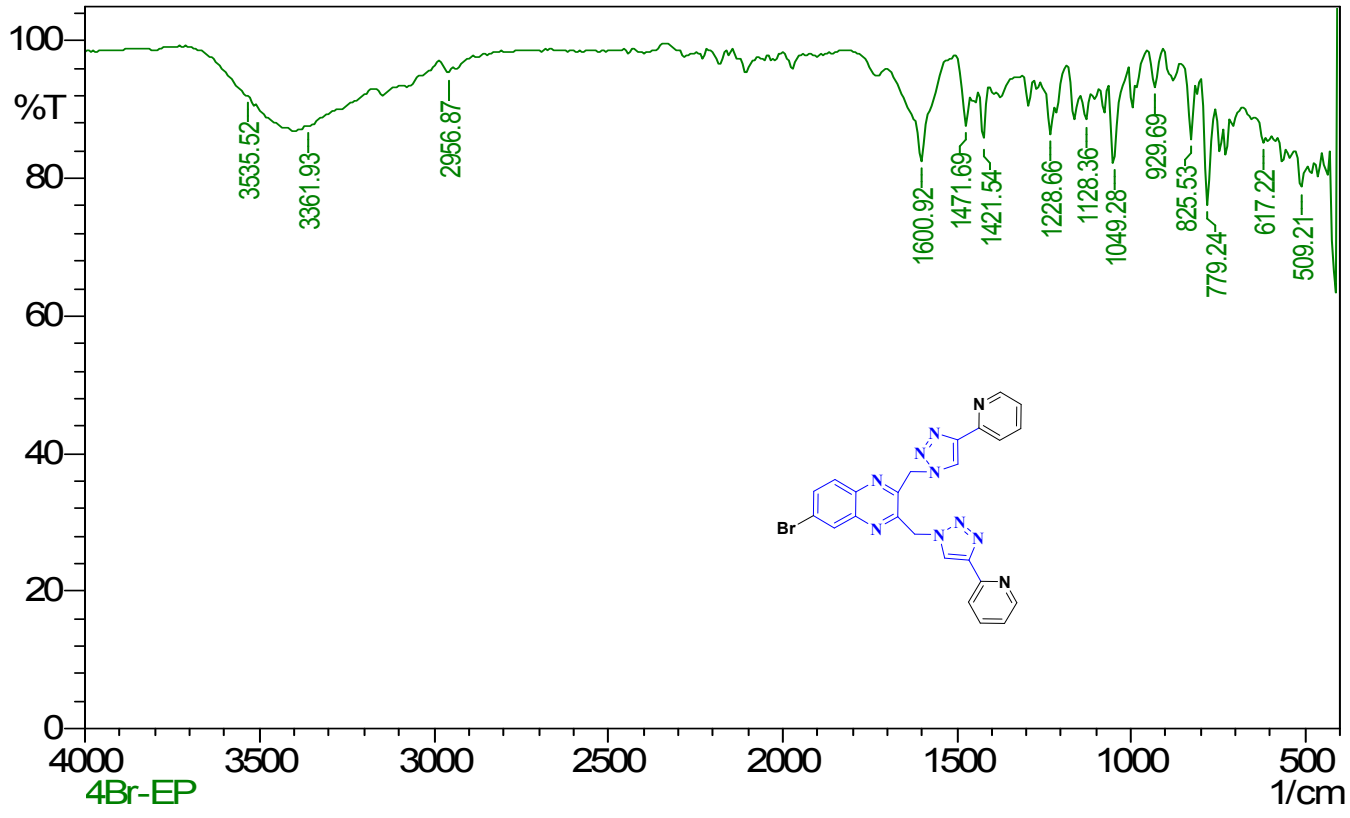

LCMS of compound 6i

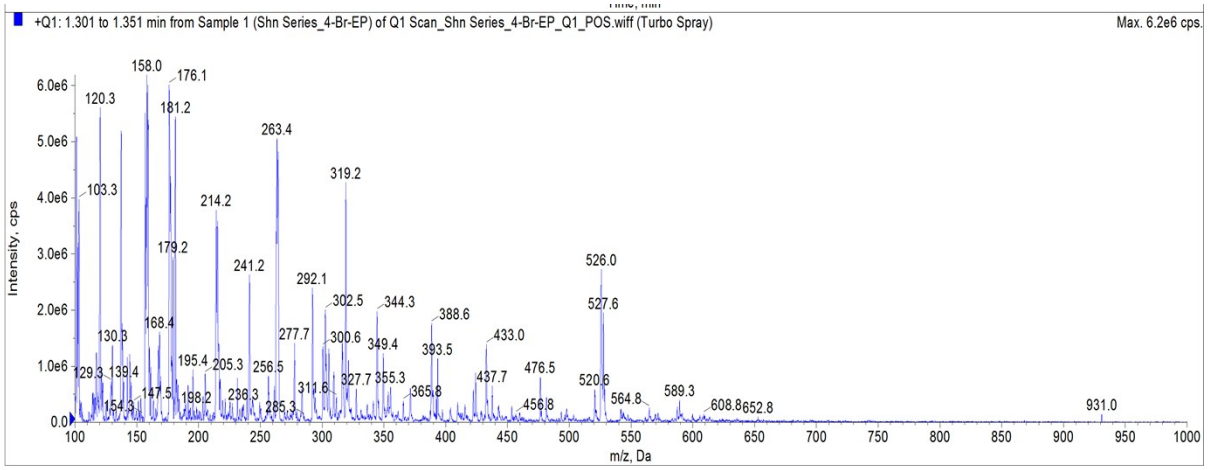

^{1}H NMR of compound 8

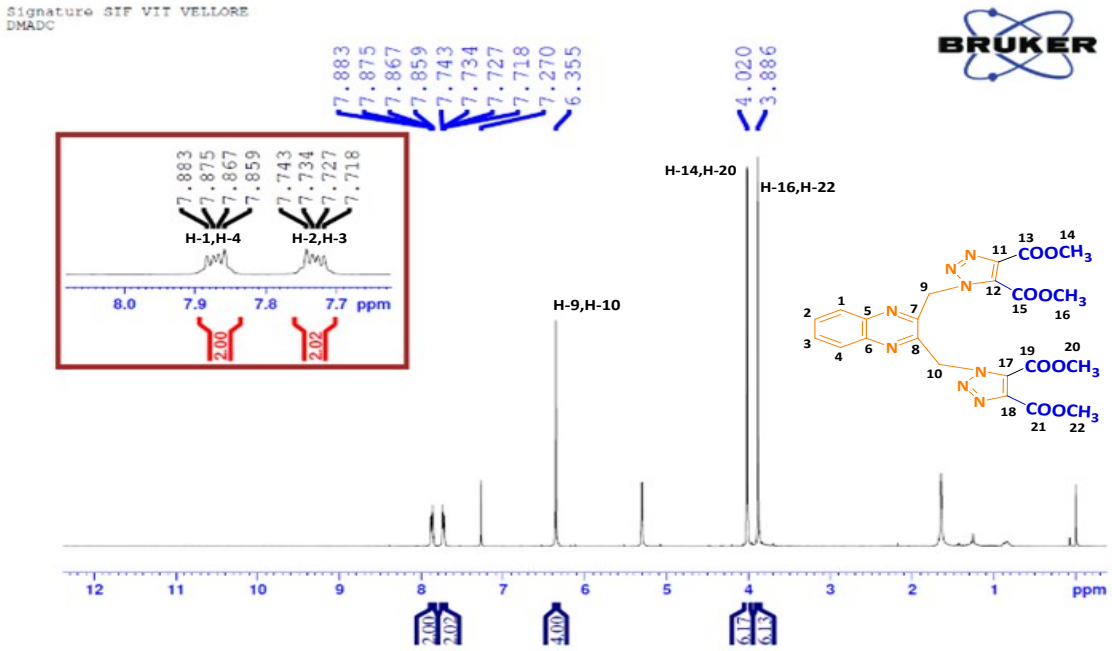

^{13}C NMR of compound 8

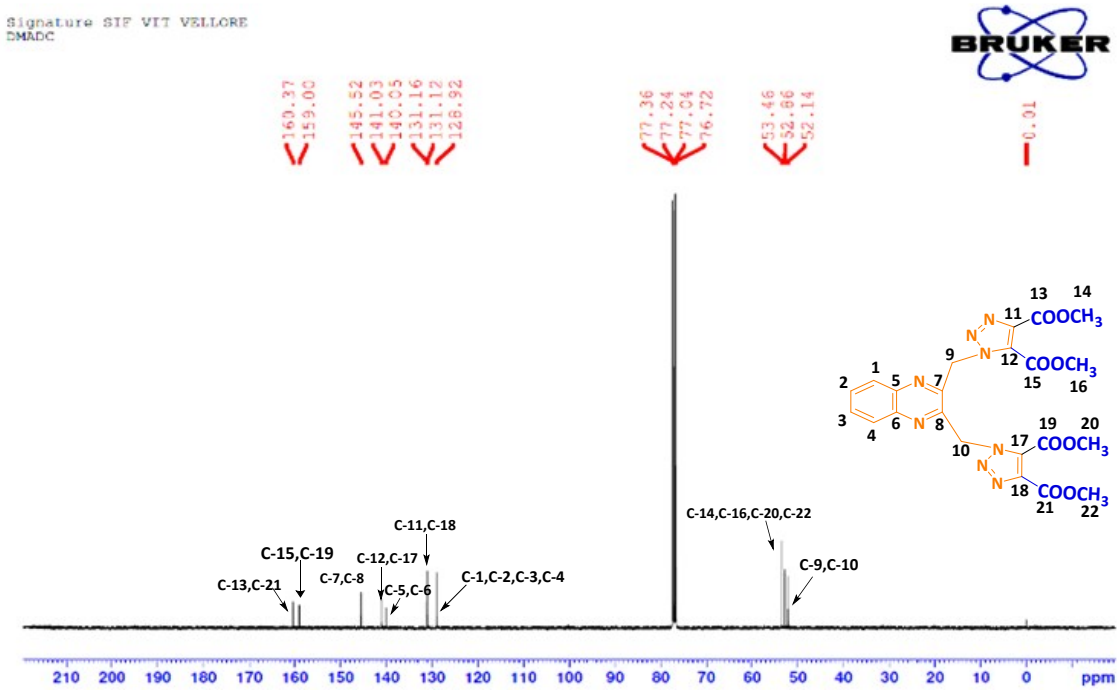

IR spectra of compound 8

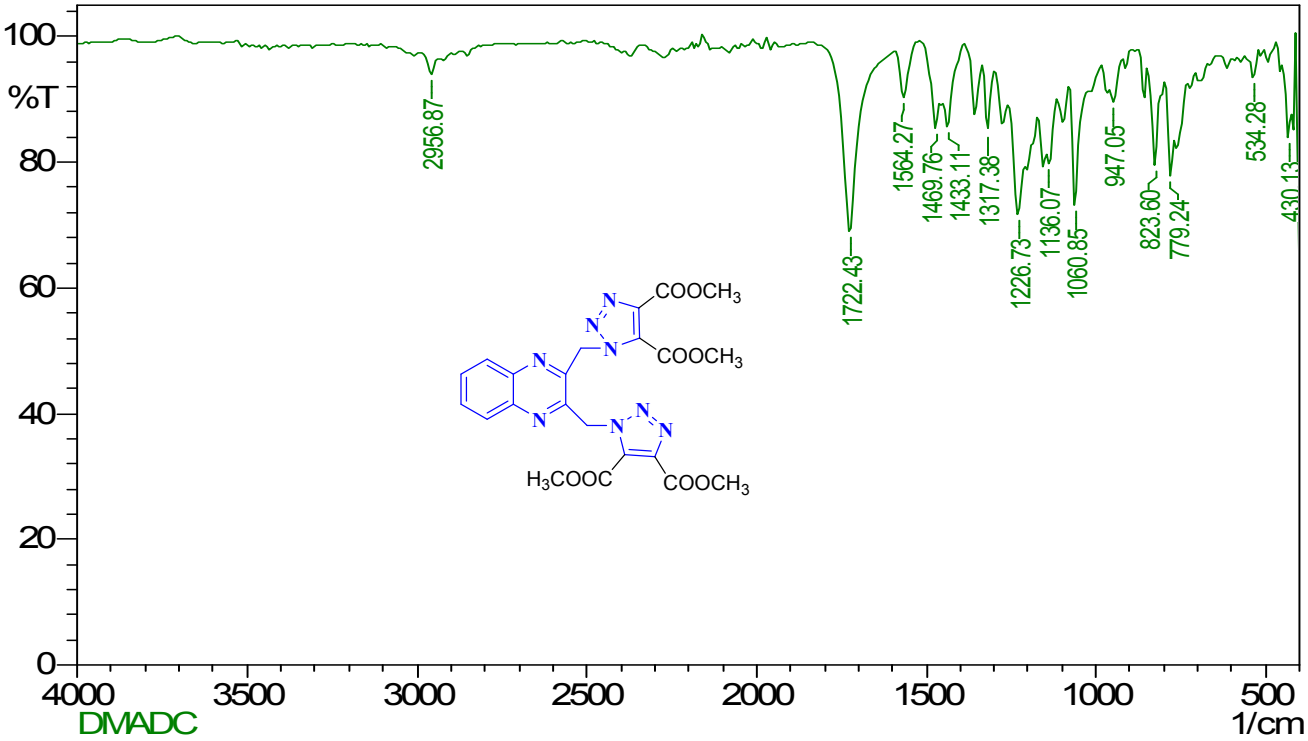

LCMS of Compound 8

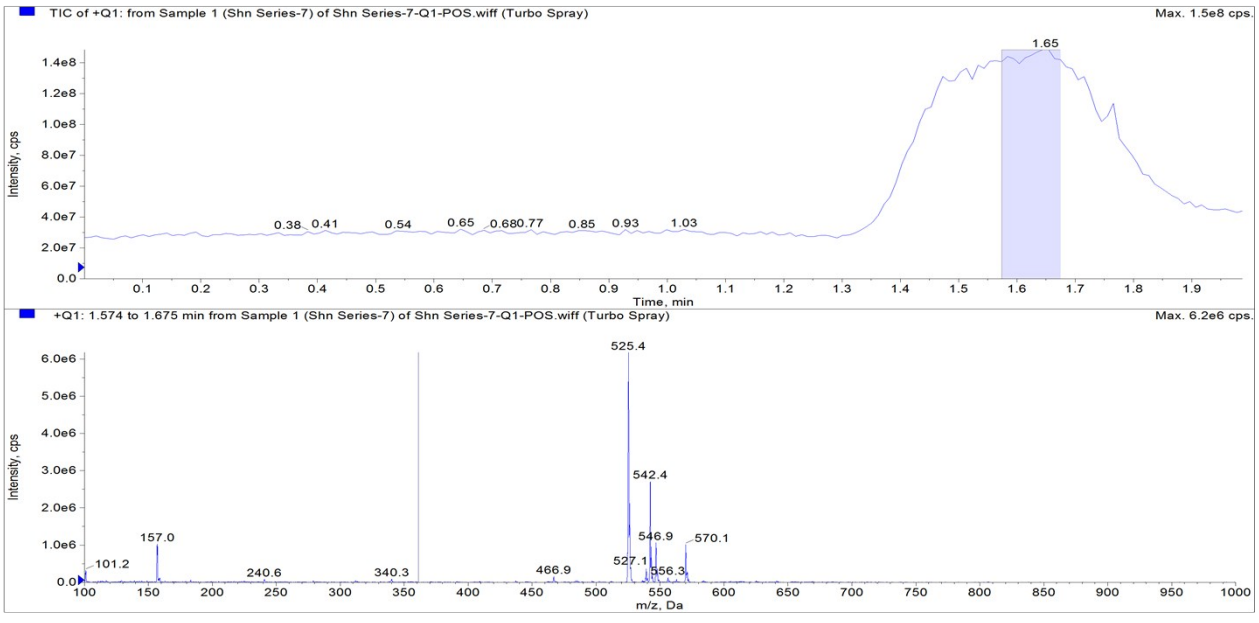

^{1}H NMR of compound 9b

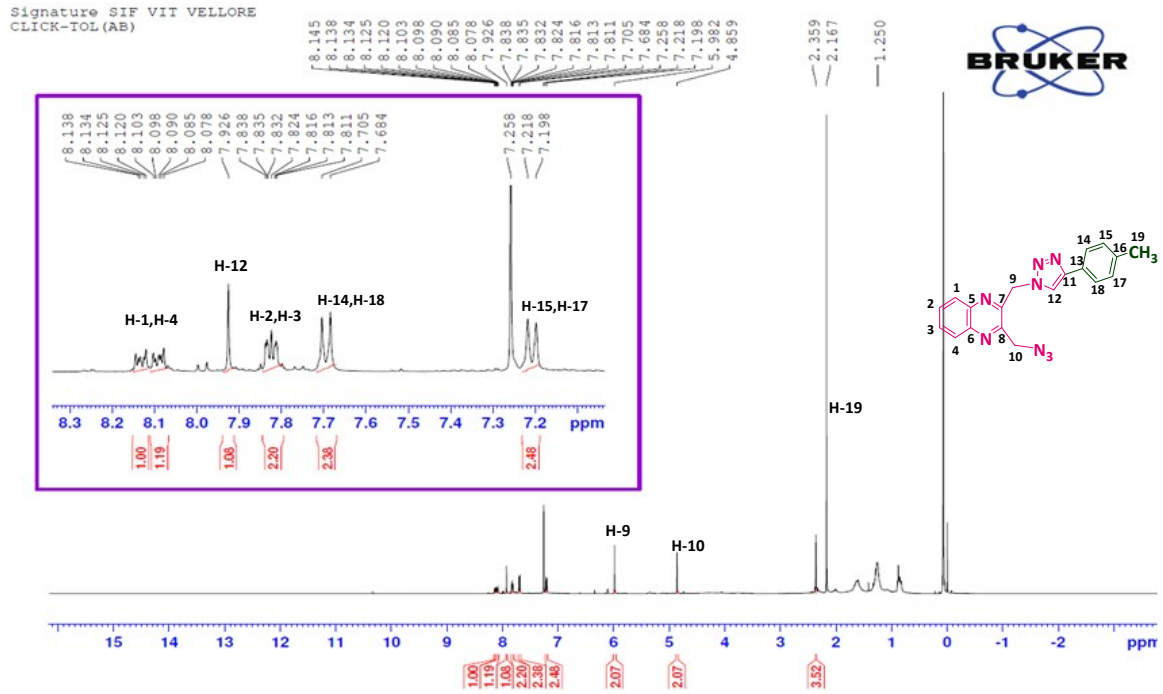

IR spectra of compound 9b

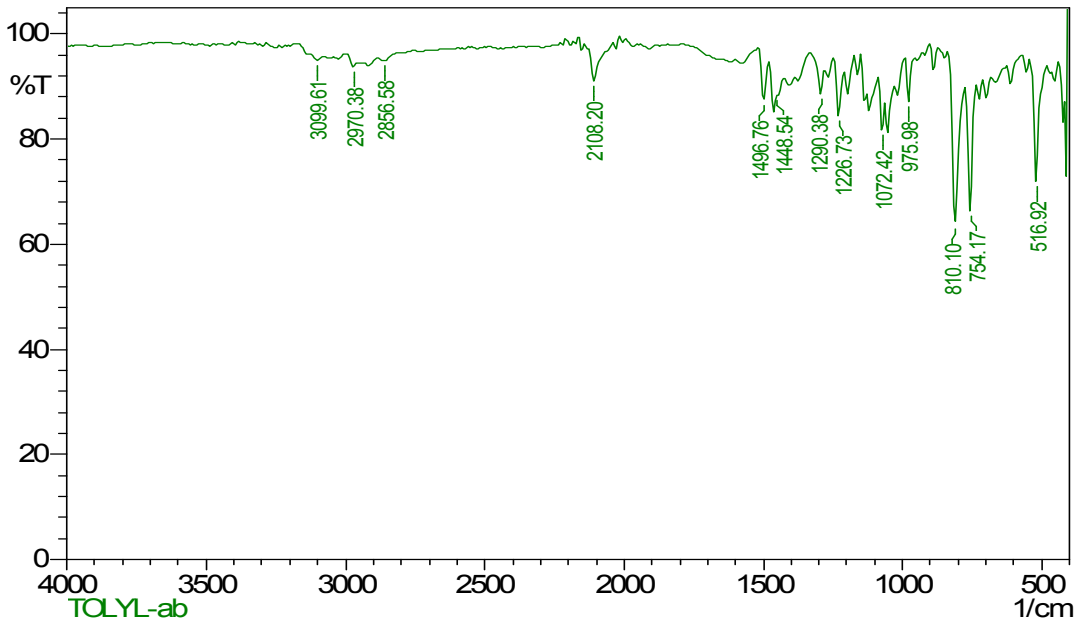

^{1}H NMR of compound 9c

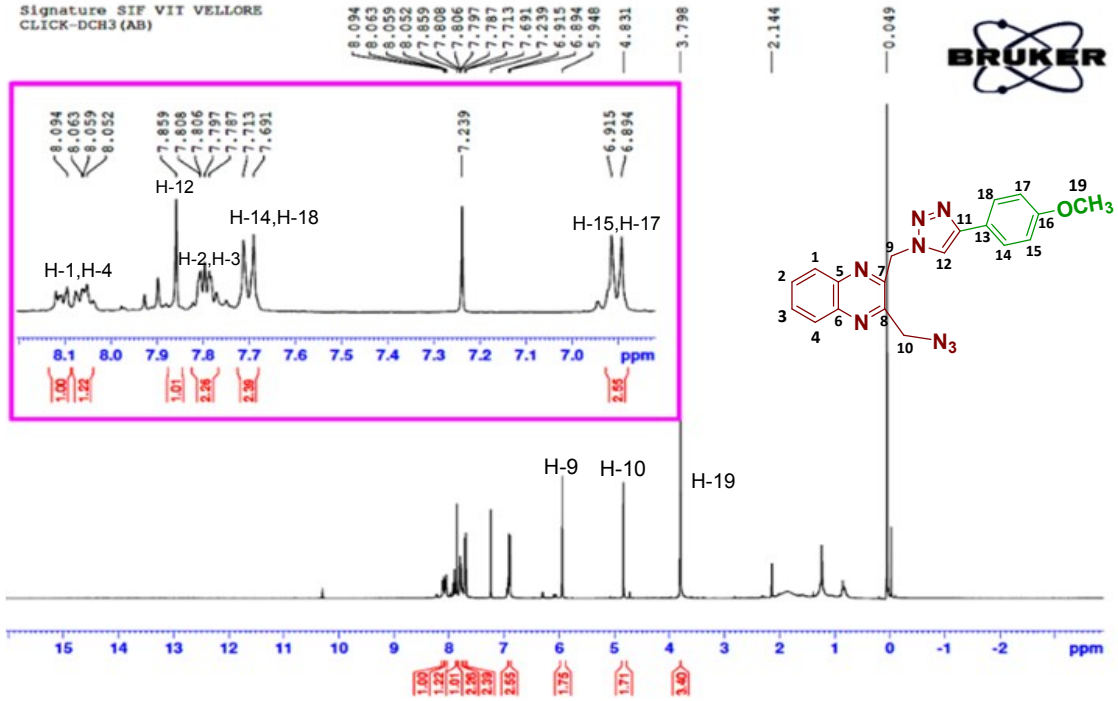

IR spectra of compound 9c

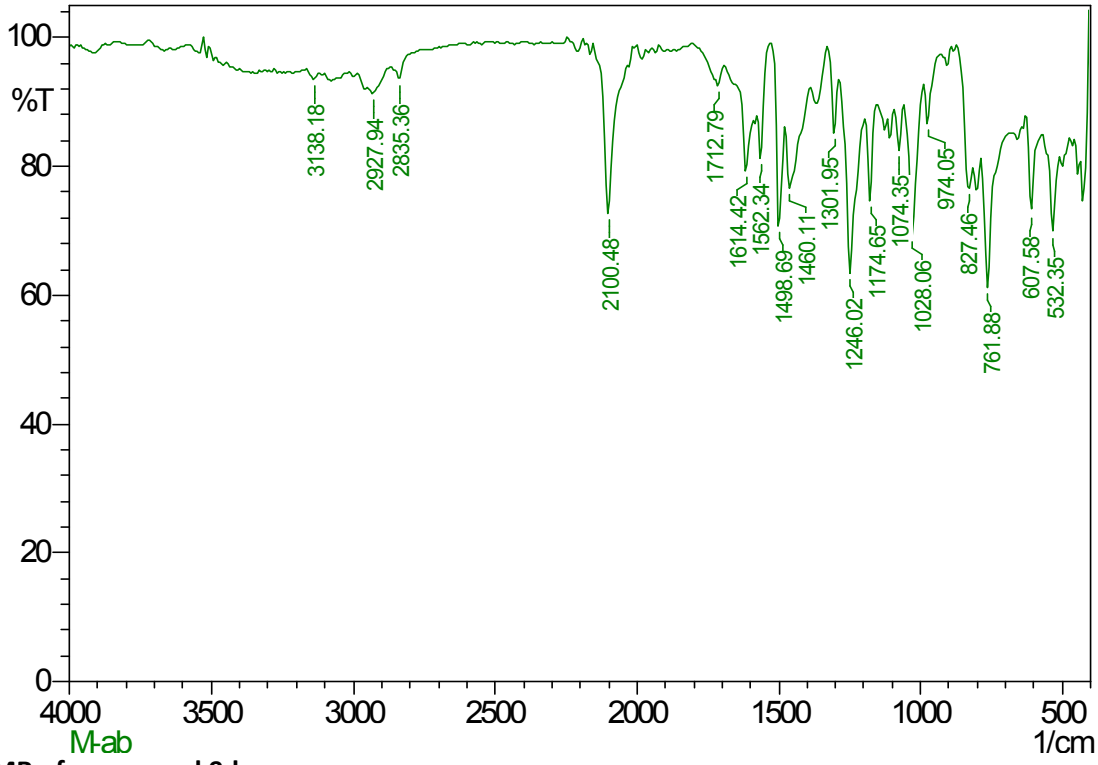

^{1}H NMR of compound 9d

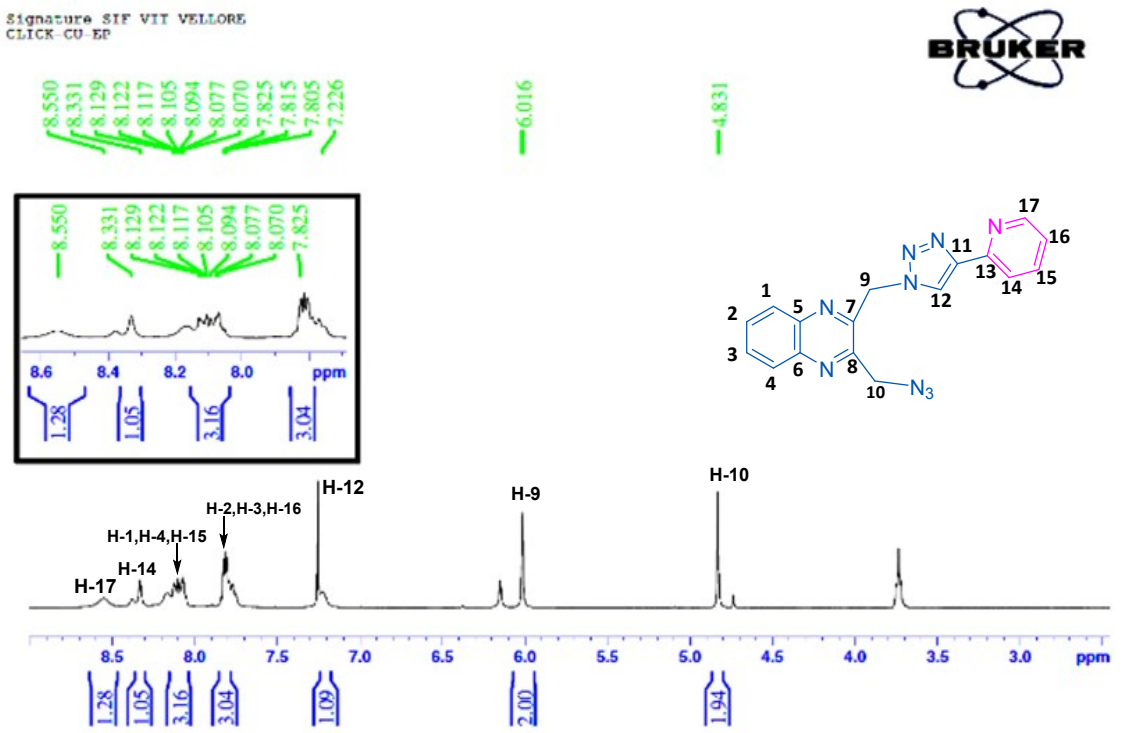

IR spectra of compound 9d

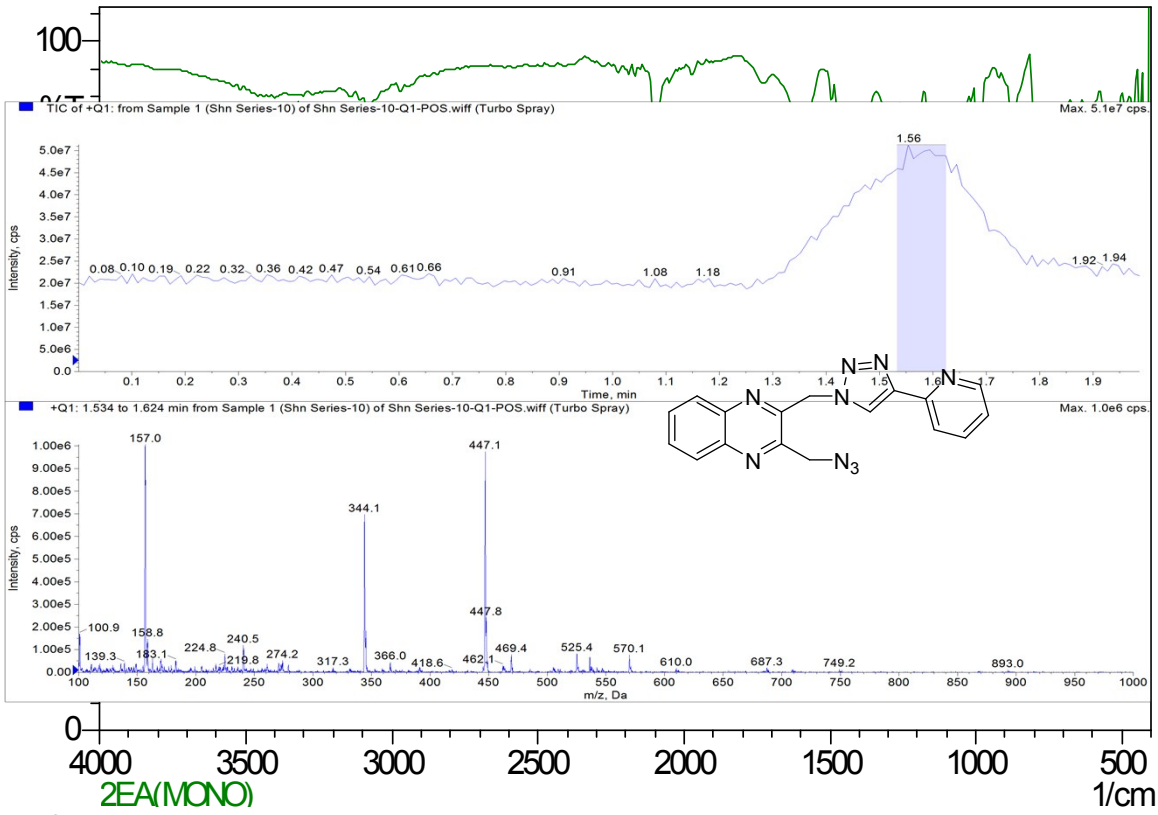

LCMS of compound 9d

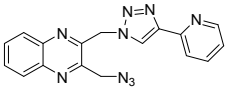

^{1}H NMR of compound 10a

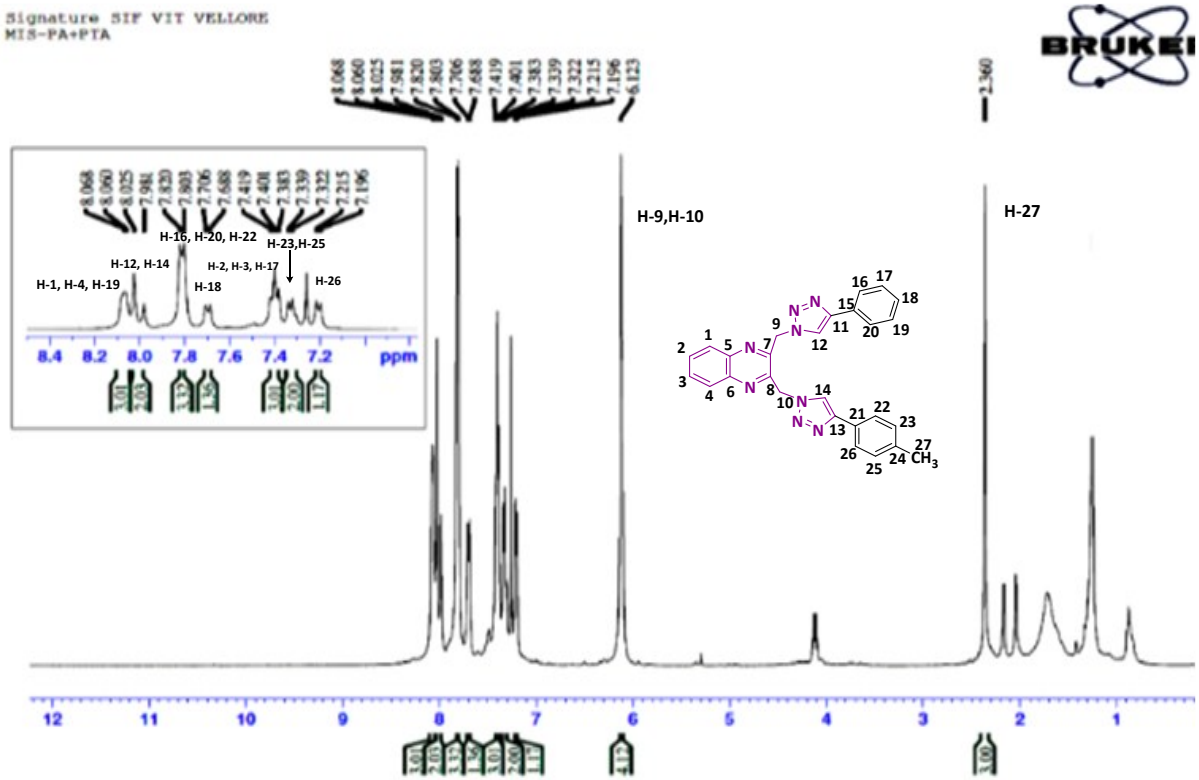

^{13}C NMR of compound 10a

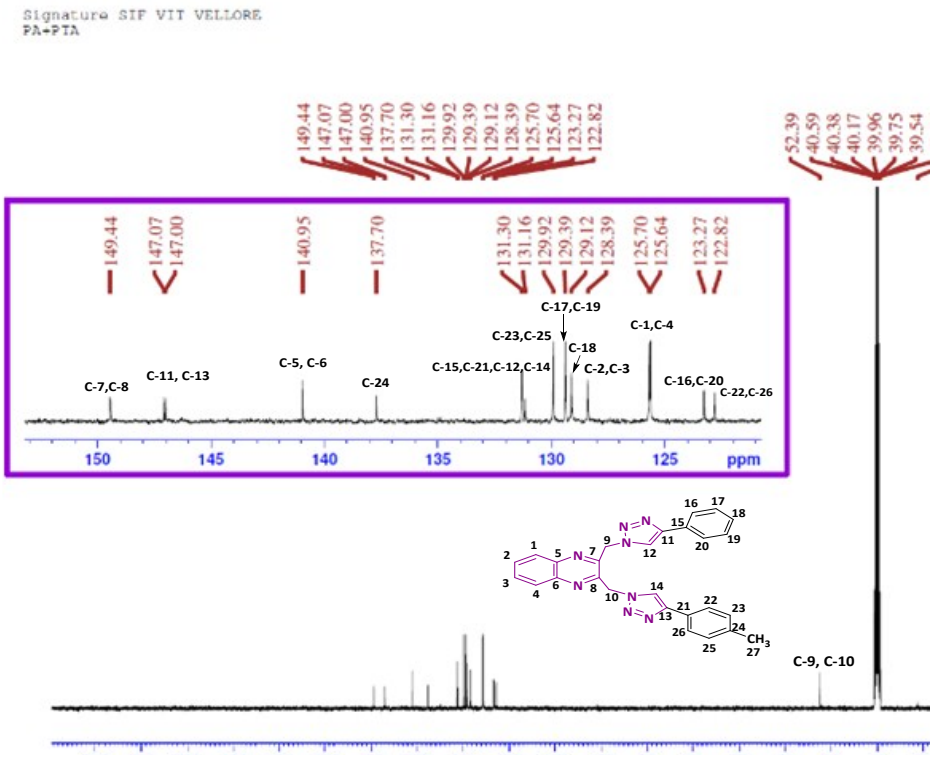

IR spectra of compound 10a

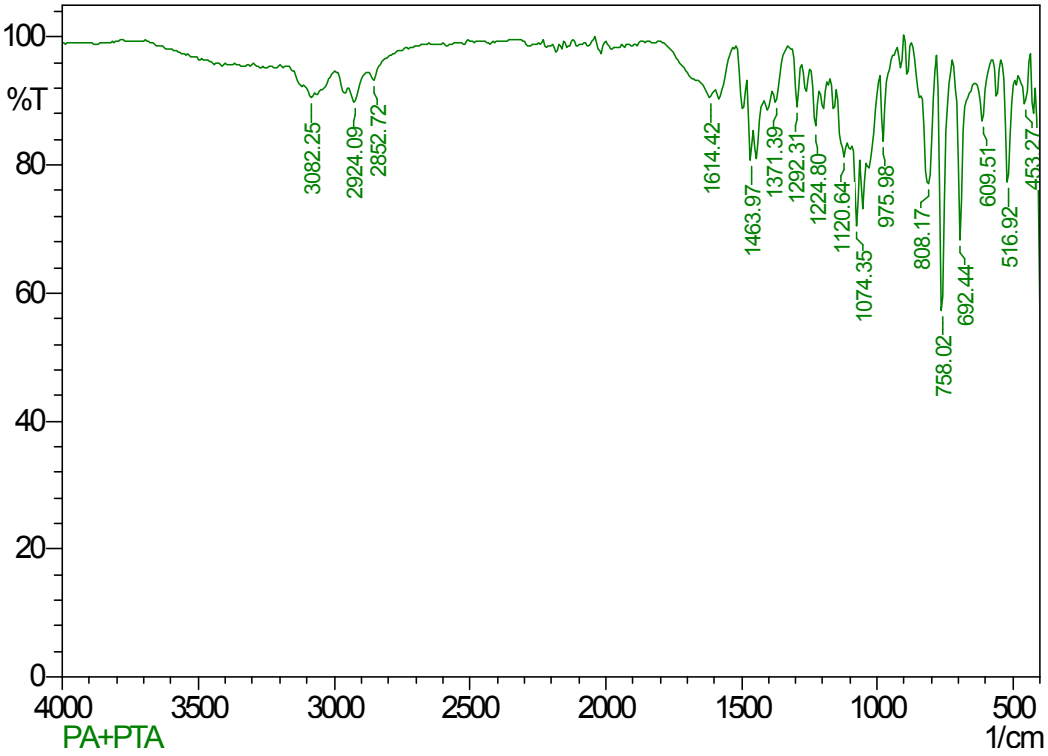

LCMS of compound 10a

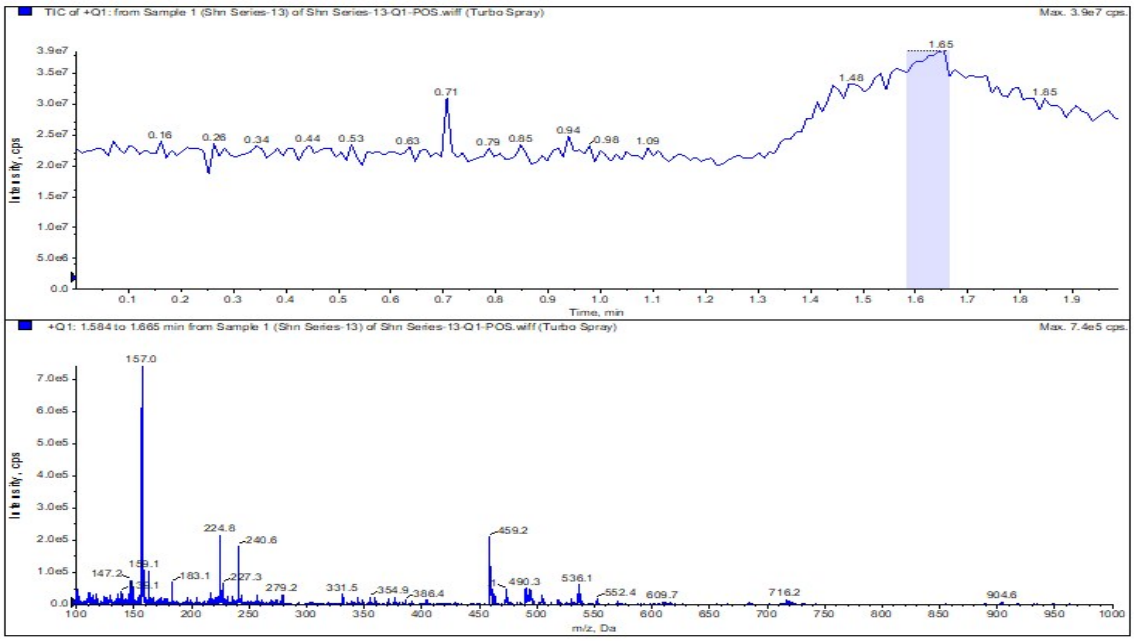

^{1}H NMR of compound 10b

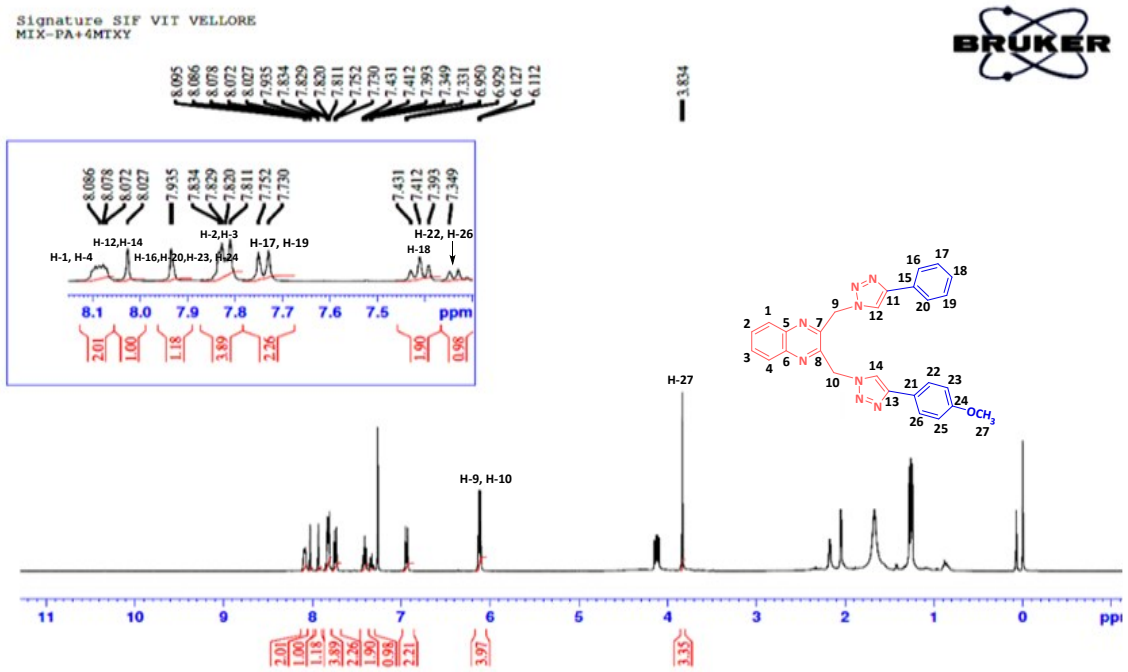

IR spectra of compound 10b

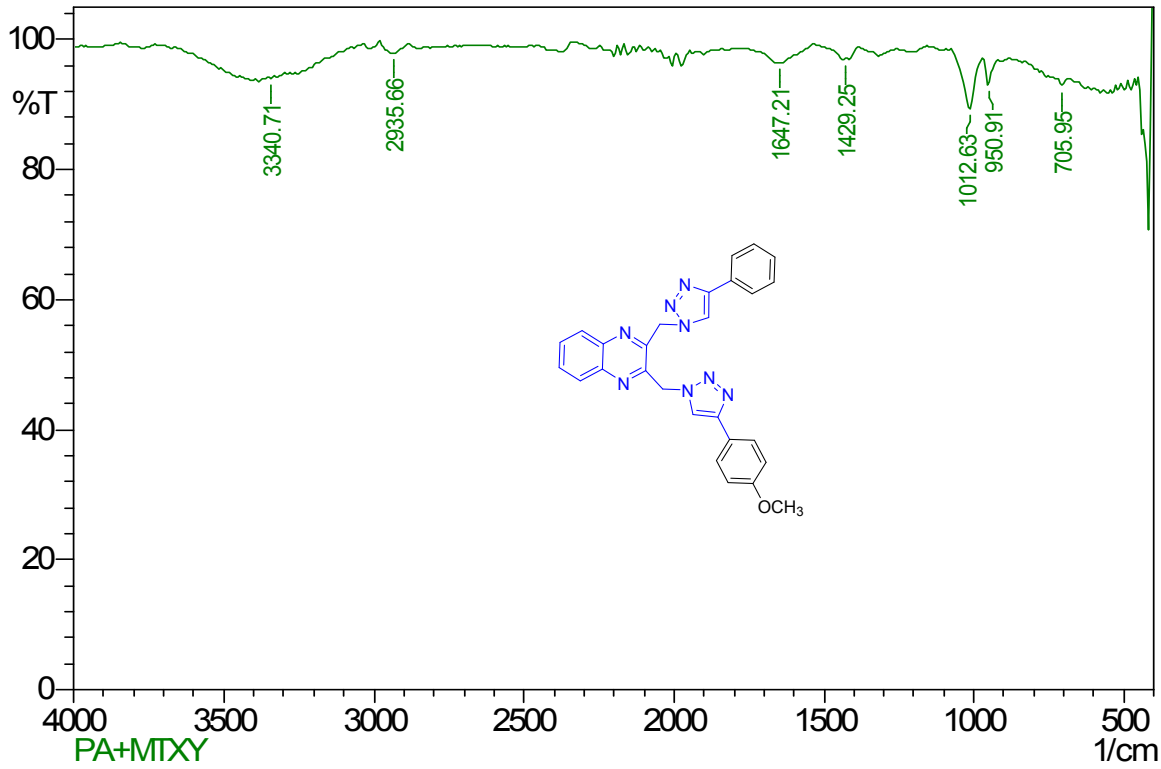

LCMS of compound 10b

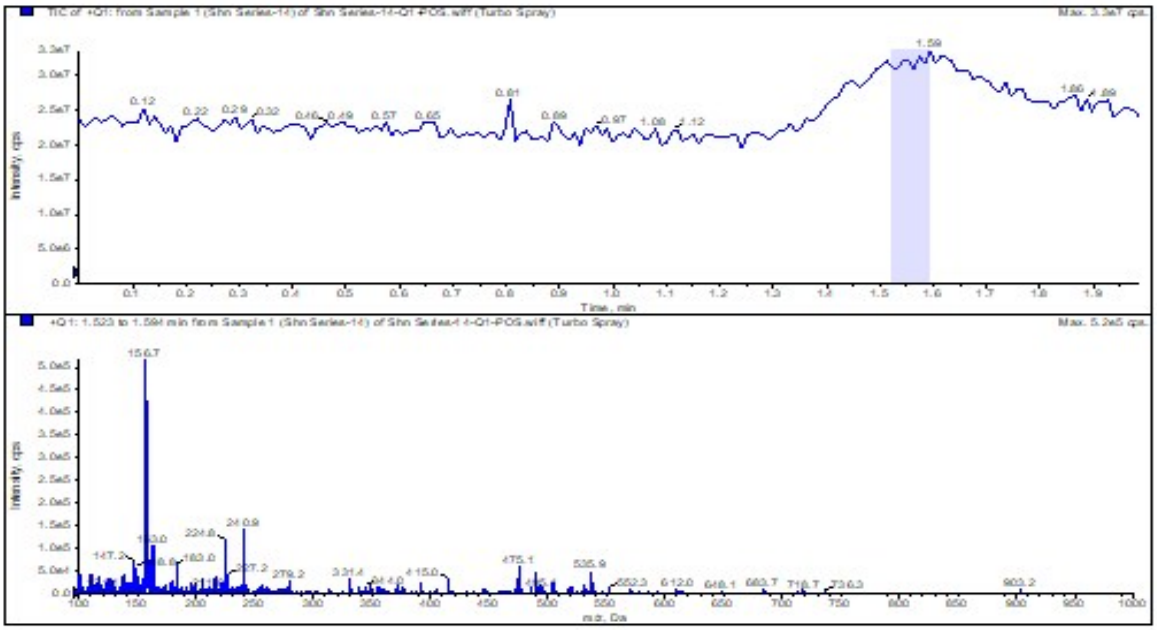

^{1}H NMR of compound 10c

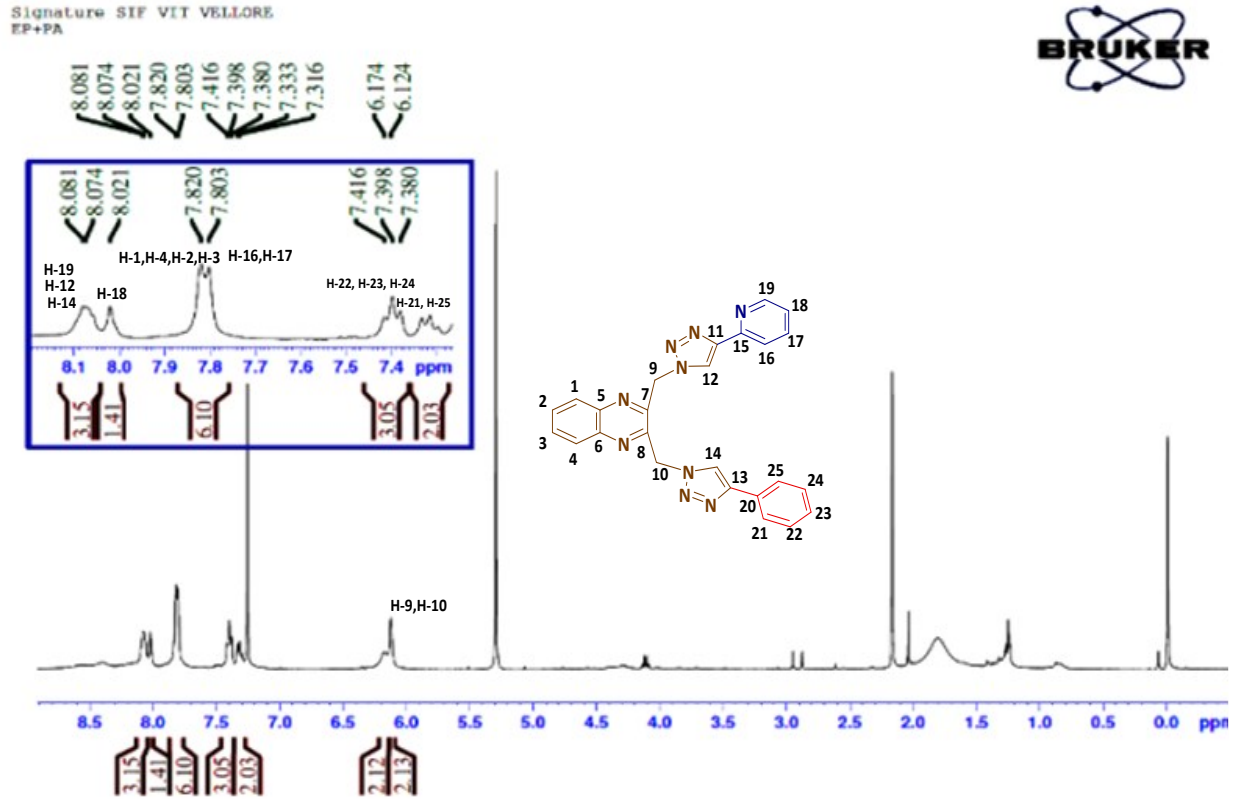

IR spectra of compound 10c

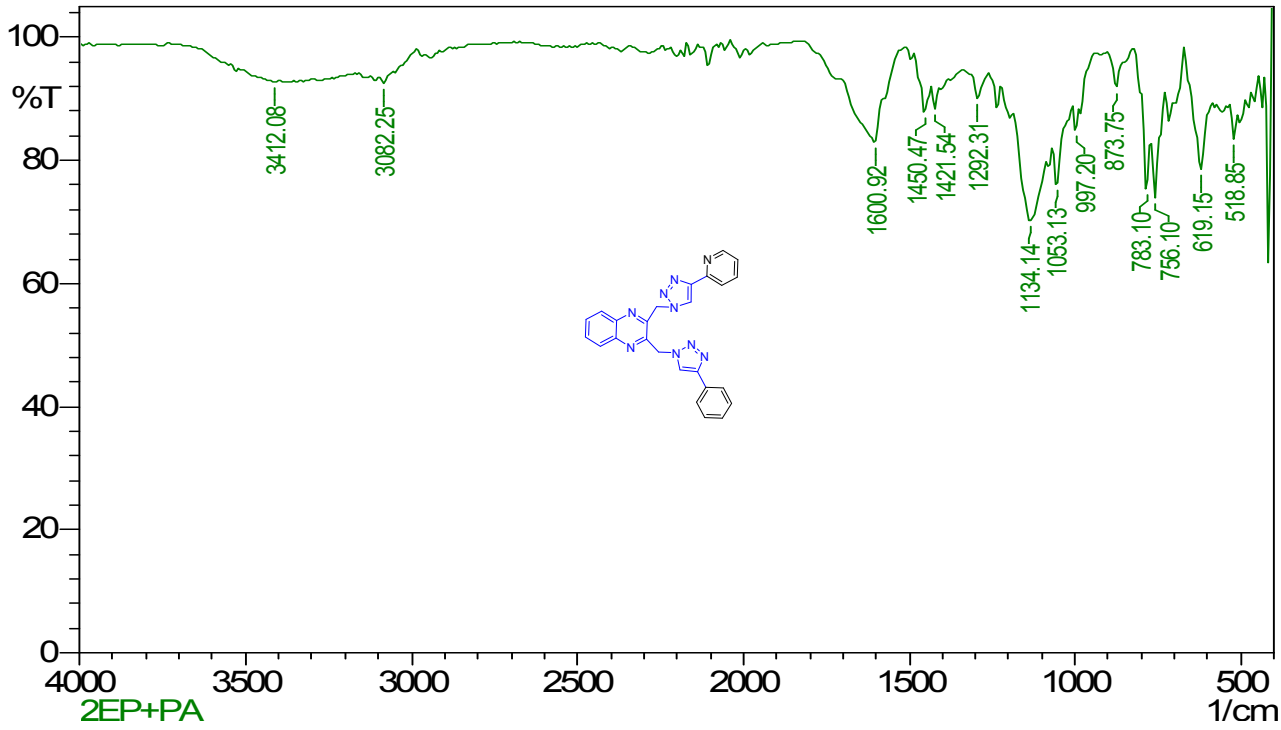

LCMS of compound 13c

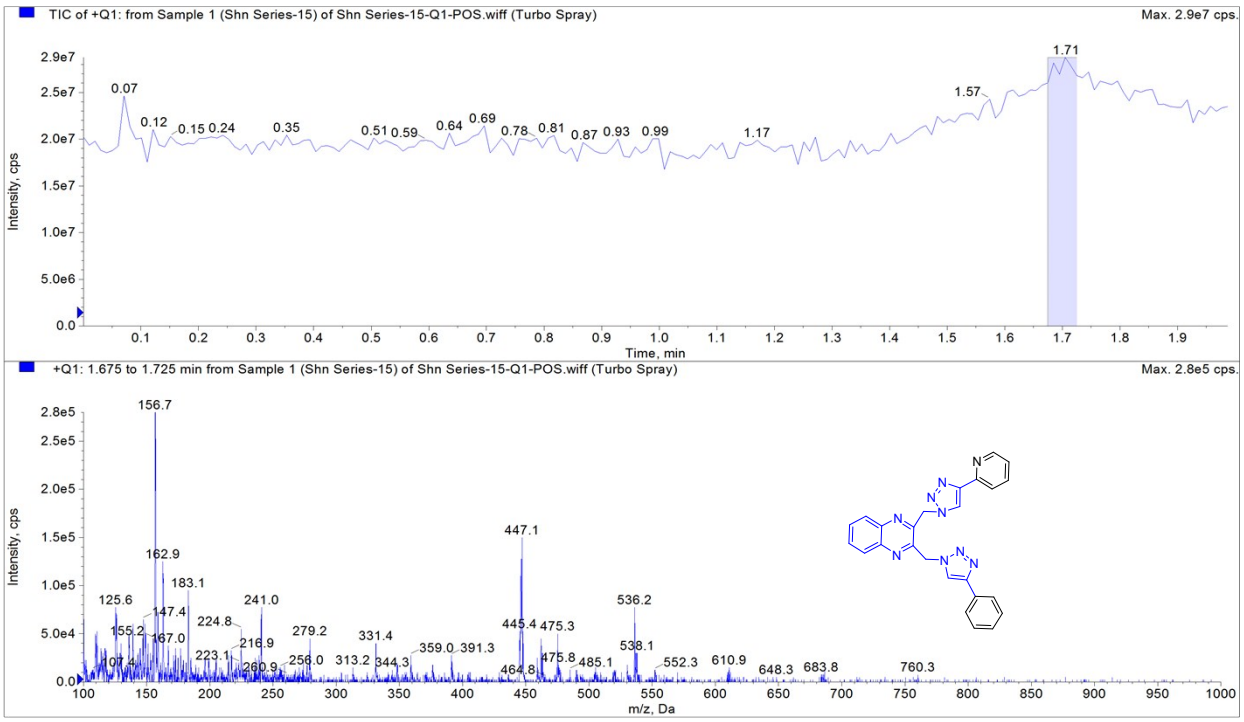

^{1}H NMR of compound 10d

.

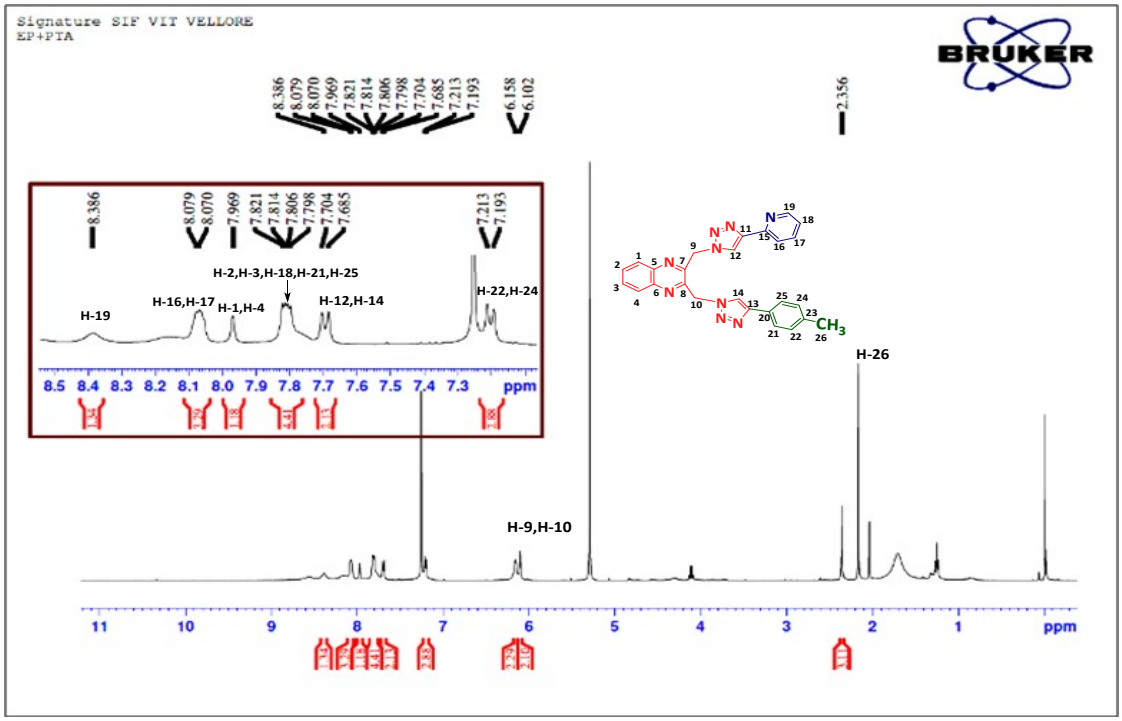

^{13}C NMR of compound 10d

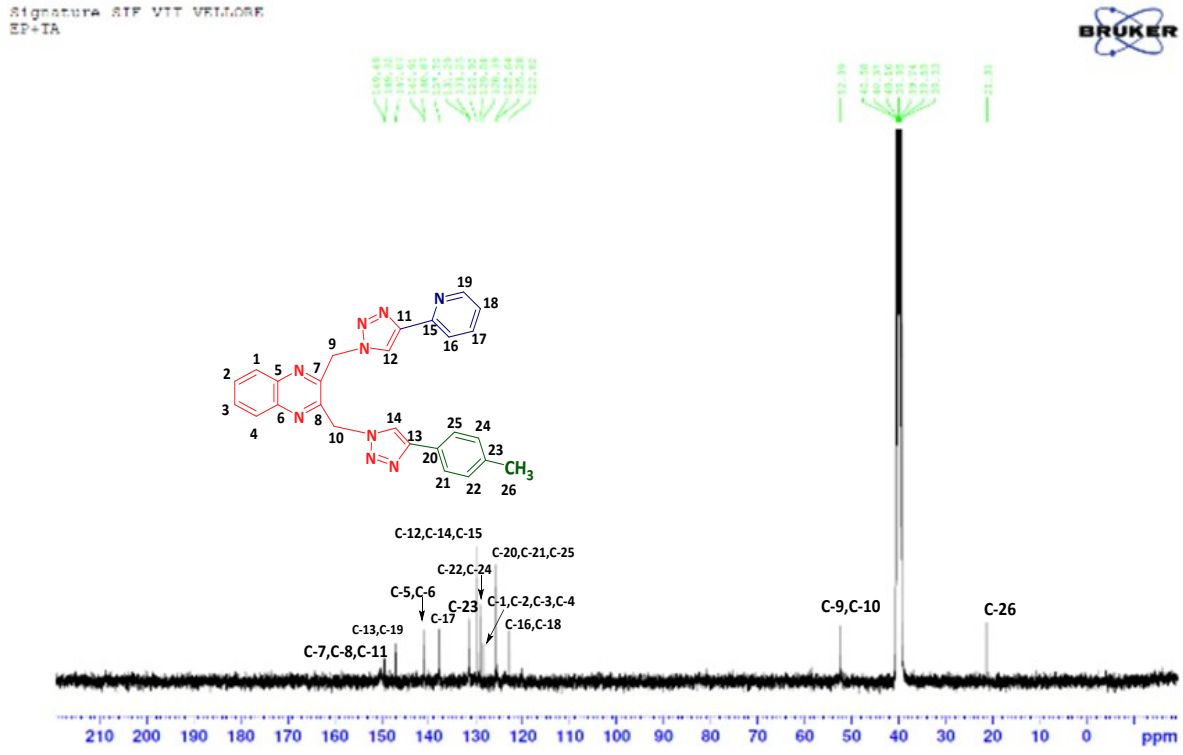

IR spectra of compound 10d

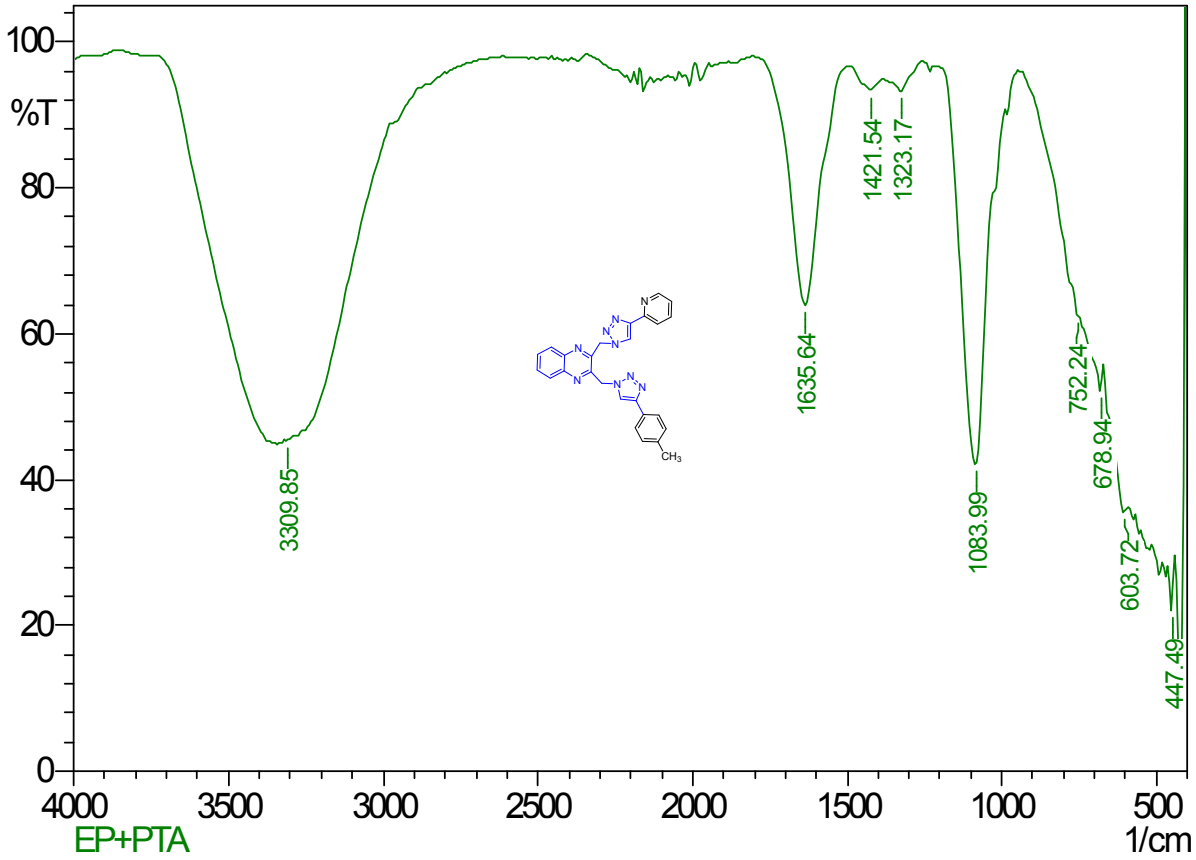

LCMS of compound 10d

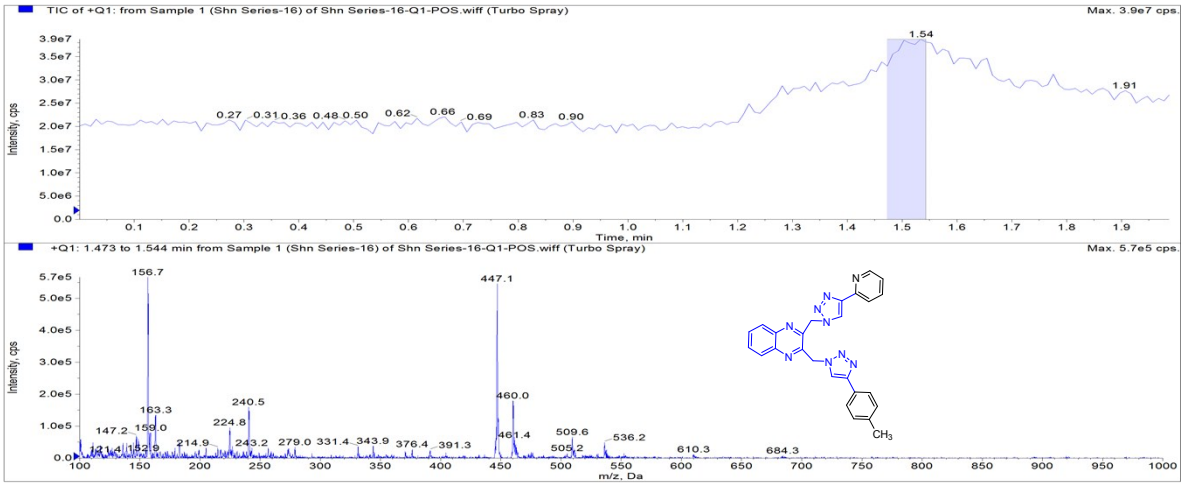

^{1}H NMR of compound 10e

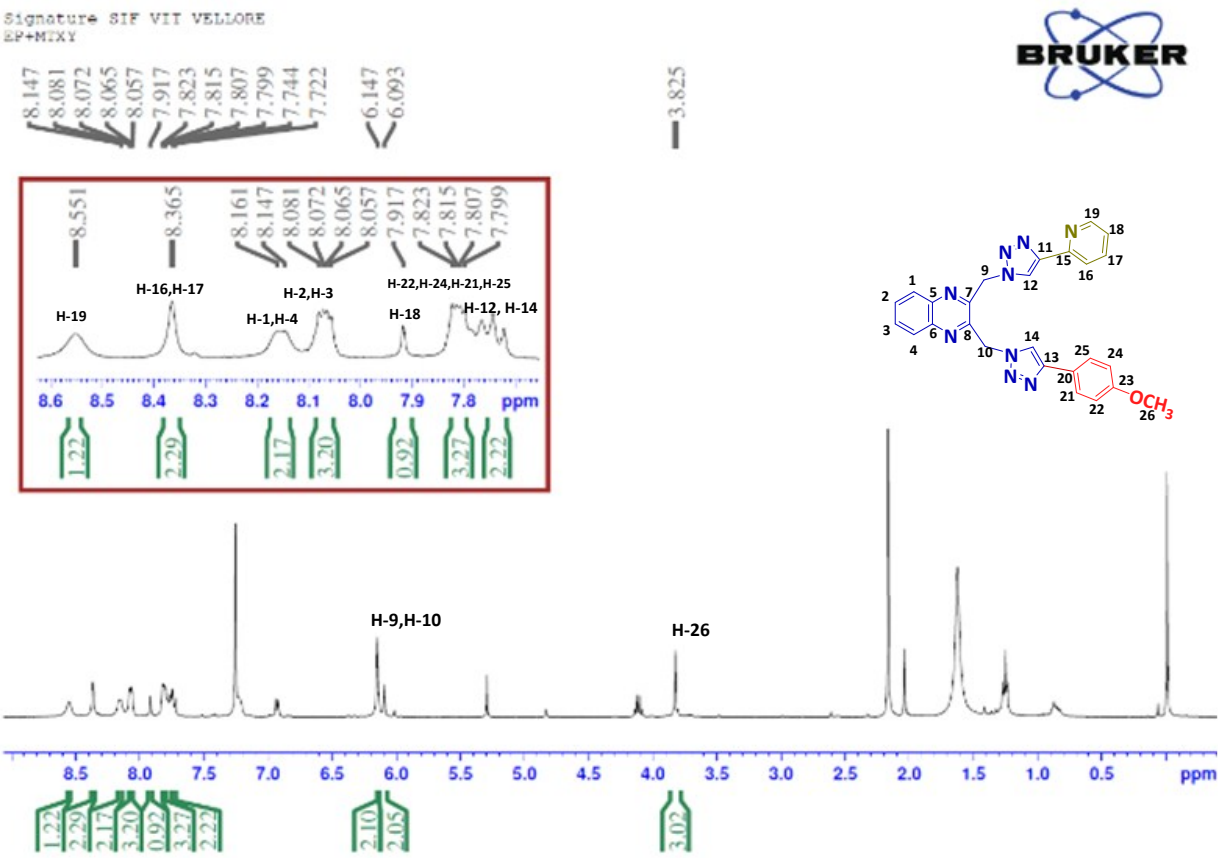

IR spectra of compound 10e

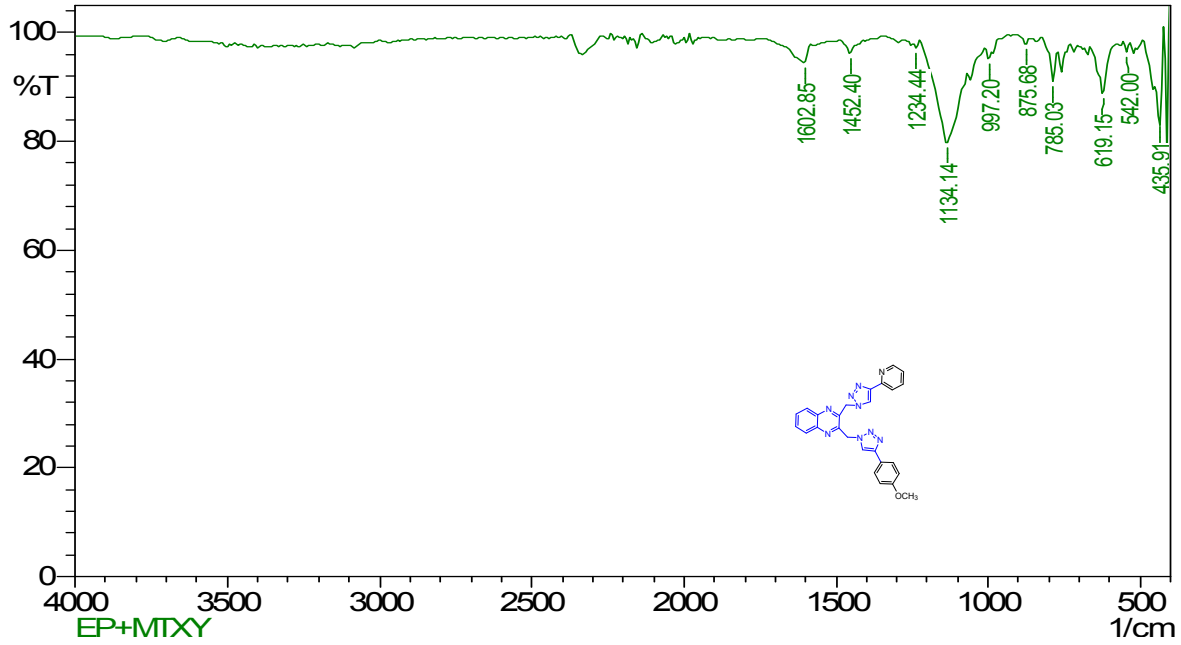

LCMS of compound 10e

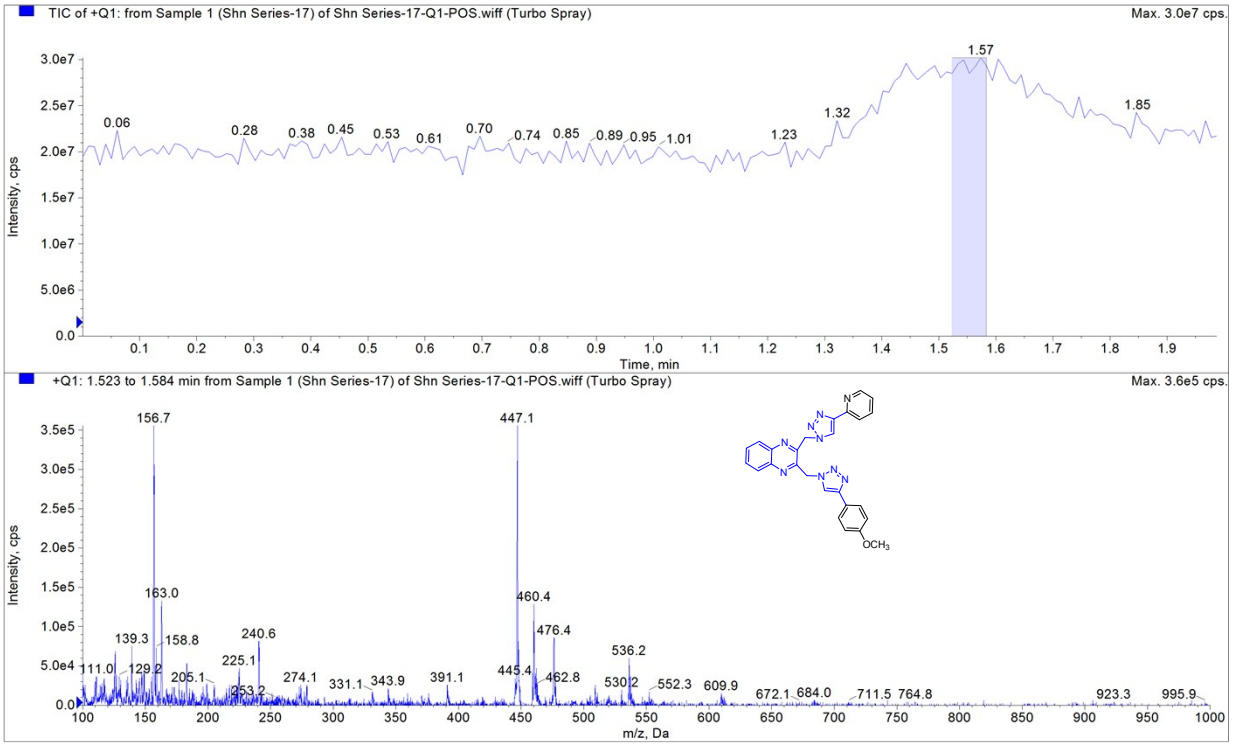

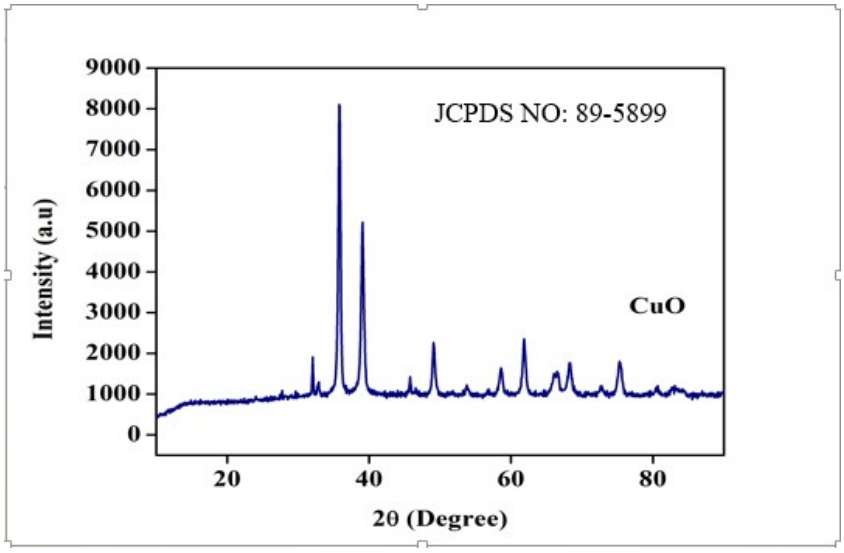

Fig. S1. X-ray diffraction pattern of CuO nanoparticle

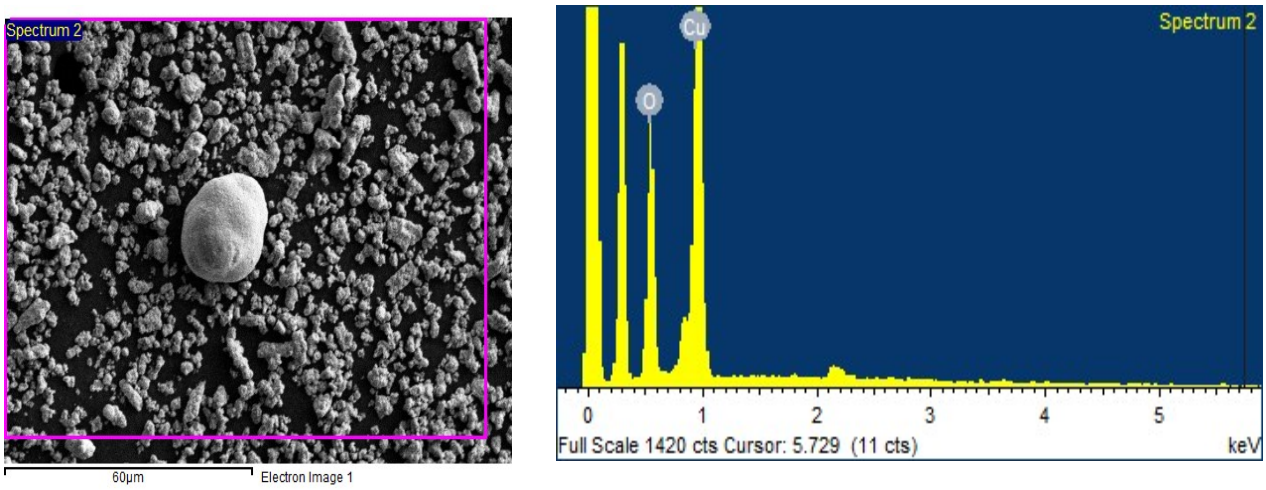

(a) **(b)**

Fig. S2 (a) SEM image and **(b)** EDX spectra of CuO

Table S1. Elemental analysis in EDX

Element	Weight %	Atomic%
O K	26.58	58.97
Cu L	73.42	41.03
Totals	100.00	

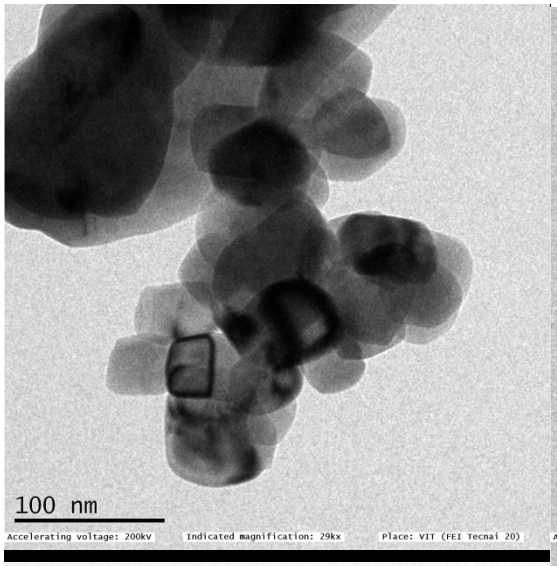
100 nm
Accelerating voltage: 200kv
Indicated magnification: 29kx
Place: VIT (FEI Tecnai 20)

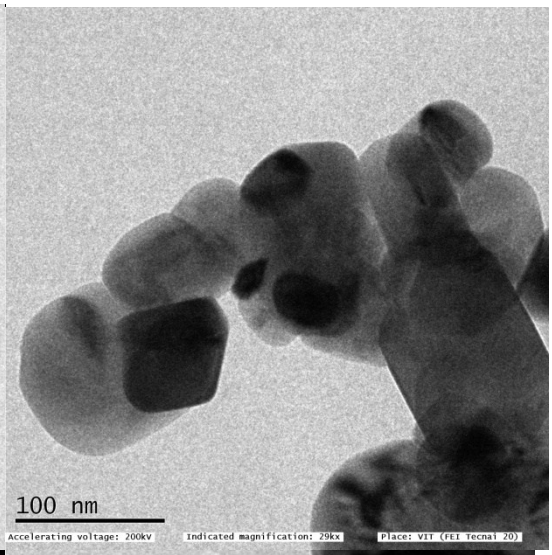
100 nm
Accelerating voltage: 200kv
Indicated magnification: 29kx
Place: VIT (FEI Tecnai 20)

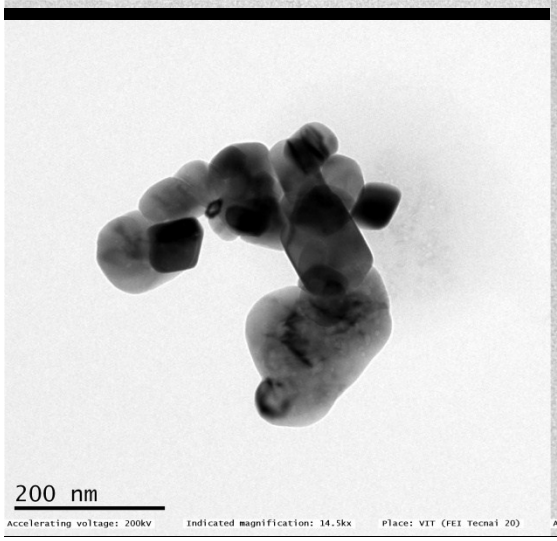
200 nm
Accelerating voltage: 200kv
Indicated magnification: 14.5kx
Place: VIT (FEI Tecnai 20)

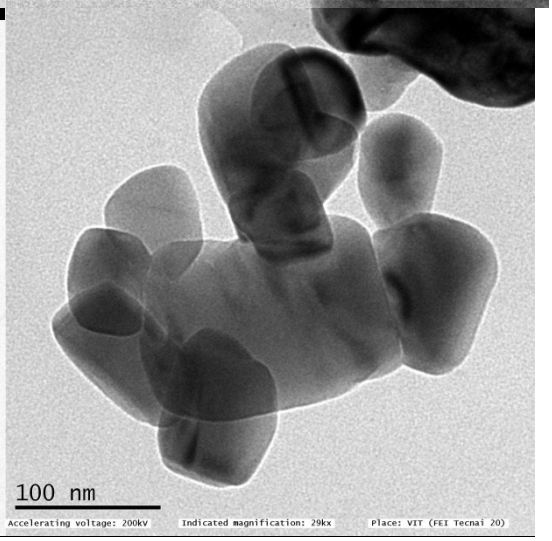
100 nm
Accelerating voltage: 200kv
Indicated magnification: 29kx
Place: VIT (FEI Tecnai 20)

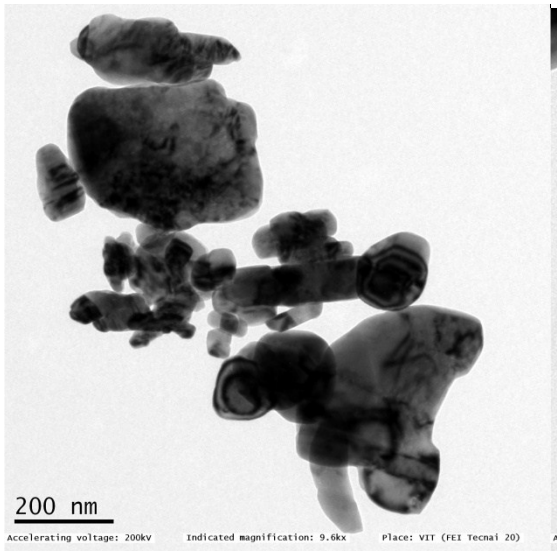
200 nm
Accelerating voltage: 200kv
Indicated magnification: 9.6kx
Place: VIT (FEI Tecnai 20)

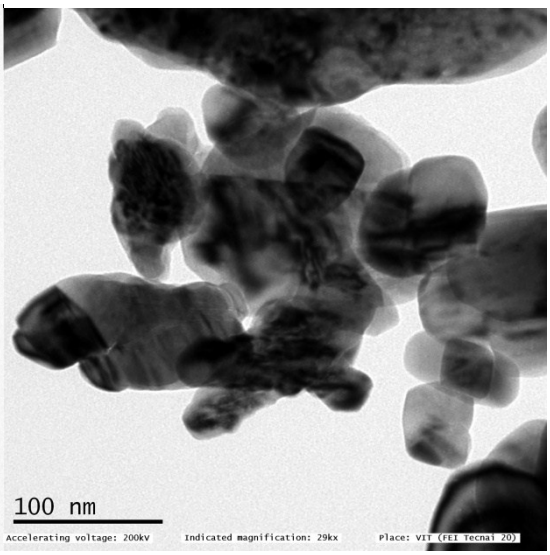
100 nm
Accelerating voltage: 200kv
Indicated magnification: 29kx
Place: VIT (FEI Tecnai 20)

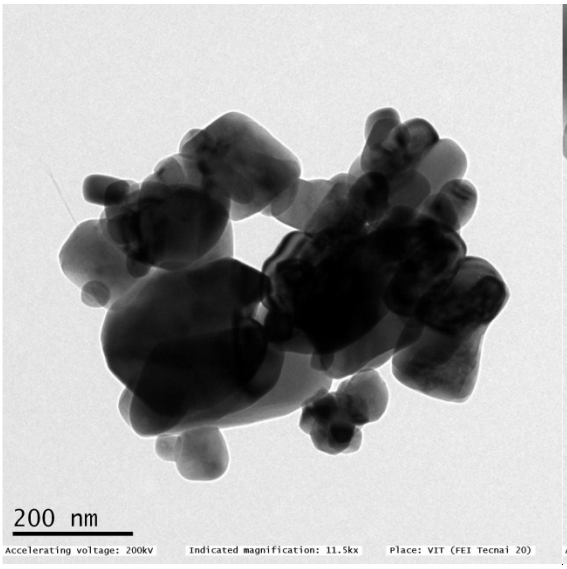
200 nm
Accelerating voltage: 200kv
Indicated magnification: 11.5kx
Place: VIT (FEI Tecnai 20)

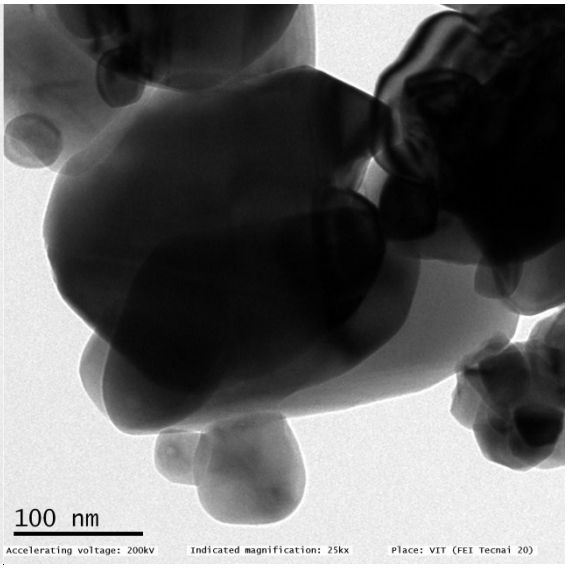
100 nm
Accelerating voltage: 200kv
Indicated magnification: 25kx
Place: VIT (FEI Tecnai 20)

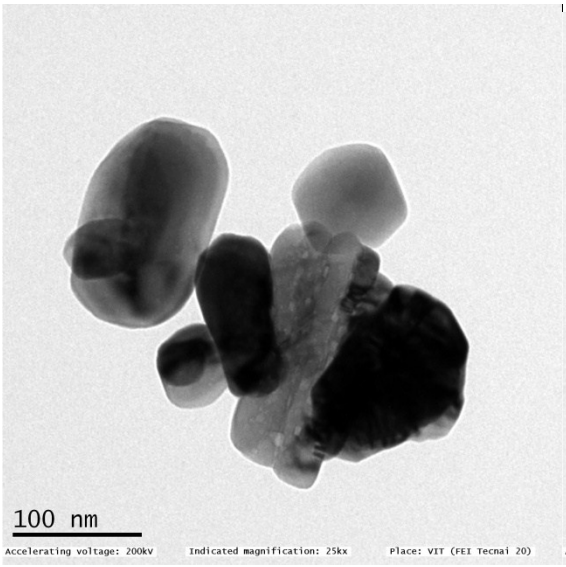
100 nm
Accelerating voltage: 200kv
Indicated magnification: 25kx
Place: VIT (FEI Tecnai 20)

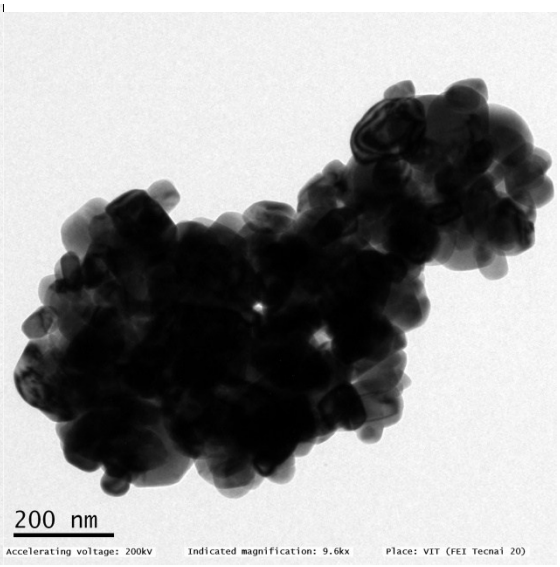
200 nm
Accelerating voltage: 200kv
Indicated magnification: 9.6kx
Place: VIT (FEI Tecnai 20)

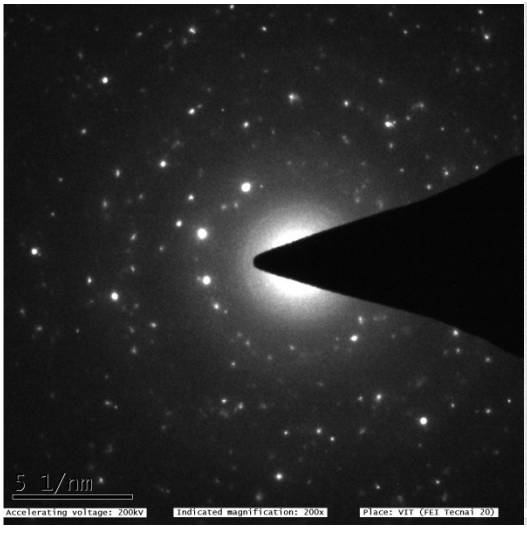
5 1/nm
Accelerating voltage: 200kv
Indicated magnification: 200x
Place: VIT (FEI Tecnai 20)

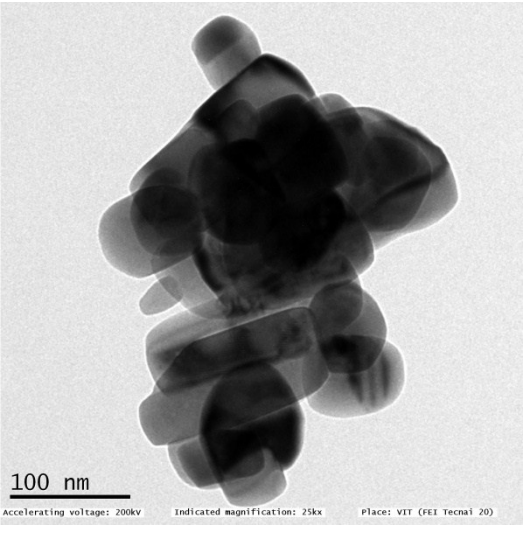
100 nm
Accelerating voltage: 200kv
Indicated magnification: 25kx
Place: VIT (FEI Tecnai 20)

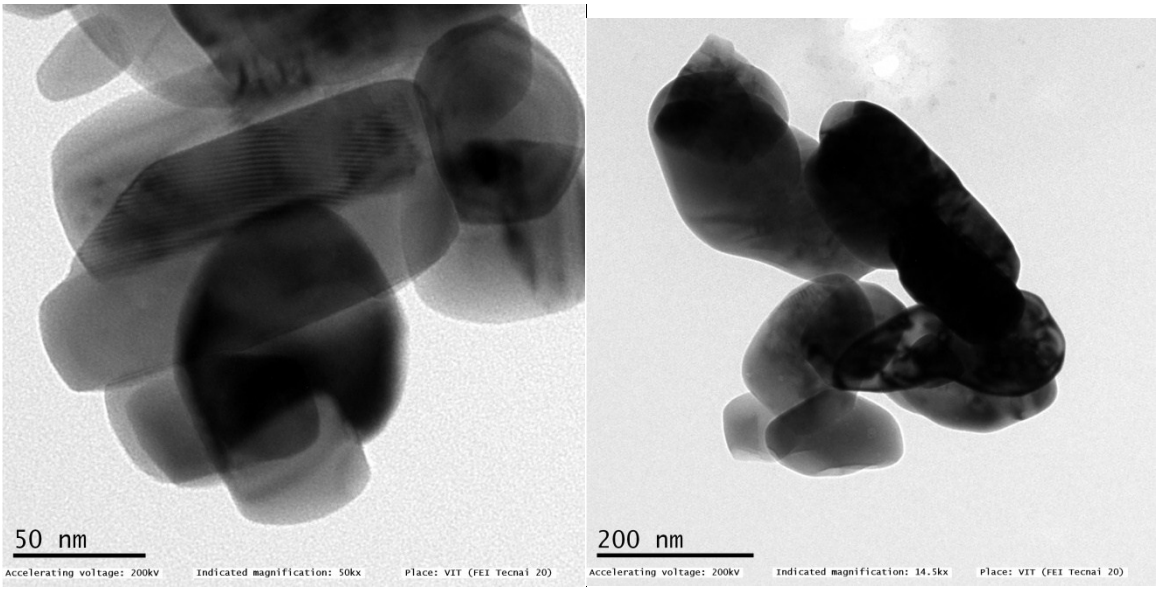

Fig. S3 TEM images of synthesized CuO nanoparticle

Table S2 Elemental analysis of CuO in TEM

Element	Series	Net unn. C	norm. C [wt.%]	Atom. C [at.%]	Error (3 Sigma) [wt.%]
Oxygen	K-series	11327	8.85	27.84	0.91
Copper	K-series	130681	91.15	72.16	8.32
Total:			100.00	100.00	

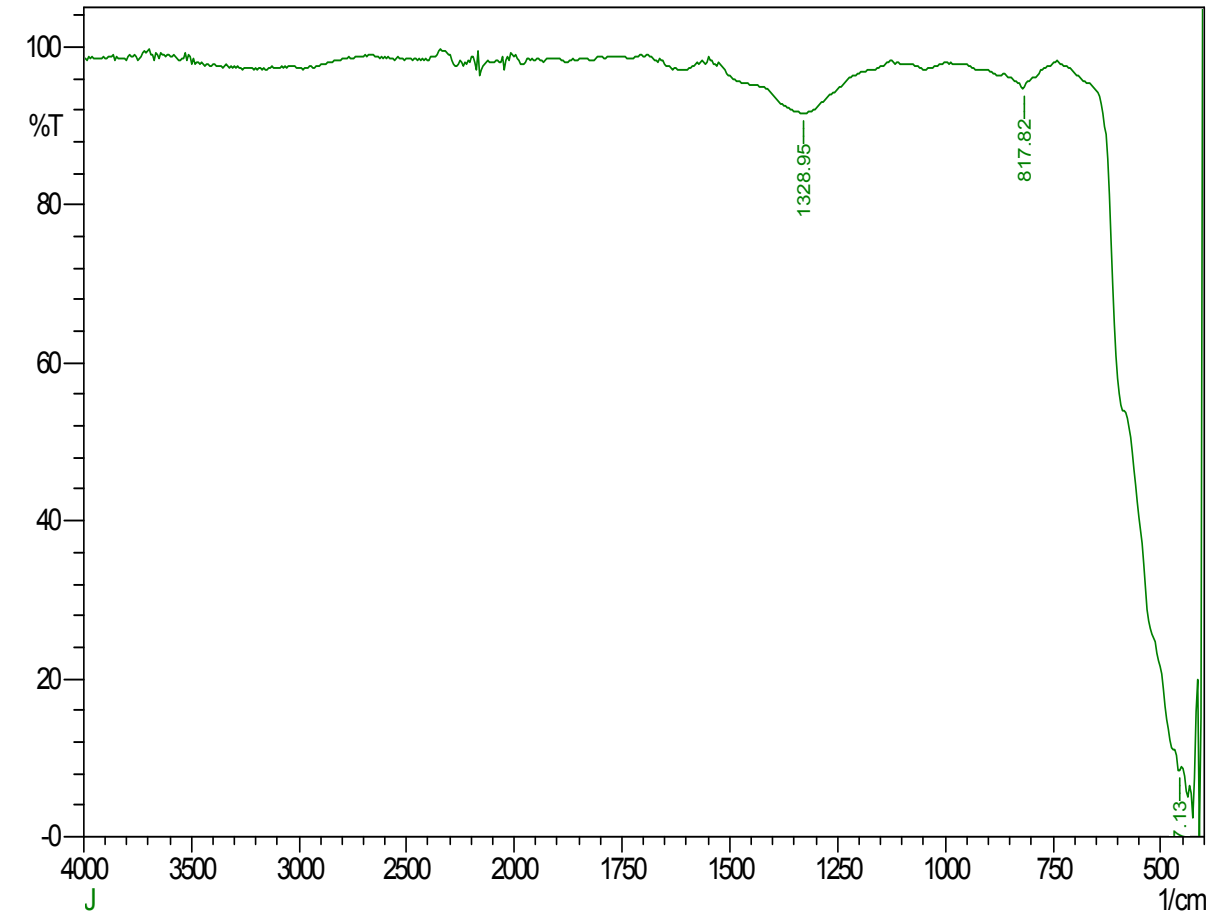

Fig. S4 IR spectra of synthesized CuO nanoparticle

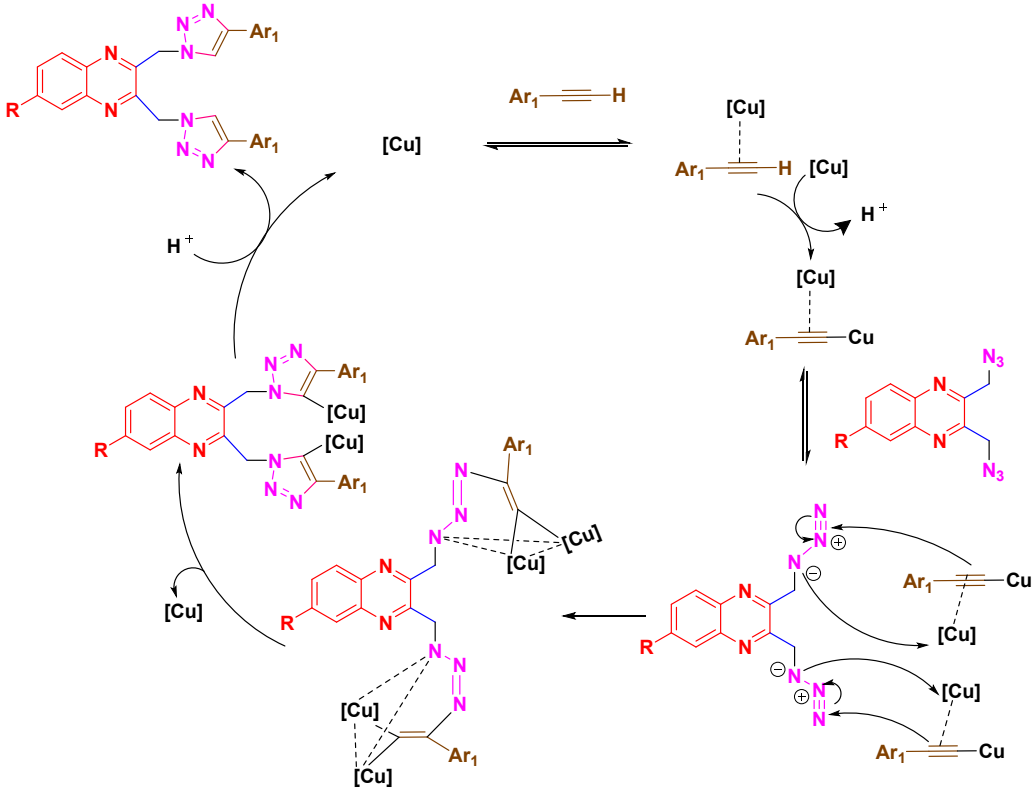

Fig. S5 Plausible catalytic pathway for Cu(II) mediated click reaction

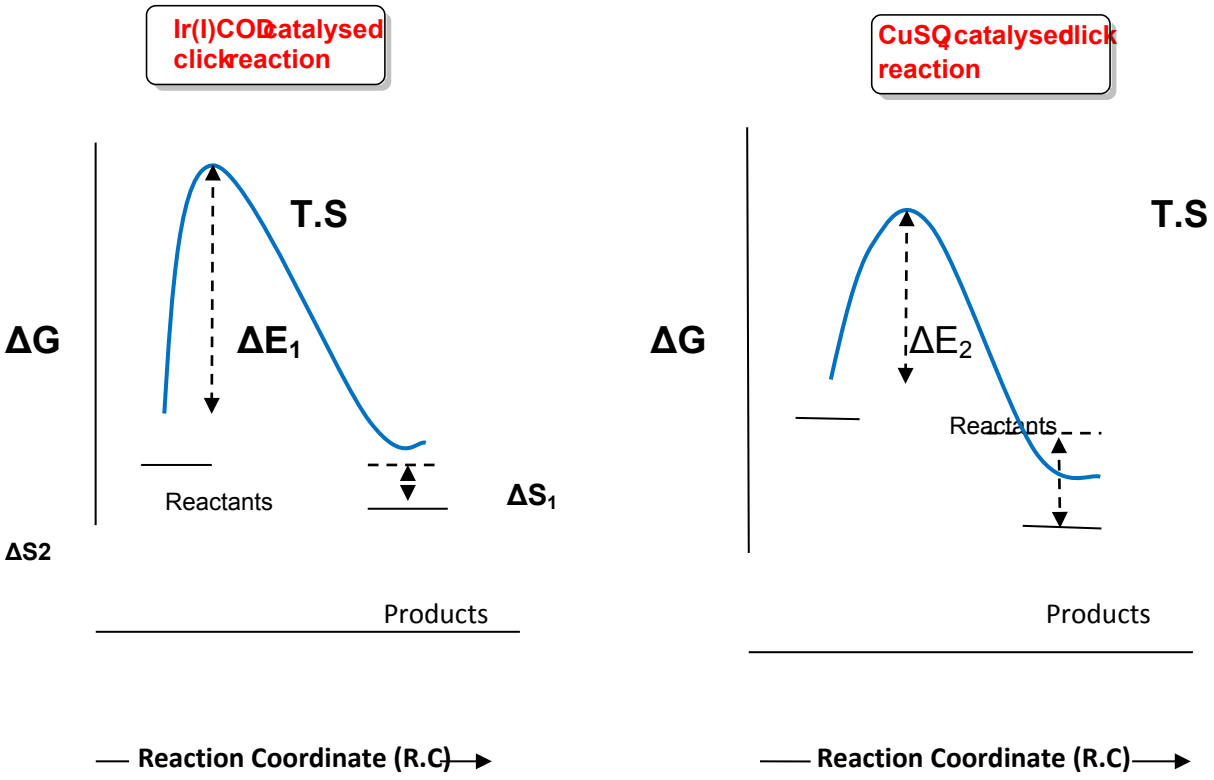

ΔE= Activation energy; ΔS= Stabilisation energy, $\Delta E_1 > \Delta E_2$ and $\Delta S_1 < \Delta S_2$ implies that Cu(I) catalysed cycloaddition stabilizes the transition state (T.S) more than that of Ir(I) catalysed click reaction.

Fig S6. Energy profile diagram for Ir(I) & Cu(II) catalysed click reaction

DNA BINDING STUDY BY ABSORPTION AND EMISSION

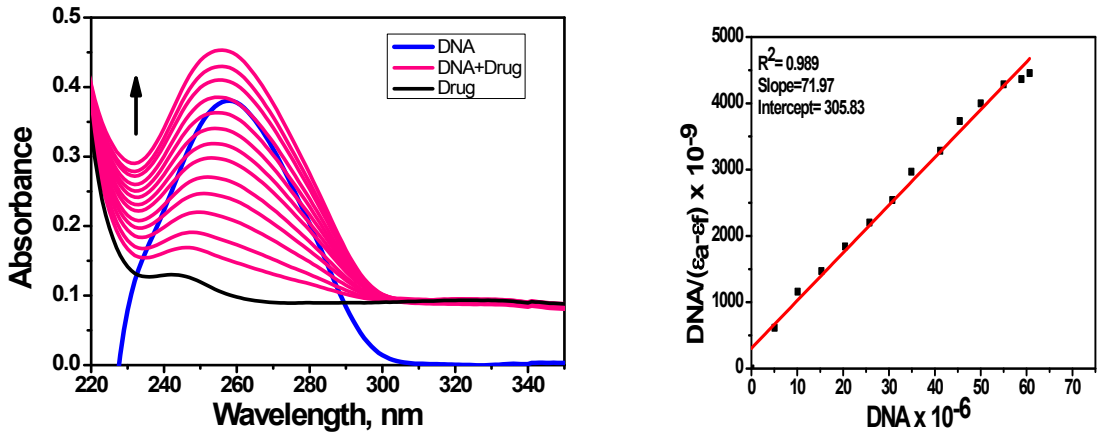

(a) (c)

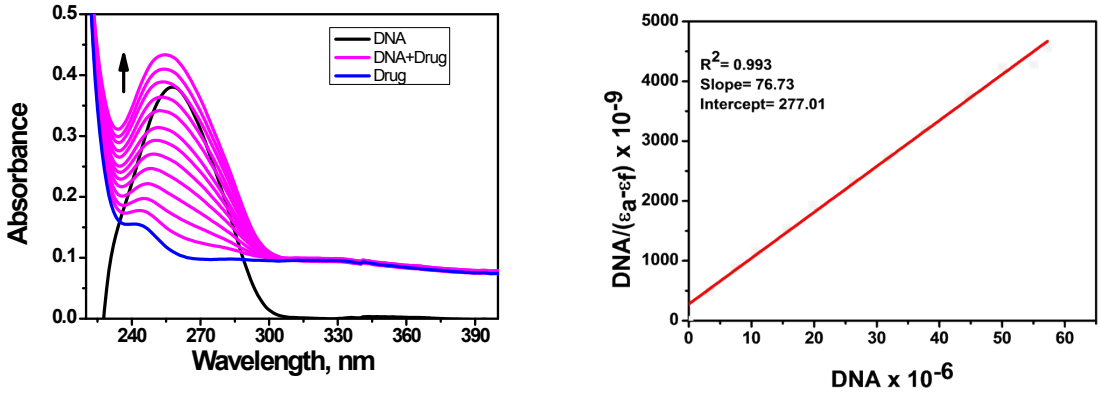

(b) (d)

Fig. S7. UV-visible titration of compound (a) **6g** and (b) **10a** in 5 mM Tris-HCl buffer with incremental addition of CT-DNA at pH 7.2. [DNA]/ (ε_a-ε_f) vs. [DNA] linear plots of compound (c) **6g** and (d) **10a**

BSA BINDING STUDY

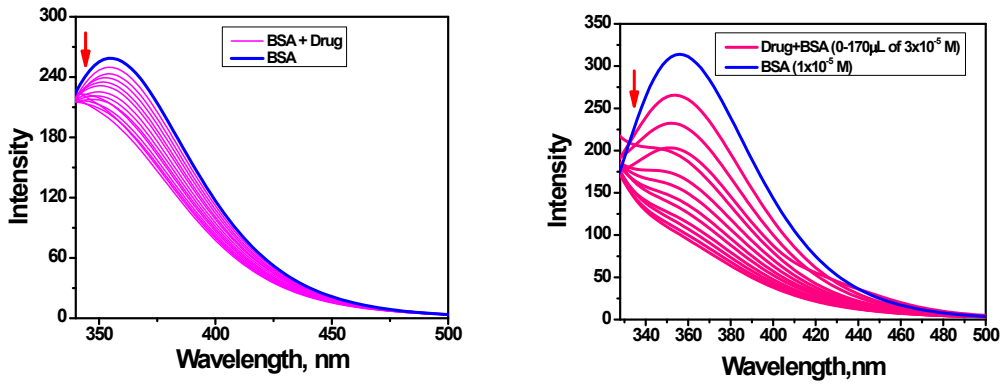

(a) (b)

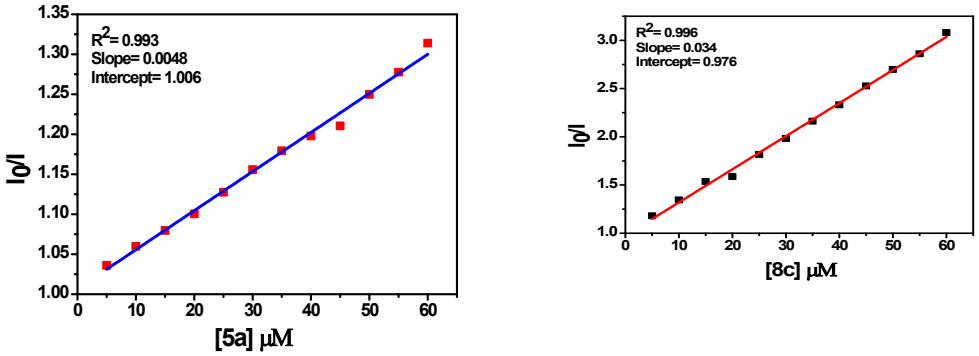

(c) (d)

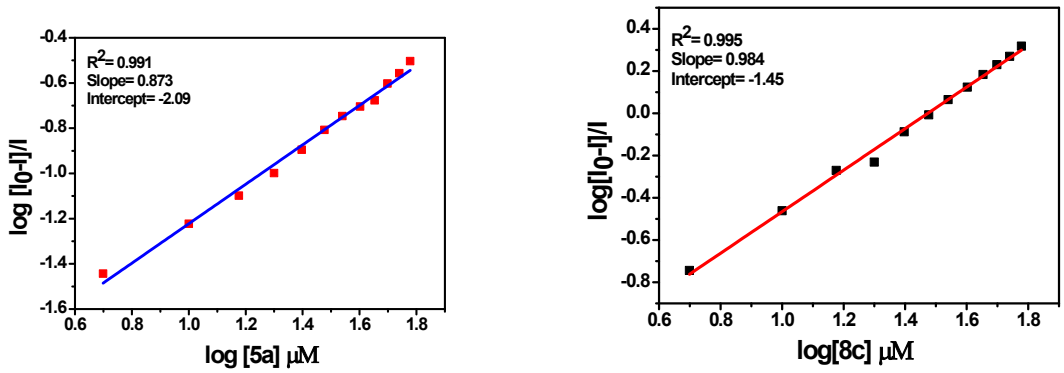

(e) (f)

Fig. S8. Fluorescence quenching of BSA on addition of compound (a) **6g** and (b) **10a** in 5 mM Tris HCl buffer at pH 7.2 (λ_{ex} = 295; λ_{em} = 350 nm). Plot of I_0/I vs. concentrations of compound (c) **6g** and (d) **10a**. Scatchard plot of log ($[I_0-I]/I$) vs. log [compound] for BSA in the presence of compound (a) **6g** and (b) **10a**.

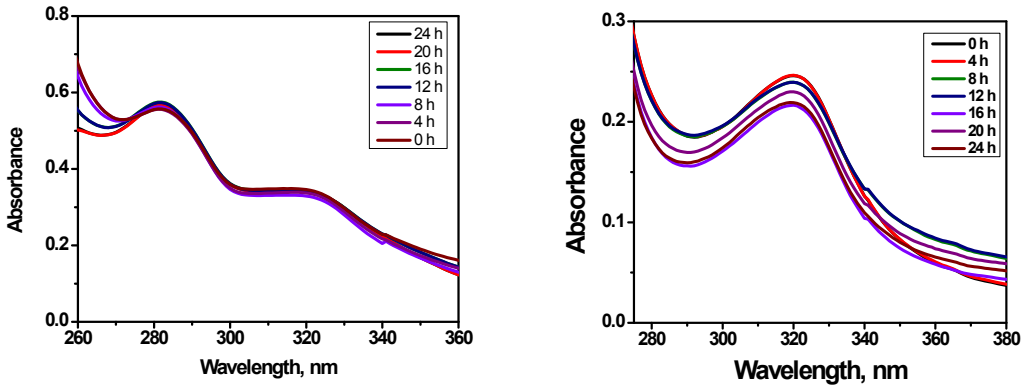

(a) (b)

Fig.S9. Stability study of compound (a) **6g** and (b) **10a** in MTT assay condition (phosphate buffer and 5% DMSO)

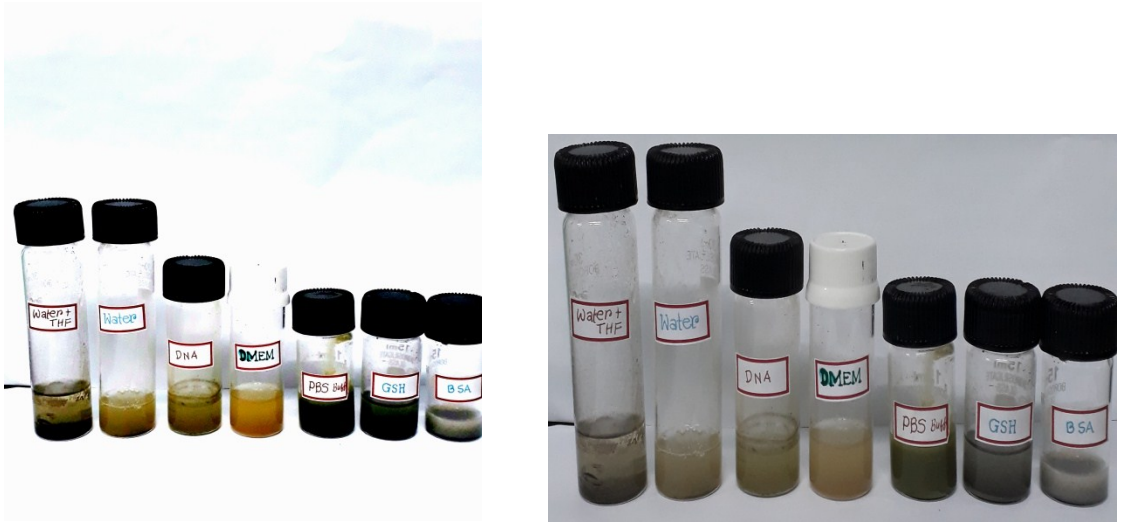

(a) **(b)**

Fig. S10. bioorthogonality study (a) before the reaction (b) after the reaction

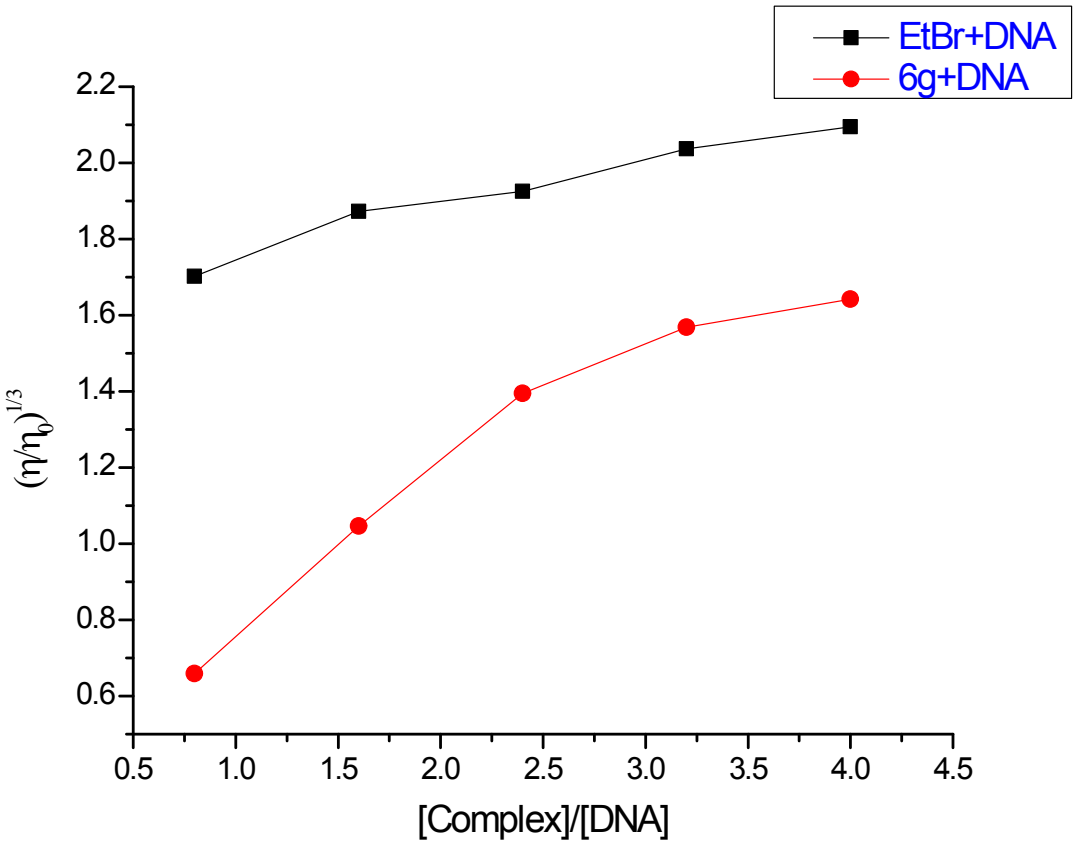

Fig. S11. Relative viscosity $(\eta/\eta_0)^{1/3}$ study of compound **6g** and EtBr

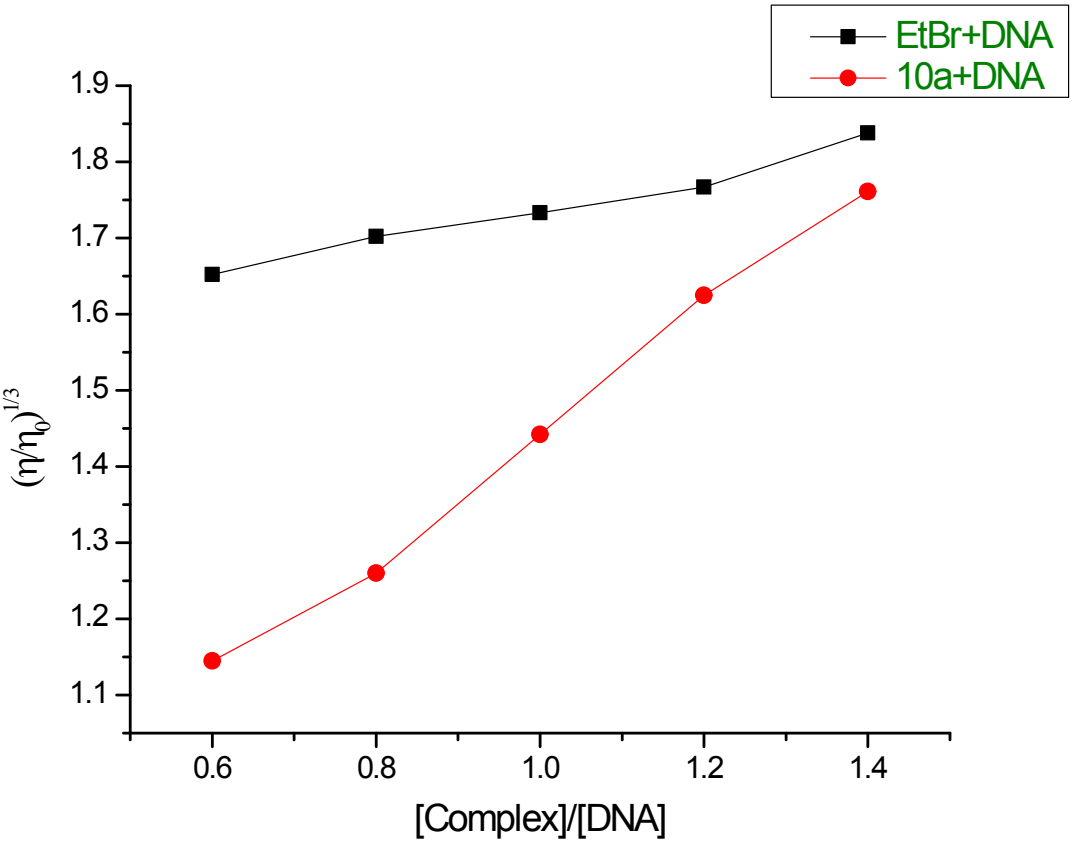

Fig. S12. Relative viscosity $(\eta/\eta_0)^{1/3}$ study of compound **10a** and EtBr

Experimental Section

***In vitro* cytotoxic activities (MTT assay)**[1]

In vitro cytotoxicity study was performed by standared MTT protocol.[2] This assay is based on the reduction of the yellow MTT tetrazolium salt (3-[4,5-dimethylthiazol-2-yl]-2,5diphenyltetrazolium bromide) by mitochondrial dehydrogenases to form a blue MTT formazan in viable cells. Synthesized triazoles were dissolved in 0.1% DMSO followed by serial dilution with medium. Two different types of cancer cell lines i.e. human colorectal adenocarcinoma cell line (Caco-2), human Epitheloid Cervix Carcinoma (HeLa), and one normal Human embryonic kidney cells (HEK-293) were used for this assay. Closely 1×10^4 cells per well for all these three cell lines were cultured in 100 µL of a growth medium in 96-well plates and incubated at 37 °C under a 5% CO_2 atmosphere. Afterward these cells were treated with different concentrations of the compounds (1-200 µM) in the volume of 100 µM/well. Cisplatin and RAPTA-C were used as standard positive control drug. After 24 h, the medium was superfluous and cell cultures mixed with 100 µl MTT reagent (1 mg/ml) and then incubated for 5 h at 37° C. After that the suspension was placed on microvibrator for 10-15 min and successively the absorbance was recorded by the ELISA reader at λ = 570 nm. The experiment was also performed in triplicate. The data were expressed as the growth inhibition percentage calculated according to the equation: % Cell viability = $[OD_{sample}\text{-}OD_{blank}/OD_{control}\text{-}OD_{blank}] \times 100$, where OD_{sample} is the measured absorbance in wells containing samples, $OD_{control}$ is the absorbance measured for cells

with a medium and a vehicle and OD_{blank} is the absorbance measured for blank well (no cells). Dose response curve was fitted in Origin 8.5 software and IC_{50} was calculated.

Cellular imaging assay[1]

Cellular imaging experiment was accomplished by using cancerous HeLa cell line obtained from NCCS. This study was conducted using 6 well plates. Cultured cells with 80% confluence were trypsinized using 1-2 ml of 1X trypsin. At that, it was transferred to fresh 15 ml falcon tube and centrifuged at 2000 rpm for 1-5 min. DMEM fresh media (80 µl) was added to the pellet formed at the bottom of the tube and the cells were seeded in 6 well plates. Subsequently, the test compounds (20 µM concentration) in PBS buffer were added to the well plates. After incubating for 2-4 h at 37 °C, all the wells were washed twice with PBS buffer (pH 7.4). Finally, the fluorescence images were recorded using the glass slides with an Olympus Fluorescence microscope at 480-550 nm excitations.[3]

DNA binding study[1]

The calf-thymus DNA (CT-DNA) binding property of the compounds was monitored by electronic spectra and competitive binding assay using a classical DNA intercalator, ethidium bromide (EtBr) by fluorescence spectroscopy.

UV–visible studies[1]

DNA binding experiments was conducted by using compound **6g** and **10a** in Tris-HCl buffer (5 mM Tris-HCl in water, pH 7.4) in water medium.[4] The concentration of CT-DNA was determined from its absorbance intensity at 260 nm and its known molar absorption coefficient value 6600 M^{-1} cm^{-1}. UV titration was performed by gradual increase of CT-DNA concentration. The sample was equilibrated with CT-DNA for about 5 min before each measurement. Then the absorbance of the compounds were measured after each 5 µL addition of CT-DNA. The intrinsic DNA binding constant (K_b) was calculated using the equation (i):

$$\frac{[DNA]}{(\varepsilon_a - \varepsilon_f)} = \frac{[DNA]}{(\varepsilon_b - \varepsilon_f)} + \frac{1}{K_b(\varepsilon_a - \varepsilon_f)} (i)$$

Where [DNA] is the concentration of DNA, ε_a is the apparent extinction coefficient observed for the compound, ε_f corresponds to the extinction coefficient of the test compund in its free form, and ε_b refers to the extinction coefficient of the test compound when fully bound to DNA. Data were plotted using Origin 8.5 software to obtain the [DNA]/(ε_a-ε_f) vs. [DNA] linear plot. The ratio of the slope to intercept from the linear fit gives the value of the intrinsic binding constant (K_b).

Ethidium bromide displacement assay[1]

The ethidium bromide fluorescence displacement assay was performed to identify the mode of binding between the potent complexes with DNA.[5] The intercalation of EthB to DNA is accompanied by strong fluorescence emission owing to the formation of the EtBr-DNA complex. Once a second molecule intercalates into DNA, there is a decrease of number of binding sites on the DNA available to EthB giving rise to reduction in the fluorescence intensity. The apparent binding constant (K_{app}) of the complex to CT-DNA was determined from the emission spectral measurements using ethidium bromide (EtBr) as a spectral probe in 5 mM Tris-HCl buffer (pH 7.4). EthB showed no apparent emission in Tris-buffer medium because of fluorescence quenching of free EthB by solvent molecules. The emission intensity gets significantly enhanced due to its intercalative binding to duplex DNA. A competitive binding of the complex to DNA is found to reduce the EthB emission

intensity. The relative binding propensity of the complex to DNA was estimated from the reduction of the emission intensity. The values of the apparent binding constant (K_{app}) were obtained by using the (ii) equation:

$$K_{app} \times [Complex]_{50} = K_{EtBr} \times [EtBr] (ii)$$

where K_{app} is the apparent binding constant of the complex studied, $[Complex]_{50}$ is the concentration of the complex at 50% quenching of DNA-bound ethidium bromide emission intensity, K_{EthB} is the binding constant of the EtBr (K_{EtBr} = 1.0 x 10^7 M^{-1}), and [EtBr] is the concentration of ethidium bromide (8 μM). The Stern-Volmer quenching constant (K_{SV}) has been calculated by using Stern-Volmer equation.[6]

Protein binding studies[1]

The interaction of the test compounds with bovine serum albumin (BSA), a structural homolog with human serum albumin (HSA) has been studied from tryptophan emission quenching experiment. The emision quenching of BSA at λ = 340 nm was observed with increasing the compound concentration, which confirms that the interaction between the compound and BSA have occurred. The compound solutions were gradually added to the solution of BSA (2 μM) in 5 mM Tris-HCl/NaCl buffer (pH 7.2) and the quenching of the emission signals at 340 nm (λex = 295 nm) were recorded. The quenching constant (K_{BSA}) has been determined quantitatively by using Stern-Volmer equation iii. Stern-Volmer plots of I_0/I vs. [Compoud] was made using the corrected fluorescence data taking into account the effect of dilution. Linear fit of the data using the equation (iii):

$$I_0/I = 1 + K_{BSA}[Q] = 1 + k_q \tau_0 [Q] (iii)$$

Where, I_0 and I are the emission intensities of BSA in the absence and in the presence of quencher of concentration [Q], gave the quenching constant (K_{BSA}) using Origin Pro 8.0 software. kq is the quenching rate constant, τ_0 is the average lifetime of the tryptophan in BSA without quencher reported as $1x10^{-8}$ s. For such static quenching interaction, the binding constant (K) and the number of binding sites (n) can be determined according to the Scatchard equation (iv) [7]:

$$\log(I_0 - I/I) = \log K + n \log[Q] (iv)$$

References

1 (a) A. Mondal, S. De, S. Maiti, B. Sarkar, A. Kumar, R. Jacob, A. Moorthy and P. Paira, *J. Photochem. Photobiol. B: Biology*, 2018, 178, 380–394; (b) Sunisha K. S., S. Banerjee, A. Mondal and P. Paira, *New J. Chem.*, 2016, 40, 10333-10343; (c) M. Chhabra, S. Sinha, S. Banerjee and P. Paira, *Bioorg. Med. Chem. Lett.*, 2016, 26, 213-217; (d) G. R. Jadhav, S. Sinha, M. Chhabra and P. Paira, *Bioorg. Med. Chem. Lett.,* 2016, 26, 2695-2700; (e) S. De, S. R. Chaudhuri, A. Panda, G. R. Jadhav, R Selva Kumar, P. Manohar, N. Ramesh, A. Mondal, A. Moorthy, S. Banerjee, P. Paira, S. K. Ashok Kumar, *New J. Chem*., 2019, 43, 3291-3302.

2 R. Menicagli, S. Samaritani, G. Signore, F. Vaglini and L. Dalla, J. Med. Chem. 2004, 47, 4649–4652.

3 M. R. Gill and J. A. Thomas, Chem. Soc. Rev. 2012, 41, 3179-3192.

4 M. Sirajuddin, S. Ali and A. Badshah, J. Photochem. Photobio. B: Bio., 2013, 124, 1–19.

5 S. Dasari and A. K. Patra, Dalton Trans. 2015, 44, 19844-19855.

6 J. Keizer, J. Am. Chem. Soc., 1983, 105, 1494–1498.

7 J. Liu, J. Tian, W. He, J. Xie, Z. Hu and X. Chen, J. Pharm. Biomed. Anal, 2004, 35, 671-677.